Adolescence in the Development of the Prefrontal Cortex and Mediodorsal Thalamus

Laura Jacqueline Benoît

Submitted in partial fulfillment of the
requirements for the degree of
Doctor of Philosophy
under the Executive Committee
of the Graduate School of Arts and Sciences

COLUMBIA UNIVERSITY

2021

Abstract

Adolescence in the Development of the Prefrontal Cortex and Mediodorsal Thalamus

Laura Jacqueline Benoît

Cognitive impairments are a hallmark of many, if not all, psychiatric disorders. They include deficits in working memory, attention, and cognitive flexibility. The prefrontal cortex (PFC) is essential for these cognitive functions and has been implicated in psychiatric disorders, including schizophrenia. The PFC receives reciprocal inputs from the thalamus, and this thalamo-PFC circuitry supports cognition. In patients with schizophrenia, who have impaired cognitive functioning, thalamo-PFC connectivity is disrupted. This finding is also seen in adolescents at high risk for the disorder, even before diagnosis.

While impaired cortical maturation has been postulated as a mechanism in the etiology of schizophrenia, the postnatal development of thalamo-PFC circuitry is still poorly understood. In sensory cortex, activity relayed by the thalamus during a postnatal sensitive period is essential for proper cortical maturation. However, whether thalamic activity also shapes maturation of the PFC is unknown.

Here, I will present evidence to support the hypothesis that adolescence represents a sensitive period, during which the PFC is susceptible to transient perturbations in thalamic input activity, resulting in persistent changes in circuitry.

In Chapter 1, I present the existing literature on schizophrenia and our current understanding of its etiology. I then review the structure and connectivity of the PFC and its inputs, including the thalamus, in the context of schizophrenia and cognition. Next, I discuss the role of adolescence in the development of these structures and circuits. Finally, I introduce the

concept of sensitive periods and outline the hypothesis that a similar process may occur in the context of the adolescent development of thalamo-PFC circuitry.

To assess cognitive functioning in mouse models, I developed an operant-based working memory task. In Chapter 2, I describe this newly developed task and demonstrate that behavioral performance in the task is susceptible to PFC lesions. Thus, the task offers a new approach to studying PFC cognitive function.

In Chapter 3, I discuss work done to address the hypothesis of adolescence as a sensitive period in the development of thalamo-PFC circuitry. I established an approach whereby I can transiently reduce activity in the thalamus during specific time windows. In this way, I compared the persistent effects of transient thalamic inhibition during adolescence and adulthood. I found that adolescent thalamic inhibition causes long-lasting deficits in cognitive behavioral performance, including the operant-based working memory task described in Chapter 2 and a cognitive flexibility task, decreased PFC cellular excitability, and reduced thalamo-PFC projection density. Meanwhile, adult thalamic inhibition has no persistent consequences on behavior or PFC excitability.

Adolescent thalamic inhibition also results in disrupted PFC cellular cross-correlations and task outcome encoding during the cognitive flexibility task. Strikingly, exciting the thalamus in adulthood during the behavioral task rescues PFC cross-correlations, task outcome encoding, and the cognitive deficit.

These data support the hypothesis that adolescence is a sensitive period in thalamo-PFC circuit maturation as adolescent thalamic inhibition has long-lasting consequences on PFC circuitry, while adult thalamic inhibition has no persistent effects. Moreover, these results highlight the role of the thalamus as a non-specific facilitator of PFC activity, expanding our understanding of this thalamic function to additional cognitive contexts. By supporting PFC

network activity, boosting thalamic activity provides a potential therapeutic strategy for rescuing cognitive deficits in neurodevelopmental disorders.

Finally, in Chapter 4, I conclude with a general discussion. I highlight major take-aways from this work as well as next steps in our exploration of these crucial neural circuits. Together, the findings outlined here offer new promise for early diagnosis and treatment options for patients with cognitive impairments and psychiatric disorders.

Table of Contents

List of Figures

Acknowledgments

None of this work would have been possible without the help and support of my colleagues, mentors, friends, and family. Over the four years that I've worked on these projects, I have been extremely lucky to have an incredible network of people, both near and far.

I thoroughly appreciate all of the invaluable advice and guidance in my projects and in science and medicine as a whole. Science is a team effort, and I have been privileged to be surrounded by people who exemplify how to be an incredible teammate. I can only hope that I carry that energy forward.

I am also enormously grateful to all of you for those non-scientific "distractions" – trips, dinners, shows, walks, sports, etc. They have allowed me to maintain a balance that has been an essential contributor to this work. And also, it's been fun!

Chapter 1: The Postnatal Development of the Prefrontal Cortex and the Mediodorsal Nucleus of the Thalamus in the Context of Schizophrenia and Cognition

1.1 Schizophrenia

Schizophrenia is a severe, chronic psychiatric disorder, with a worldwide prevalence approaching 1 percent (McGrath et al., 2008; Moreno-Küstner et al., 2018). It is one of the most disabling and economically impactful medical conditions, identified by the World Health Organization in the top 30 illnesses contributing to the global burden of disease and top 10 global leading causes of disability (Murray, 1990). In addition to the effects of schizophrenia itself, people with the disorder are at a higher risk for co-occurring disorders, including other psychiatric disorders such as substance use disorders (Buckley et al., 2009) and metabolic conditions such as type II diabetes (Hoffman, 2017; Olfson et al., 2015; Pillinger et al., 2017), multiplying the impact on people and families affected by the disorder. In the US, meta-analyses have identified large racial disparities, with black Americans being at least 2.4 times more likely than white Americans to be diagnosed with schizophrenia (Barnes, 2004; Chien & Bell, 2008; Olbert et al., 2018; Schwartz & Blankenship, 2014). Similar racial disparities were seen when analyzing lifetime rates of psychotic symptoms. Given that race is a social construct with no biological basis, this racial discrepancy points to the complex pathogenesis of schizophrenia, which includes many environmental and psychosocial factors (Stilo & Murray, 2019).

1.1.1 Pre-Diagnosis

The typical onset of schizophrenia is seen in late adolescence (Gogtay et al., 2011), with prodromal symptoms seen sometimes years before diagnosis (Häfner et al., 1994). Given these

early indicators, schizophrenia is thought to have a developmental origin, with risk factors identified in both the prenatal and postnatal periods (Insel, 2010; Millan et al., 2016; Paus et al., 2008; Sakurai & Gamo, 2019; Weinberger & Berman, 1996; Welham et al., 2009). For instance, gestational exposure to infection has been implicated in the development of schizophrenia (Brown & Derkits, 2010; Insel, 2010), and during adolescence, exposure to various perturbations, including cannabis and stress, increases risk of later illness development (Arseneault et al., 2002; Gomes & Grace, 2017).

These widespread risk factors further underline the complex pathogenesis of schizophrenia, which makes prevention and early diagnosis very challenging. However, early treatment of schizophrenia is associated with improved outcomes (Häfner & Maurer, 2006; McEvoy, 2007). As a result, one area of interest lies in the identification of early indicators, which could help prevent many of the long-term effects of untreated psychosis. Some studies have begun to look at potential early markers, such as changes in white matter, in patients at clinical high risk for psychosis (Di Biase et al., 2021). Meanwhile, whole-brain resting state functional imaging of patients with diagnosed mental disorders has shown a highly consistent network organization across individuals, but the small differences that do exist may be predictive of the diagnosis (Spronk et al., 2021). These studies, among others, have spurred further research into the identification of biological markers, specifically in regional interconnectivity, that can help diagnose schizophrenia, ideally in the early stages before the first psychotic episode.

Due to our incomplete understanding of these early biological markers for psychiatric disorders, there is some debate in the field about whether the appropriate early interventions should focus on early symptoms or simply reducing exposure to known risk factors (Malhi et al., 2021; Woods et al., 2021). However, both sides of this debate can agree that the most

productive path forward comes from a better understanding of the biological processes involved in the etiology of these disorders.

1.1.2 Diagnosis

Schizophrenia is characterized by three major categories of symptoms: positive, negative, and cognitive. The Diagnostic and Statistical Manual of Mental Disorders (DSM-5) designates that for diagnosis, a patient must experience positive symptoms (i.e., delusions, hallucinations, or disorganized speech) and/or negative symptoms (i.e., diminished emotional expression, avolition, or catatonia), which must coincide with social and/or occupational dysfunction (*Diagnostic and statistical manual of mental disorders: DSM-5™, 5th ed*, 2013).

1.1.3 Cognitive Symptoms

While only positive and negative symptoms are used in the diagnosis of the disorder, cognitive symptoms (i.e., deficits in attention or working memory (Huang et al., 2019)) are equally prominent and severely compromise functional outcomes for patients with schizophrenia (Bowie et al., 2008; Green et al., 2000; Millan et al., 2012b). However, most currently available therapeutics target other symptoms, leaving the cognitive impairments untouched, or even worse (Hill et al., 2010; Millan, 2006; Millan et al., 2012b). Moreover, these cognitive deficits are seen throughout the entire course of the disorder, including before diagnosis (Davidson et al., 1999), at the first psychotic episode (Saykin et al., 1994), and in later stages of the disorder (Breier et al., 1991; Heaton et al., 1994), indicating that they cannot simply be attributed to the chronicity of the disorder or long-term consequences of anti-psychotic medications and treatments. In addition to schizophrenia, cognitive impairments have also been demonstrated in most, if not all, psychiatric disorders, including mood, anxiety, panic, and developmental disorders (Kolb & Whishaw, 1983; Millan et al., 2012a; Weinberger & Berman, 1996). Despite the widespread nature of these symptoms and their importance on quality of life, treatment of

cognitive symptoms remains elusive. Given this clinical discrepancy, recent research has focused on understanding the circuitry and mechanisms involved in cognition and cognitive deficits.

1.2 Prefrontal Cortex

Decades of research have identified the prefrontal cortex (PFC), an evolutionarily conserved part of the frontal lobe, as an important center for cognitive function (*Frontal lobe function and dysfunction*, 1991). Several reports have demonstrated a striking resemblance between the cognitive deficits observed in patients with frontal lesions and deficits seen in schizophrenia, suggesting that alterations in the PFC may play a role in cognitive symptoms in this disorder (Kolb & Whishaw, 1983; Kraepelin et al., 1919; Muller et al., 2002). Indeed, functional imaging studies have confirmed the importance of the PFC in cognition and support the hypothesis that cognitive deficits arise from disruptions to PFC activity (Ingvar & Franzen, 1974; Karlsgodt et al., 2009; Weinberger & Berman, 1996).

One area of interest lies in understanding the role of intrinsic PFC circuitry and its external inputs. As with other parts of cortex, the PFC has a multi-layered architecture, with distinct cellular and molecular characteristics distributed across the layers (Santana & Artigas, 2017). It is made up of several different cellular populations, which form synaptic connections with other cells within the PFC as well as other cortical and subcortical regions.

1.2.1 Pyramidal Neurons

Excitatory, glutamatergic pyramidal neurons make up approximately 75% of the total neuronal population in the PFC (Beaulieu, 1993; Volk & Lewis, 2010). While the total number of neurons in the PFC is not changed in patients with schizophrenia (Thune et al., 2001), there is evidence of changes in arborization (Konopaske et al., 2018), dendritic spines (Black et al.,

2004; Garey et al., 1998; Glantz & Lewis, 2000), protein markers (Arion et al., 2015; Glantz & Lewis, 1997; Mirnics et al., 2000; Perrone-Bizzozero et al., 1996), and other cellular characteristics such as somal size (Pierri et al., 2001; Rajkowska et al., 1998). One major hypothesis proposes that excessive synaptic pruning may account for the changes in dendritic arborization (Boksa, 2012; Rapoport & Gogtay, 2008). However, the precise mechanisms contributing to these changes remain elusive. Some hypothesize that existing abnormalities in glutamate transmission may be revealed by excessive pruning (Deakin et al., 1989; Sherman et al., 1991) or that normal developmental synapse elimination may be disrupted (Feinberg, 1982; McGlashan & Hoffman, 2000). Recent work has also looked at the role of microglia in the immune system and complement activity in mediating this pruning (Sekar et al., 2016; Sellgren et al., 2019; Yilmaz et al., 2021). Altogether, it is clear that the PFC and its pyramidal cell population are implicated in schizophrenia in numerous ways.

1.2.2 Interneurons

The second major cellular population in the PFC consists of inhibitory GABAergic interneurons, which make up approximately 25% of the PFC neuronal population (Beaulieu, 1993; Volk & Lewis, 2010). As with the pyramidal cells, many abnormalities have also been identified in the interneuron population, including changes in a GABA synthesizing protein, GAD67 (Hashimoto et al., 2008a). Other GABA-associated proteins have also been implicated in schizophrenia, indicating that both the production and reuptake of GABA is compromised in the PFC in schizophrenia (Hashimoto et al., 2008b; Ohnuma et al., 1999).

PFC interneurons are often described in subpopulations with distinct characteristics. Populations that express the neuropeptide somatostatin (Morris et al., 2008) or cholecystokinin (Eggan et al., 2008) have been shown to be affected in schizophrenia. Much of the research has traditionally focused on interneurons that express that calcium-binding protein, parvalbumin

(PV), which make up approximately 25% of PFC GABAergic neurons (Condé et al., 1994) and receive inputs from pyramidal cells (Melchitzky et al., 2001). In schizophrenia, the total number of PFC PV neurons is unchanged (Hashimoto et al., 2003; Woo et al., 1997), but protein expression is altered in PV cells (Cruz et al., 2009; Hashimoto et al., 2003; Volk et al., 2002; Woo et al., 1998), resulting in impairments in GABA signaling (Volk & Lewis, 2010). Moreover, PV interneurons are of particular interest because they are crucial for the generation of gamma oscillatory activity (Buzsáki & Wang, 2012). Gamma oscillations have been shown to play an important role in cognitive functioning and are disrupted in patients with schizophrenia (Chen et al., 2014; Cho et al., 2006; Hirano et al., 2015; Kirihara et al., 2012; Light et al., 2006; Tanaka-Koshiyama et al., 2020; Uhlhaas & Singer, 2012).

1.3 The development of the PFC in schizophrenia

The importance of the PFC in schizophrenia has also been highlighted in neurodevelopmental models, which suggest that disruptions to PFC maturation during adolescence may lead to schizophrenia (Feinberg, 1982; Rapoport et al., 2012; Weinberger, 1987). Specifically, Feinberg's hypothesis states that in schizophrenia, aberrant activity-dependent pruning during adolescence may lead to persistent changes in PFC circuit function (Feinberg & Campbell, 2010). In addition to dendritic pruning (Boksa, 2012; Schafer & Stevens, 2013), there are several other markers of PFC adolescent development that are disrupted during adolescence in the progression of schizophrenia (Millan et al., 2016). For instance, during adolescence, the PFC undergoes a period of volumetric reduction. Cytokines related to this process are shown to be elevated in the circulation in people at clinical high risk for psychosis (Cannon et al., 2015). Similarly, grey matter loss in the PFC is already seen in adolescents at clinical high risk (Dazzan et al., 2011).

One crucial component of PFC maturation is interneuron development, as dysregulation of the interneurons can lead to an excitatory/inhibitory imbalance and disruption of neural oscillatory activity, which in turn leads to impaired cognition (Kann, 2016; Lewis, 2012; Lewis et al., 2012; Marín, 2012; Millan et al., 2012b; Uhlhaas, 2013; Woo et al., 2010). GABA-glutamatergic coupling is also crucial for proper PFC maturation as it impacts subcortical circuits, and its disruption can lead to psychosis (Bodatsch et al., 2015; Marín, 2012; Uhlhaas, 2013).

With the extensive impact of interneuron development on subsequent psychiatric health, there are numerous factors that have been identified in this process. For instance, adolescent NMDA receptor hypoactivity can have implications for proper gamma oscillatory activity (Woo et al., 2010). In addition, the expression of PV undergoes changes during adolescence, which are altered in schizophrenia (Samantha J. Fung et al., 2010). The Na-K-Cl co-transporter, a GABA-A receptor-associated protein (Deidda et al., 2014; Morita et al., 2014), and Kv3 potassium channels (Kann, 2016; Marín, 2012; Uhlhaas, 2013; Woo et al., 2010; Yanagi et al., 2014), which are responsible for the rapid repolarization of GABAergic interneurons, also play important roles in neural circuit maturation and in PFC interneurons' ability to mediate cognition, and they are implicated in schizophrenia. Intracellular neuregulin 1-ERBB4 is important for migration of cortical interneurons and axon myelination, and its levels are altered in schizophrenia (Karam et al., 2010; Marín, 2012; Mei & Nave, 2014). Extracellular matrix disruptions (Berretta, 2012) and abnormal regulation by neurotrophins, such as BDNF (Mondelli et al., 2011), can also have long-term consequences on proper interneuron development and later psychosis. Altogether, this work points to numerous important processes that occur in the adolescent development of PFC interneurons that impact cognitive functioning and psychiatric health later in life.

1.4 PFC Inputs

The PFC also receives inputs from a variety of cortical and subcortical regions (Divac et al., 1978; Hoover & Vertes, 2007; Markowitsch et al., 1978). These inputs are highly heterogeneous, including dopaminergic projections from the ventral tegmental area (Bjorklund et al., 1978; Clarkson et al., 2017; Gee et al., 2012; Robinson & Sohal, 2017; Seamans & Yang, 2004; Seong & Carter, 2012), serotonergic projections from the raphe nuclei (Garcia-Garcia et al., 2017; Vertes et al., 1999), cholinergic projections from the basal forebrain (Bigl et al., 1982), noradrenergic projections from the locus coeruleus (Chandler, 2016), and glutamatergic excitatory projections from the contralateral PFC, the amygdala, the hippocampus, and the thalamus. The excitatory glutamatergic projections converge onto the same PFC pyramidal cell populations, with a distinct regional organization along the pyramidal cells (Little & Carter, 2012). The projections from the amygdala (Salzman & Fusi, 2010), hippocampus (Sigurdsson & Duvarci, 2016), and thalamus (Ouhaz et al., 2018; Parnaudeau et al., 2018) are also disrupted in patients with cognitive deficits.

1.4.1 Amygdala

The amygdala is traditionally viewed as the emotional center of the brain and separate from cognitive processes. Due to its connections with the PFC, we now understand that there are many interactions between emotion and cognition that make the two processes inseparable (Lang & Davis, 2006; Salzman & Fusi, 2010). Indeed, there are many complex cognitive-emotional behaviors that rely on the integration of regions that have been conceptualized as either affective or cognitive (Barbas & Zikopoulos, 2007; Murray & Izquierdo, 2007; Pessoa, 2008; Price, 2007). For instance, the uncinate fasciculus (UF) is a white matter tract that projects from limbic structures, like the amygdala, to the frontal lobe. Human studies have found

disruptions to the UF in patients with schizophrenia, and this finding has been associated with cognitive deficits and later disorder progression (Singh et al., 2016).

Interestingly, different psychotic disorders show differential connectivity, with patients with schizophrenia showing reduced amygdalar-PFC functional connectivity (Anticevic et al., 2014b; Ho et al., 2019; Hoptman et al., 2010; Tian et al., 2011) and patients with bipolar disorder I with psychosis showing an increased connectivity between the regions (Ho et al., 2019). Meanwhile, it has been well-documented that patients with schizophrenia have a reduced amygdalar volume (Ho et al., 2019; Okada et al., 2016; van Erp et al., 2016), but because this is not seen in patients with other psychotic disorders and has typically been identified later in the disorder progression, the volumetric reduction may also be related to exposure to anti-psychotic medications, which can result in brain tissue loss (Fusar-Poli et al., 2013).

Altogether, this body of evidence clearly implicates the amygdala in patients with schizophrenia. With the discrepancies seen in the phenotypes across different psychotic disorders and the later manifestation of these findings, the amygdalar metrics can best be used to monitor disorder progression or cognitive and emotional symptoms.

1.4.2 Hippocampus

The hippocampus is another subcortical region that projects to the PFC. It is a complex structure that plays an important role in learning and memory. It is implicated in patients with schizophrenia, with abnormal activation during certain behaviors, such as memory tasks (Heckers & Konradi, 2010). The functional connectivity between the PFC and the hippocampus is also altered in patients with schizophrenia (Fletcher, 1998; Heckers et al., 1998; Liang et al., 2006; Pettersson-Yeo et al., 2011; Weinberger et al., 1992). This dysconnectivity was seen both at rest (Zhou et al., 2008) and during cognitive tasks, such as working memory tasks (Henseler

et al., 2010; Meyer-Lindenberg et al., 2005; Rasetti et al., 2011). Furthermore, an effective connectivity study found that the hippocampal influence over the PFC was reduced in schizophrenia (Benetti et al., 2009).

Anatomically, numerous studies have also identified a reduction in hippocampal volume in patients with early-onset schizophrenia (Barr et al., 1997; Sumich et al., 2002; Szeszko et al., 2003). While this finding is established in early stages of the disorder, it also persists in chronic schizophrenia (Nelson et al., 1998). In addition, patients with schizophrenia have changes in cerebral blood flow in the hippocampus, which is linked to hippocampal hypermetabolism (DeLisi et al., 1989; Kawasaki et al., 1992; Malaspina et al., 2004; Medoff et al., 2001), and this phenotype has been tied to symptom severity (Liddle et al., 1992; Molina et al., 2003; Silbersweig et al., 1995). Interestingly, this hippocampal hypermetabolism has been shown to precede the volume loss, suggesting that the hypermetabolism, driven by glutamate, may be the cause for this hippocampal atrophy (Schobel et al., 2013). As with the amygdala, anatomical abnormalities have also been identified in the major fiber bundle that connects the hippocampus to the frontal lobe, in this case, the fornix (Zhou et al., 2008).

Altogether, the hippocampus along with its connection to the PFC are clearly impaired in patients with schizophrenia, and this disruption is important for cognitive symptoms and functioning.

1.4.3 Thalamus

Another major excitatory input to the PFC that has been greatly studied in the context of cognitive functioning and psychiatric disorders comes from the thalamus. The thalamus is a heterogeneous structure located deep in the brain, which is made up of multiple nuclei, with each nucleus projecting to and receiving inputs from largely non-overlapping areas (EG & McCormick, 2007). First order thalamic nuclei receive sensory inputs from the periphery and

project to primary sensory and motor cortical areas (Guillery, 1995). For instance, the lateral geniculate nucleus receives input from the retina before projecting to the primary visual cortex (Bickford, 2016; Sherman & Guillery, 1998). Meanwhile, higher order nuclei receive their inputs directly from the cortex, with nuclei like the mediodorsal nucleus of the thalamus (MD) exhibiting reciprocal connectivity with the PFC (Harris et al., 2019; Ray & Price, 1992).

While the thalamus has traditionally been viewed as a simple relay station (Jones, 2012; Levin et al., 1991), it is now clear that thalamic nuclei play a more substantial regulatory role in coordinating cortical activity, especially the higher order nuclei (Giraldo-Chica & Woodward, 2017; Mukherjee et al., 2020; Sherman, 2016). For instance, in addition to the MD projections to pyramidal cells in the PFC, the MD also projects onto PFC PV interneurons, contributing to additional complexity in these thalamocortical projections (Canetta et al., 2020; Delevich et al., 2015; Mukherjee et al., 2020).

The thalamus is one of the major brain regions that has been implicated in schizophrenia (Cronenwett & Csernansky, 2010; Giraldo-Chica & Woodward, 2017; Glahn et al., 2008; Pergola et al., 2015; Sim et al., 2006). Thalamic volume has been shown to be reduced in patients with schizophrenia, even in early stages of the disorder (Huang et al., 2015; Huang et al., 2017; Rao et al., 2010). Imaging studies have demonstrated a hyperconnectivity between the thalamus and sensory regions and hypoconnectivity between the thalamus and cerebellar and prefrontal regions (Anticevic et al., 2014a; Cheng et al., 2015; Damaraju et al., 2014; Klingner et al., 2014; Kubota et al., 2013; Li et al., 2016; Marenco et al., 2012; Neil D. Woodward et al., 2012). The thalamo-PFC decreased correlation has also been measured in patients during cognitive testing (Giraldo-Chica et al., 2017; Mitelman et al., 2005; Pinault & Deschenes, 1998; Woodward et al., 2012), where it has been linked to impairments in functioning.

Unlike the amygdalar findings, these thalamic phenotypes have been observed in early stages of the disorder as well as in patients at clinical high risk for schizophrenia, even before diagnosis. For instance, decreases in thalamic volume have been seen in younger patients with psychosis or at clinical high risk (Harrisberger et al., 2016; Lunsford-Avery et al., 2013). While many of these studies have looked at overall thalamic volume, more recent work has also identified the specific thalamic nuclei that are most impacted. These young patients have been shown to have reduced volumes of the pulvinar, MD, and ventrolateral nuclei (Huang et al., 2020). Interestingly, this study also correlated these volumes with cognitive impairments, finding that smaller nuclei was associated with worse cognitive performance, especially for the pulvinar nucleus and, to a lesser extent, the MD (Huang et al., 2020).

In addition, thalamic dysconnectivity with the PFC and other regions is also seen at rest in younger adolescents at clinical high risk for schizophrenia, before diagnosis (Anticevic et al., 2015), and in early stages of the disorder (Woodward & Heckers, 2016b). Remarkably, this thalamic dysconnectivity is more apparent in those who are later diagnosed with the disorder (Anticevic et al., 2015). These findings have been replicated and show an intermediate level of thalamic dysconnectivity in those at clinical high risk, with those in the early stages of the disorder demonstrating the same levels as people with chronic schizophrenia (Fryer et al., 2021). Moreover, adolescents at clinical high risk or with early schizophrenia also demonstrate disrupted PFC circuitry during working memory tasks (Fryer et al., 2013). Together, these studies establish that the thalamic dysconnectivity begins prior to the full onset of schizophrenia, with an increase in severity for those who ultimately develop the disorder. Meanwhile, the effects of chronic psychosis or long-term anti-psychotic medications do not appear to worsen this phenotype. These findings raise the intriguing possibility that thalamo-PFC dysconnectivity could be part of the developmental etiology of schizophrenia (Anticevic et al., 2014a; Anticevic et al., 2015; Cho et al., 2016; Woodward & Heckers, 2016a).

1.5 The MD-PFC circuit in animal models

It is clear that the PFC and its inputs, including the MD, are greatly implicated in schizophrenia and cognitive dysfunction. As a result, researchers have used animal models to better explore the mechanisms involved in the functioning of these circuits. A large body of work in rodent and primate models has focused on the role of this reciprocal MD-PFC circuit. It has been shown to be essential in many cognitive behaviors, including working memory and cognitive flexibility (Alcaraz et al., 2018; Bolkan et al., 2017; Chakraborty et al., 2016; Dias et al., 1996; Dunnett et al., 1999; Ferguson & Gao, 2018; Granon et al., 1994; Hsiao et al., 2020; Kupferschmidt & Gordon, 2018; Larsen & Divac, 1978; Parnaudeau et al., 2018; Rikhye et al., 2018a; Rikhye et al., 2018b; Saalmann, 2014; Schmitt et al., 2017; Spellman et al., 2021; Stamm & Weber-Levine, 1971; Watanabe & Funahashi, 2012). Both the PFC and the MD are individually important for cognitive functioning, as lesions or other disruptions to either region lead to cognitive impairments (Benoit et al., 2020; Dunnett et al., 1999; Ouhaz et al., 2021; Parnaudeau et al., 2013; Rikhye et al., 2018a). Furthermore, upon acute inhibition of either MD-to-PFC or PFC-to-MD projections, cognitive functioning is also impaired (Alcaraz et al., 2018; Bolkan et al., 2017; Marton et al., 2018), while stimulation of these projections enhances behavioral performance in cognitive tasks (Bolkan et al., 2017; Schmitt et al., 2017). Together, these findings not only identify the PFC and MD as crucial players in cognition; they also underscore the bidirectionality of the reciprocal circuit.

Many of the behavioral paradigms that have implicated the MD-PFC circuit are delay-containing cognitive tasks. As a result, it has been of great interest to discover the mechanisms at play during these crucial delay periods. Activity in both PFC and MD during the delay period have been implicated in proper task functioning (Bolkan et al., 2017; Watanabe & Funahashi, 2012). Analysis of PFC cellular activity has indicated subsets of neurons whose activity tile over

the course of the delay to maintain the trial-specific information (Bolkan et al., 2017). However, upon MD inhibition, this tiling is disrupted, along with behavioral performance. This study, along with others, has led to the hypothesis that the thalamic inputs to the PFC may act as a non-specific amplifier supporting PFC task-specific activity (Bolkan et al., 2017; Hsiao et al., 2020; Parnaudeau et al., 2018; Rikhye et al., 2018a; Rikhye et al., 2018b; Schmitt et al., 2017). Thus, broad excitation from the MD to the PFC allows the PFC to maintain rule specificity or trial information during the task. It has also been proposed that the MD acts as a selectivity gating mechanism to allow for modulation of PFC signaling, affecting the functional connectivity of specific task-relevant cortical ensembles (Rikhye et al., 2018a; Rikhye et al., 2018b; Schmitt et al., 2017). In this way, while the MD may not encode trial-specific information, it is sensitive to the overall task context. Within this cognitive task context, non-specific MD activity can enhance PFC ensembles, reinforcing the cue or trial information encoded within these ensembles and allowing for improved task performance (Bolkan et al., 2017; Schmitt et al., 2017).

While these studies provide consistent evidence for the role of the MD as a non-specific amplifier of PFC encoding, other studies in primates have indicated specific stimulus or spatial representations in thalamic activity during the delay period (Tanibuchi & Goldman-Rakic, 2003; Watanabe & Funahashi, 2004a, 2004b, 2012). The reasons for this discrepancy may be related to a number of factors, including the species and the task used, and further exploration of MD activity during cognitive behavioral testing should continue to study this question.

1.6 The postnatal development of the MD and PFC

This literature has offered important insights into the role of the MD-PFC circuit in the adult. However, clinical work, as illustrated above, also implicates the development of this circuit during vulnerable periods. Therefore, several groups have outlined the developmental milestones of the thalamus, PFC, and thalamo-PFC projections in rodents (Bitzenhofer et al.,

2020; Caballero et al., 2014; Caballero et al., 2020; Chini & Hanganu-Opatz, 2021; Delevich et al., 2021; Ferguson & Gao, 2014; Goodwill et al., 2018; Konstantoudaki et al., 2018; Miyamae et al., 2017a; Paus et al., 2008; Rios & Villalobos, 2004; Van Eden & Uylings, 1985; Yang et al., 2014a).

By birth, the MD projections to the PFC have already arrived in both the developing deeper cortical layers as well as the cortical plate, which will later develop into the superficial layers of the PFC (Figure 1.1) (Van Eden, 1986). These projections continue to increase after birth, reaching a peak around P10, and after a period of steep cell loss at P13, they show a gradual increase in density that levels off before P60 (Ferguson & Gao, 2014; Rios & Villalobos, 2004). Meanwhile, the volume of the PFC increases in the postnatal period, peaking around P24. At that point, it decreases, reflecting a period of dendritic pruning in PFC pyramidal neurons, a process which has its fastest rate around P30 (Marmolejo et al., 2012; Pattwell et al., 2016; Zuo et al., 2005). It has been postulated that this pruning could result in part from refinement of thalamo-cortical synaptic contacts during this period (Ferguson & Gao, 2014).

These developmental trajectories support the hypothesis that the MD plays a vital role in the postnatal development of the PFC in two primary ways: (1) the early presence of MD afferent fibers across the PFC layers from birth indicate that these thalamic afferent fibers may play a role in the laminar development of the PFC (Van Eden et al., 1991); and (2) the changes in PFC volume follow the changes in density of the MD projections, suggesting that the refinement of the thalamic projections may inform the subsequent PFC development (Ferguson & Gao, 2014; Rios & Villalobos, 2004; Van Eden, 1986; Van Eden & Uylings, 1985).

Furthermore, as discussed above, Feinberg's hypothesis states that, in schizophrenia, aberrant activity-dependent pruning during adolescence may lead to persistent changes in prefrontal circuit function (Feinberg, 1982; Feinberg & Campbell, 2010). There is some debate

over the exact ages that define adolescence in mice, but, given the context outlined in this section, it is reasonable to use the period post-weaning (postnatal day P20-21) through the major volumetric changes of these regions (P50-60) as this window includes many of the major developmental milestones that are presumed to occur in adolescence (Ferguson & Gao, 2014).

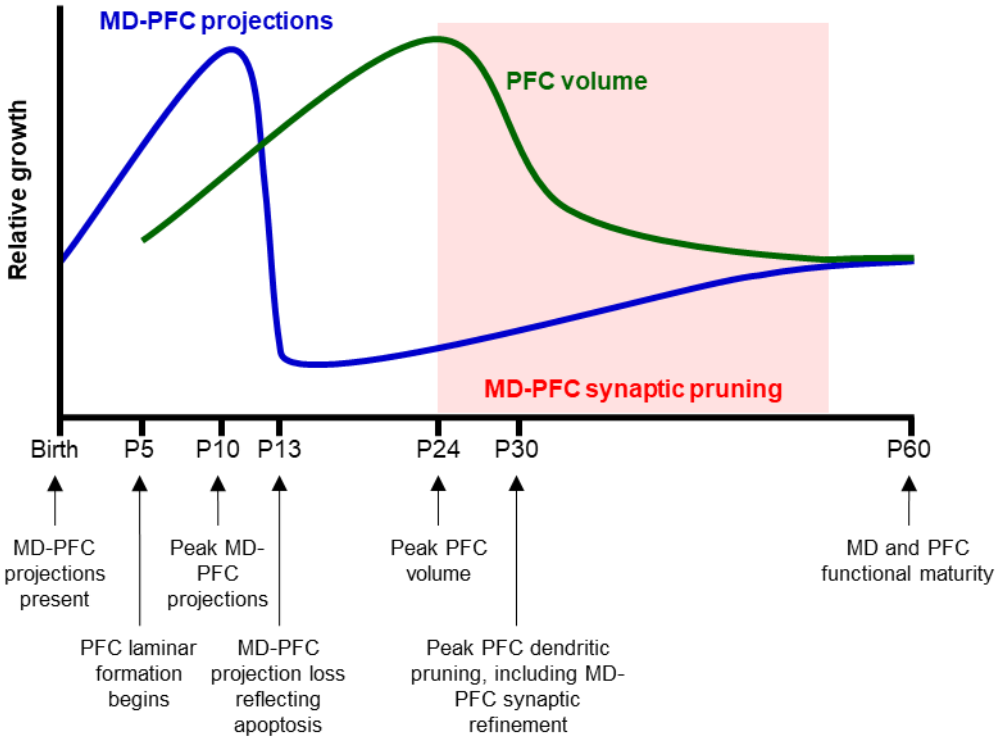

Figure 1.1. Developmental trajectory of MD-PFC projections and PFC volume in mice. In the typical development of the mouse, MD-PFC projections (blue line) have already arrived at birth. They increase in density in early life before a steep period of loss at P13 and a subsequent gradual increase in density that has stabilized by P60. Meanwhile, PFC volume (green line) increases in early life, peaking around P24. Next, there is a period of gradual decrease in PFC volume, in part due to MD-PFC synaptic refinement (red shading), all of which stabilizes by P60. The early presence of MD-PFC projections and the changes in MD-PFC projections preceding and informing PFC volumetric changes indicate that MD-PFC input maturation may influence PFC development. Adapted from (Ferguson & Gao, 2014).

1.7 Sensitive Periods

Given the extensive maturation of the PFC during this period, it has been hypothesized that adolescence may represent a “sensitive period” in the development of the region (Bicks et al., 2020; Canetta et al., 2021; Yamamuro et al., 2020). Sensitive periods denote developmental

time windows when brain circuits are particularly receptive to certain kinds of inputs, sometimes requiring that input for proper development. As such, changes to those inputs during the sensitive period can lead to long-lasting changes in the anatomy and function of the circuit (Hensch, 2004; Takesian & Hensch, 2013b). Frequently, these windows represent periods in which the refinement of brain circuitry and function is particularly susceptible to changes in neuronal activity.

A classic example is in the visual system, where transient developmental monocular deprivation can permanently impair acuity in the deprived eye (Wiesel & Hubel, 1963). This impairment in function persists even after the deprivation in visual input is reversed, as the thalamo-cortical inputs representing the closed eye are permanently disrupted in an activity-dependent manner. In addition to the visual system, sensitive periods have also been identified and characterized in other sensory systems, including somatosensory (Crair & Malenka, 1995; Feldman et al., 1998) and auditory (Caras & Sanes, 2015; de Villers-Sidani et al., 2007) cortices.

While sensitive periods in the circuit refinement of sensory cortices have been well-documented (Caras & Sanes, 2015; de Villers-Sidani et al., 2007; Sun et al., 2019; Wiesel & Hubel, 1963), recent evidence suggests that similar transient changes in activity during postnatal development can have lasting changes in the PFC (Bicks et al., 2020; Bitzenhofer et al., 2021a; Canetta et al., 2021; Larsen & Luna, 2018a). Primarily, these studies have focused on changes to intrinsic components of PFC circuitry, such as interneuron or layer II/III pyramidal neuron activity (Bicks et al., 2020; Bitzenhofer et al., 2021b; Canetta et al., 2021). Interestingly, these studies cover slightly different, but overlapping, periods, which span from P7 to P50. Given the developmental time points outlined above, this large epoch encompasses periods of intense growth and subsequent refinement in the PFC. This opens the possibility that there may

be multiple sensitive periods throughout postnatal development that might influence different aspects of circuit development.

Some have also highlighted several mechanisms found in sensory sensitive periods, including facilitators like BDNF expression (Anomal et al., 2013; Deidda et al., 2015; Hanover et al., 1999; Huang et al., 1999) and NMDA receptor changes (Chen et al., 2000; Erisir & Harris, 2003) and brakes like perineuronal net formation (Balmer et al., 2009; McRae et al., 2007; Nabel & Morishita, 2013; Takesian & Hensch, 2013a) and myelination (Bavelier et al., 2010; McGee et al., 2005; Yang et al., 2012). These facilitators and brakes have also been identified in PFC adolescent development (Baker et al., 2017; Flores-Barrera et al., 2014; Hill et al., 2012; Larsen & Luna, 2018b; Mount & Monje, 2017). These markers also span the early postnatal through late adolescent periods, further supporting the notion that overlapping developmental processes may occur throughout early life. In addition, PV cell activity is important in sensitive period plasticity (Baho & Di Cristo, 2012; Chattopadhyaya et al., 2007; Fu et al., 2012; Wu et al., 2012), and PV cells in the PFC also undergo important periods of maturation during this time (Miyamae et al., 2017b; Yang et al., 2014a).

While thalamic input activity has been shown to be important for sensory cortex maturation, including the visual cortex (Caras & Sanes, 2015; de Villers-Sidani et al., 2007; Takesian & Hensch, 2013b; Wiesel & Hubel, 1963), the role of thalamic input activity to the PFC during this time period remains unexplored. Given the importance of PFC inputs in cognitive functioning and schizophrenia as well as the role of MD inputs in PFC development, a better understanding of the impact of developmental thalamic dysfunction on the PFC will offer crucial insights into the etiology of psychiatric disorders and cognition.

1.8 Conclusions

There is a growing body of literature surrounding the etiology of schizophrenia and the development of cognitive circuits. In this chapter, I have outlined the extensive evidence implicating the PFC and its inputs, such as the MD, in the disorder. I have also outlined the roles of the MD-PFC circuit in cognition. In addition, it is clear that adolescence is a period of vulnerability in the progression of disorders such as schizophrenia and represents a period of intense maturation for the PFC and its associated circuitry. As a result, several groups are now studying the mechanisms at play during adolescence in the PFC. One leading hypothesis is that adolescence represents a sensitive period in PFC development, with recent studies supporting this theory.

However, several open questions remain. First, it is still unclear what role the inputs to the PFC have during this sensitive period. The adolescent development of the MD indicates that it may play an integral role in PFC development, but this has yet to be fully explored. Second, the evidence so far points to a very large window for the sensitive period. Future work will need to explore the mechanisms at play in subsections of the adolescent window. We may find that different aspects of PFC circuitry mature during separate or overlapping periods. Third, there are numerous developmental processes that occur during adolescence in the PFC, including synaptic pruning, interneuron development, etc. Future work should explore which of these processes can be disrupted and the long-term consequences. As noted in the previous point, there may be different processes impacted in different time windows. Fourth, in sensory sensitive periods, one area of research has focused on the possibility of re-opening sensitive periods to reverse the effects of developmental insults (Hensch & Bilimoria, 2012). It remains to be seen whether similar processes may be possible for PFC development. This work would have great implications for treatment of psychiatric disorders.

This thesis delineates work done to address the first of these questions: to better understand the role of thalamo-PFC inputs during adolescence in long-term PFC function and cognition. To address this question, first, a new cognitive behavioral paradigm was developed to test working memory deficits and PFC dysfunction in mice. Second, I established a model to transiently reduce activity in the MD and midline thalamus. This model was then used to compare the long-term effects of adolescent and adult thalamic inhibition on cognitive behavioral performance and PFC cell properties. I found that adolescent, but not adult, thalamic inhibition impaired subsequent PFC functions and behavior, confirming that adolescence is indeed a sensitive period. Next, I explored the effects of adolescent thalamic inhibition on MD-PFC projection cell density and PFC cellular activity during a cognitive flexibility task, finding that both metrics were disrupted by our manipulation, highlighting additional long-term consequences of this adolescent manipulation. Finally, I acutely enhanced thalamic activity to rescue the behavioral and PFC activity impairments caused by the adolescent thalamic inhibition. This finding indicates that, even following a developmental thalamic disruption, cognitive functioning can still be salvaged in the adult.

Altogether, these findings point to the importance of thalamic activity during adolescence in the development of the thalamo-PFC circuit and PFC function. This work also offers hope for potential treatments that could rescue functioning even following developmental disturbances.

Chapter 2: Medial Prefrontal Lesions Impair Performance in an Operant Delayed Non-Match to Sample Working Memory Task*

2.1 Abstract

Cognitive functions, such as working memory, are disrupted in most psychiatric disorders. Many of these processes are believed to depend on the medial prefrontal cortex (mPFC). Traditionally, maze-based behavioral tasks, which have a strong exploratory component, have been used to study the role of the mPFC in working memory in mice. In maze tasks, mice navigate through the environment and require a significant amount of time to complete each trial, thereby limiting the number of trials that can be run per day. Here, we show that an operant-based delayed non-match to sample (DNMS) working memory task, with shorter trial lengths and a smaller exploratory component, is also mPFC-dependent. We created excitotoxic lesions in the mPFC of mice and found impairments in both the acquisition of the task, with no delay, and in the performance with delays introduced. Importantly, we saw no differences in trial length, reward collection, or lever-press latencies, indicating that the difference in performance was not due to a change in motivation or mobility. Using this operant DNMS task will facilitate the analysis of working memory and improve our understanding of the physiology and circuit mechanisms underlying this cognitive process.

*This chapter was published as an article in Behavioral Neuroscience in 2020. **Benoit, L. J.**, Holt, E. S., Teboul, E., Taliaferro, J. P., Kellendonk, C., & Canetta, S. (2020). Medial prefrontal lesions impair performance in an operant delayed nonmatch to sample working memory task. *Behavioral Neuroscience, 134*(3), 187–197. https://doi.org/10.1037/bne0000357. PMID: 32134300

L.J.B., S.E.S., and C.K. designed the experiments. L.J.B. performed the experiments and analyzed the data. E.S.H. and E.T. assisted in the performance of the experiments. L.J.B., S.E.S., and C.K. interpreted the results and wrote the paper.

2.2 Introduction

Cognitive deficits are a hallmark of most, if not all, psychiatric disorders. Cognitive processes, which range from attention and working memory to social cognition and the use of language, can be disrupted in psychotic, stress-related, developmental, and mood disorders (Kolb & Whishaw, 1983; Millan et al., 2012a; Weinberger & Berman, 1996). Importantly, these symptoms are often predictors of long-term functional outcomes (Green et al., 2000). However, most currently available therapeutics target other symptoms of these disorders, leaving the cognitive impairments untouched, or even worse (Hill et al., 2010; Millan, 2006). Given this current therapeutic limitation, it is incumbent upon us to better understand the underlying neurobiology of these cognitive behaviors in order to develop more effective treatments.

Decades of research have identified the prefrontal cortex (PFC), an evolutionarily conserved part of the frontal lobe, as an important center for cognitive function (*Frontal lobe function and dysfunction*, 1991). Several reports demonstrated a striking resemblance between the cognitive deficits observed in patients with frontal lesions and those deficits seen in schizophrenia, suggesting alterations in the PFC may play a role in cognitive symptoms seen in this disorder (Kolb & Whishaw, 1983; Kraepelin et al., 1919). Therefore, the study of the roles that prefrontal circuits play in cognitive functions is essential to furthering our understanding of the pathophysiology of schizophrenia, or any disorder with alterations in PFC circuitry.

In addition to patient-based research, much of our current knowledge of the role of PFC circuitry in behavior is based on animal studies. Using primates and rodents, researchers have manipulated specific brain circuits to determine their role in cognitive behaviors. To assess spatial working memory in rodents, a delayed non-match to sample (DNMS) T-maze task is frequently used (Bolkan et al., 2017; Kellendonk et al., 2006; Parnaudeau et al., 2018; Parnaudeau et al., 2013). In this task, the animal is trained to run from the start arm of a T-

shaped enclosure to the available open arm during the initial sample phase, where it receives a reward. The animal then returns to the start arm, where it is held for a variable delay period. In the subsequent choice phase, both arms of the maze are opened, and the animal must go to the opposite arm (“non-match”) from the one that was presented during the sample phase in order to receive a reward. Longer delays increase task difficulty and are accompanied by a decrease in performance.

Previous work in rodents has shown that this DNMS T-maze task is dependent on the medial PFC (mPFC) both during the acquisition of the task, when there is a short delay, and upon introduction of longer delays, which increasingly tax working memory (Aultman & Moghaddam, 2001; Bolkan et al., 2017; Granon et al., 1994; Kellendonk et al., 2006). During the introduction of longer delays, the inputs to the mPFC that contribute to different phases of this task have been further explored. Input from the mediodorsal nucleus of the thalamus (MD), a higher order thalamic nucleus has been shown to be important during the delay (maintenance) phase, while input from the ventral hippocampus (vHip) is critical for the sample (encoding) phase (Bolkan et al., 2017; Spellman et al., 2015). In addition, activity in mPFC-to-MD projections is necessary during the choice (selection) phase (Bolkan et al., 2017; Parnaudeau et al., 2018).

These studies have provided important insight into the circuits involved in different aspects of spatial working memory. However, in the T-maze only a limited number of trials can be completed on a given day due to the long trial lengths. For example, in our hands the initial sample phase lasts 17 seconds on average, with individual delay lengths lasting up to 120 seconds. This long trial length, combined with the distances needed to travel to obtain each reward, limits the number of trials that can be completed in a given day. As a result, it is harder to detect small effect sizes when two different experimental manipulations are compared.

Moreover, a reduced number of trials per day also limits the number of conditions or manipulations that can be introduced on a given day (e.g. testing multiple delay lengths in the same day). Finally, the ability to have more trials per day facilitates the analysis of *in vivo* physiological data collected during task performance. In addition to long trial lengths, the T-maze also has a strong explorative spatial component, with the animal navigating through long maze arms while encoding and subsequently retrieving a memory. With shorter time scales in a smaller, enclosed operant box, the working memory tested is less dependent on interference from navigating through the arms.

As an alternative to this traditional DNMS T-maze task, several operant versions have been developed, which are inherently less exploratory, allow many more trials per day to be conducted, and facilitate the simultaneous collection of data from a large number of animals. One version, developed by Rossi et al., allows the mice to select one of two levers during the initial sample phase (Rossi et al., 2012). The levers are then removed, and subsequently reinserted after a given delay; the mouse must choose the lever it did not pick in the sample phase in order to correctly earn a reward in the choice phase. While performance in this task deteriorated in a delay-dependent manner and was impaired by mPFC lesion, there are several strategies the animal can develop to solve the task that avoid using working memory. For example, after selecting the initial sample lever, the mouse can immediately wait in front of the opposite lever until it appears, effectively overriding the need to utilize working memory during the delay time. To circumvent this limitation, an alternative task has been developed in which mice press an initial sample lever to initiate a delay phase, but then must make an entry to a noseport on the opposite wall at the end of the delay phase in order to trigger the presentation of both levers during the choice phase. However, while versions of this task have been shown to be dependent on the dorsomedial striatum (Akhlaghpour et al., 2016) and hippocampus (Goto & Ito, 2017), it is imperative to know whether it is also dependent on the mPFC.

In this study, we implemented an operant-based DNMS task, similar to that used by Akhlaghpour et al (Akhlaghpour et al., 2016) and Goto et al (Goto & Ito, 2017), in which mice performed as many as 160 trials per day, to establish its dependence on the mPFC. We found that mPFC lesions impaired both the acquisition of the task, which was done in the absence of a delay, and task performance after introduction of different delays. We further showed that trial length, reward collection, and lever-press latencies were unchanged by the lesion, indicating that an underlying decrease in motivation was not responsible for the impaired task performance in mPFC lesioned animals. Thus, the DNMS operant-based task will serve as a useful complement to the DNMS T-maze task, facilitating the study of prefrontal circuitry and physiology in working memory.

2.3 Results

The goal of this study was to investigate the role of the mPFC in an operant-based DNMS working memory task. To address this question, we created an excitotoxic lesion of the structure using an injection of ibotenic acid, or conducted a sham surgery using an injection of phosphate buffered saline (PBS), before training the mice in the DNMS working memory task (Figure 2.1a).

2.3.1 Confirmation of the lesion location.

Post-hoc histology showed that the lesioned region typically encompassed both the prelimbic and infralimbic portions of the mPFC. In some animals, the lesion also spread to anterior portions of the cingulate cortex (Cg1 and Cg2). No spread was seen to any of the motor or sensory cortices. The lesioned regions showed a number of distinct characteristics including 1) a loss of cell density, 2) an accumulation of non-cellular Nissl clumps, and 3) a contraction of the lesioned region, which were used to define the lesion boundaries (Figure 2.1 b, c, d).

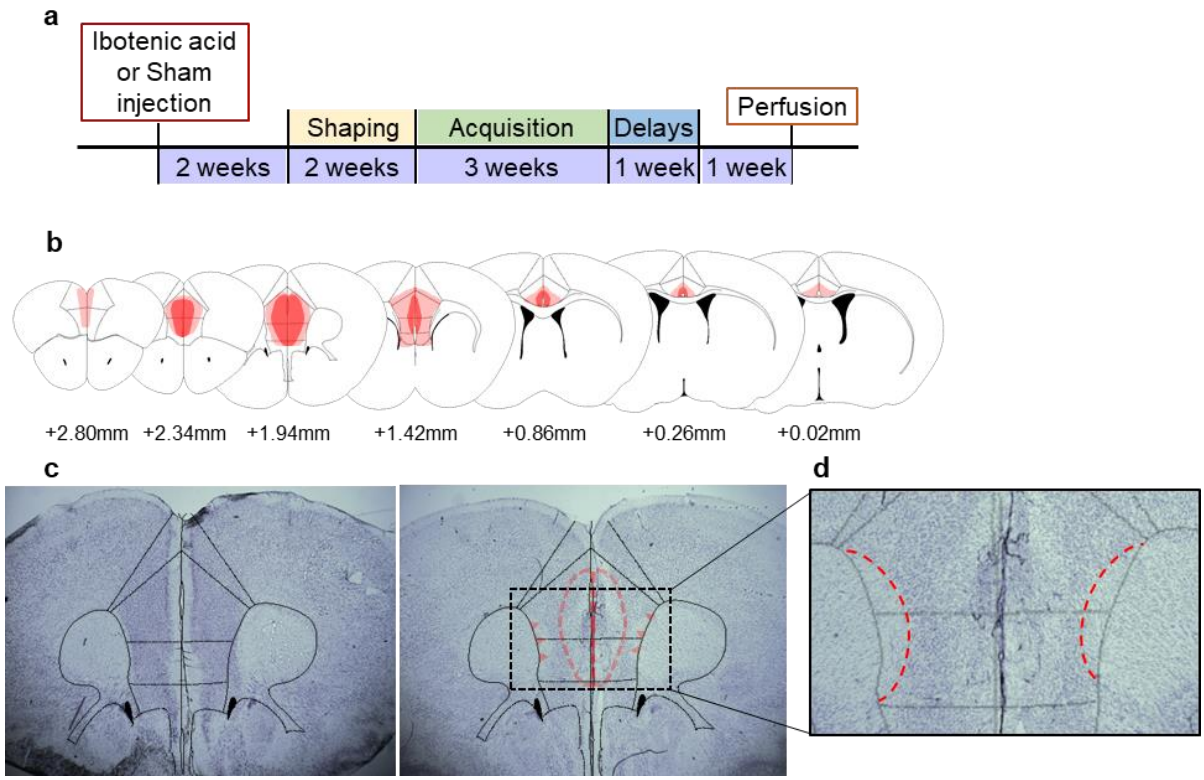

Figure 2.1. Experimental Timeline and Extent of Lesion. a) Timeline of experimental procedures. b) Schematic representation of the maximal (light) and minimal (dark) extent of damage caused by the mPFC ibotenic acid injection in coronal slices. c) Example Nissl staining from a sham (left) and lesion (right) coronal slice. Dashed lines outline area with lower cell density and accumulation of Nissl found with dead tissue. Arrowheads indicate the shift of the white matter tract as a result of contraction of the medial regions. d) Higher magnification of example lesion coronal slice from c. Solid outlines show control region borders from the Paxinos and Watson Mouse Brain Atlas. Dashed lines outline the shifted border of the white matter tract.

2.3.2 Acquisition performance is impaired by the mPFC lesion.

Following a post-surgical recovery period, the mice began the first stages of training, which involved shaping in operant boxes with a reward milk dipper, levers, and noseport (Figure 2.2a), as described in the Methods section. The shaping was learned similarly across the two groups. To learn the lever press, the sham group took 1.438 ± 1.031 days, and the lesion group took 1.412 ± 0.795 days. An unpaired t-test showed that the groups were not significantly different from one another (p=0.9363). Similarly, to learn to poke the noseport, the sham group took 1.688 ± 0.793 days, and the lesion group took 1.706 ± 0.686 days, with an unpaired t-test

showing no significant difference between the groups (p=0.9436). The mice then learned the DNMS task with a 0-second delay; this period represents the acquisition stage of the task (Figure 2.2b). Mice with an mPFC lesion were significantly slower to acquire the task, requiring more days of training to reach a criterion level of performance (Figure 2.2c, d). While all animals began with a chance level of 50% performance, sham mice were able to learn the task more quickly. A two-way repeated measures ANOVA showed a significant main effect of lesion over time (p=0.0234) and a significant time x lesion interaction (p=0.0108). Bonferroni post-hoc analysis found the sham group performance to be significantly higher than the lesion group performance during training days 7 and 8 (day 7: p=0.0067; day 8: p=0.0191). While the sham mice were able to reach a criterion of 3 consecutive days above 80% performance in 8.56±2.58 days (mean ± standard deviation (SD)), the lesion mice took 12.24±4.12 days to reach the same level of performance.

Given this deficit in performance, we wanted to know whether other aspects of the behavior were affected. We found no difference between the groups for any other parameters measured. Total time to complete each trial did not change with training and was not different between groups (Figure 2.2e, f). Similarly, the latency between pressing the sample and choice levers were also the same across both groups (Figure 2.2g). This indicated that there was no gross motor impairment in the lesioned animals and suggested that the performance deficit of the lesioned group was not the result of a longer ‘experienced delay time’ in the task. There was also no change in the latency between the choice lever selection and reward retrieval (Figure 2.2h), nor was there a difference in the percentage of rewards retrieved, with both groups retrieving over 99% of offered rewards (Figure 2.2i). These similarities indicate that the difference in behavior is likely not a result in a change in motivation to earn the milk reward. Finally, the percentage of aborted trials (recorded when the animal failed to make the second noseport entry in the 5-second time limit) was below 5% for both groups, with no animal

aborting more than 12% of trials (Figure 2.2j), indicating that the animals in both groups had similar numbers of trials on each day in which to learn the task. Together, these data indicate that both the sham and lesion groups experienced the task similarly during the acquisition stage. However, the lesion group still took longer to acquire the task.

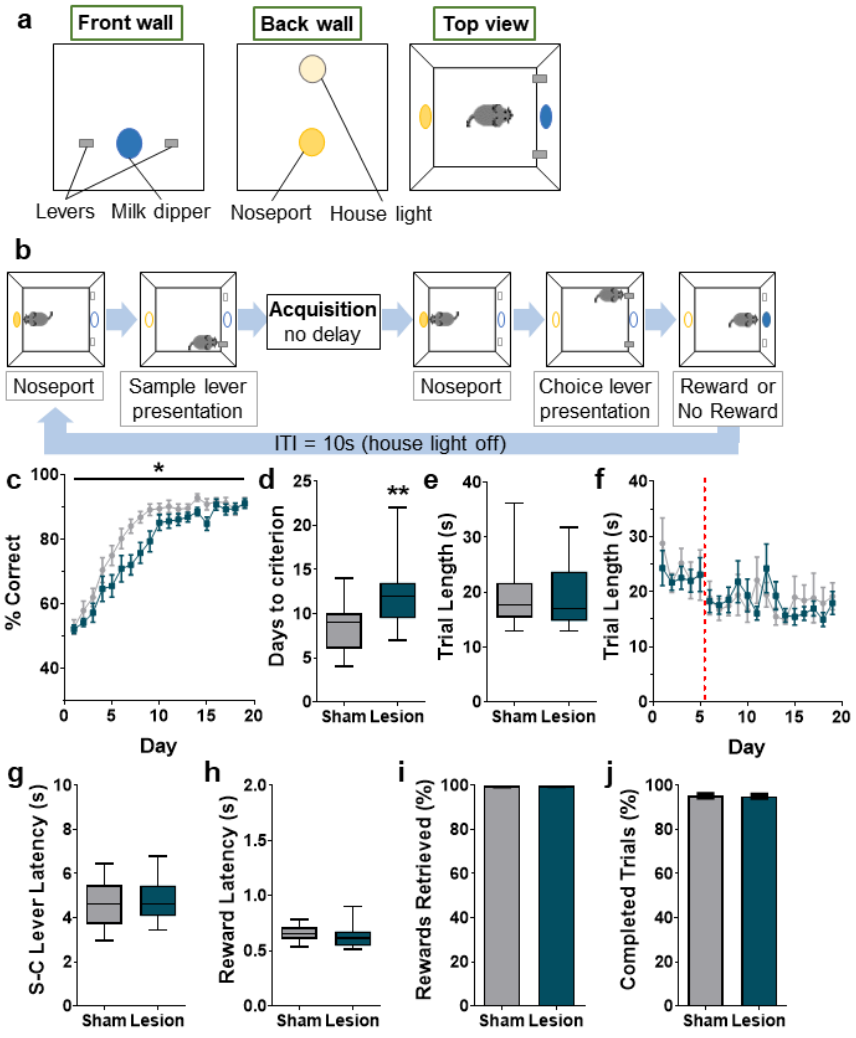

Figure 2.2. Acquisition of an operant DNMS task is impaired by an mPFC lesion. a) Layout of the operant box. Left: Front wall, containing a milk dipper and two levers, one on either side of the dipper. Center: Back wall, containing a noseport and a 1.0-amp house light. Right: Top view of the operant box. The milk dipper and levers on the front wall are represented on the right side of the image, and the noseport on the back wall is represented on the left side of the image. b) Schematic illustration of the trial sequence for the acquisition of the task, including a 0-second delay. c) Performance of sham (light) and lesion (dark) groups over the 19 days of acquisition indicated as the percentage of correct trials on each day (n=16 sham mice, 17 lesion mice; two-way repeated-measures ANOVA (rmANOVA), main effect of lesion, F (1,31)=5.687,

*p = 0.0234; time x lesion interaction, F (18,558)=1.951, *p = 0.0108). d) Number of days to reach the criterion of 3 consecutive days with a performance above 80% correct (two-tailed unpaired t-test, sham vs. lesion, t=3.048, df=31, **p = 0.0047). e) Mean length of each trial throughout acquisition (two-tailed unpaired t-test, t=0.1582, df=31, p=0.8753). f) Length of each trial for each day of acquisition. Dashed line represents the introduction on Day 6 of the imposed time limit for the second noseport entry. In the first five days of acquisition, there was unlimited time for the second noseport entry (two-way rmANOVA, main effect of time, F (4,110)=0.9300, p=0.4494; main effect of lesion, F (1,31)=0.2091, p=0.6507; time x lesion interaction, F (4,110)=0.3293, p=0.8578). Starting with Day 6, there was a 5-second time limit imposed on the second noseport entry (two-way rmANOVA, main effect of time, F (13,403)=1.240, p=0.2479; main effect of lesion, F (1,31)=0.004387, p=0.9476; time x lesion interaction, F (13,403)=1.064, p=0.3888). g) Latency between sample lever press (S) and choice lever press (C) throughout acquisition (two-tailed unpaired t-test, t=0.7222, df=31, p=0.4756). h) Latency between choice lever press and reward retrieval throughout acquisition (two-tailed unpaired t-test, t=0.7522, df=31, p=0.4576). i) Percentage of rewards awarded that were retrieved (two-tailed unpaired t-test, t=0.6377, df=31, p=0.5283). j) Percentage of trials that were completed, not aborted (two-tailed unpaired t-test, t=0.1954, df=31, p=0.8464).

2.3.3 Delay performance is impaired by the mPFC lesion.

When every animal had reached the acquisition criterion, the delay testing began. Delays (2, 4, 8, or 16 seconds) were introduced between the sample and choice lever presentations (Figure 2.3a). Each delay condition was randomly interspersed within a given day, and the testing was repeated over several days. The performance was summed across the last four days of testing for the data presented in Figure 2.3. The baseline level of performance with a 0-second delay, taken as the average performance across the last 3 days of acquisition, was not significantly different between the groups (mean ± SD, sham: 90.65±5.93%, lesion: 89.90±5.74%). However, the performance with delays was impaired for the lesion group compared with the sham group (Figure 2.3b). A two-way repeated measures ANOVA showed a significant main effect of the lesion across delays (p=0.0075) and a significant delay x lesion interaction (p=0.0014). This impairment was driven by the differences in performance in the 2- and 4-second delay conditions, where sham mice performed above or close to criterion level (2s: 83.27±7.84%; 4s: 77.41±6.31%), but lesion animals performed worse (2s: 74.84±9.38%; 4s: 65.01±11.35%). Bonferroni post-hoc analysis for each delay condition showed a significant

difference between the groups at those two delays (p-values: 2s: 0.0209, 4s: 0.0002), and a trend-level difference between the groups' performances at the 8-second delay condition (p=0.0919, sham: 69.25±10.36%, lesion: 62.34±9.91%), but no effect at the 16-second delay condition (p>0.9999, sham: 59.85±7.41%, lesion: 56.64±6.58%) where the performance for both groups was close to chance (50%).

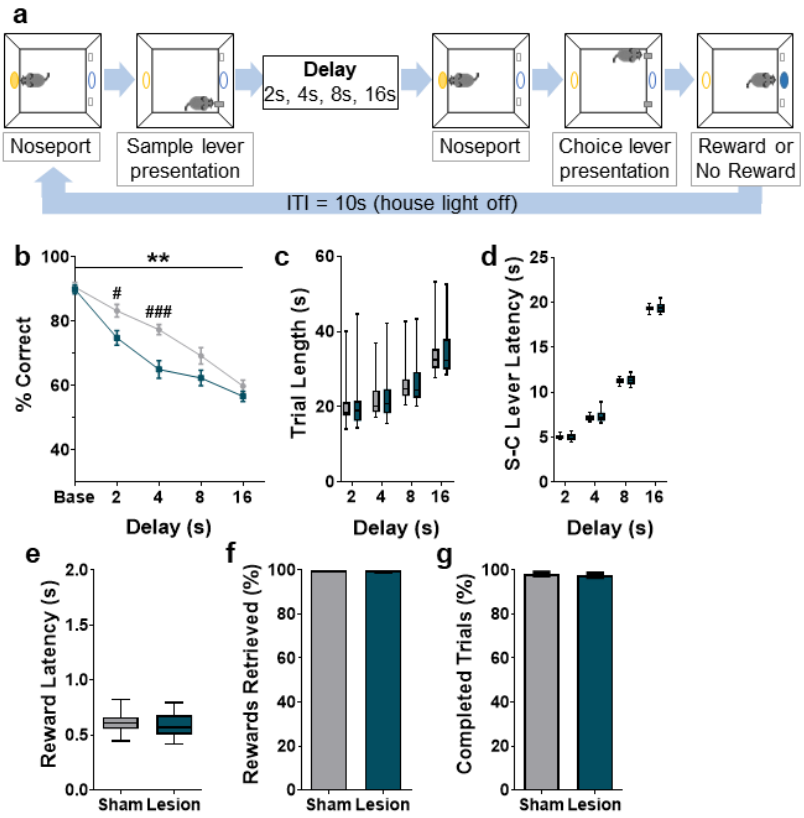

Figure 2.3. Delay performance of an operant DNMS task is impaired by an mPFC lesion. a) Schematic illustration of the trial sequence for the task, including randomly interleaved 2-, 4-, 8-, and 16-second delays. b) Performance of sham (light) and lesion (dark) groups indicated as the percentage of correct trials for each of the four delay lengths as well as baseline ('Base': mean performance from the last 3 days of acquisition; n=16 sham mice, 17 lesion mice; two-way rmANOVA, main effect of lesion, $F(1,31)=8.179$, **p = 0.0075; delay x lesion interaction, $F(4,124)=4.729$, **p = 0.0014; Bonferroni post-hoc corrected p-values: 2-s $t=2.907$, $df=155$, #p=0.0209; 4-s $t=4.279$, $df=155$, ###p=0.0002). c) Mean length of each trial for each delay length (two-way rmANOVA, main effect of lesion, $F(1,31)=0.1205$, p=0.7308; delay x lesion interaction, $F(3,93)=0.05374$, p=0.9835). d) Latency between sample lever press (S) and choice lever press (C) for each delay length (two-way rmANOVA, main effect of lesion, $F(1,31)=0.5730$, p=0.4548; delay x lesion interaction, $F(3,93)=1.485$, p=0.2238). e) Latency between choice lever press and reward retrieval throughout delays (two-tailed unpaired t-test,

t=0.3436, df=32 p=0.7334). f) Percentage of rewards awarded that were retrieved (two-tailed unpaired t-test, t=0.6530, df=31, p=0.5186). g) Percentage of trials that were completed, not aborted (two-tailed unpaired t-test, t=0.6034, df=31, p=0.5507).

As with the acquisition stage, we also measured other parameters to assess whether the difference in performance might be accounted for by differences in behavior other than working memory. As before, trial length and the latency between sample and choice lever presses for each delay condition were the same between groups (Figure 2.3c, d). Similarly, the latency to collect the reward and the percentage of rewards retrieved were similar between groups (Figure 2.3e, f), as were the percentage of completed trials (Figure 2.3g). Cumulatively, these findings suggest that mPFC lesioned mice show an impairment in performance of a DNMS working memory task, that is not due to motor or motivational impairments.

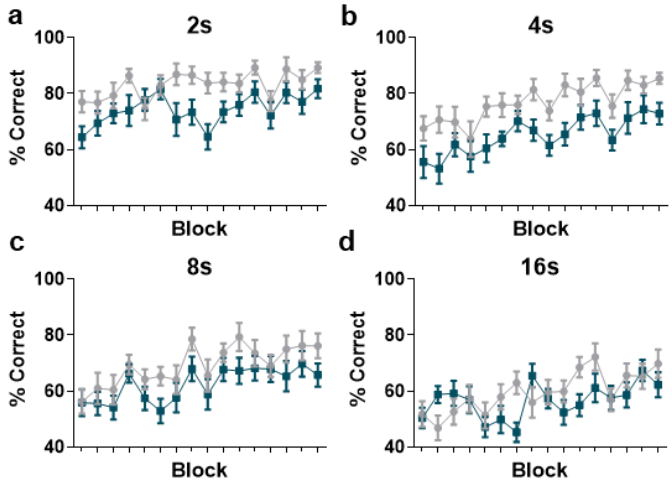

Figure 2.4. Delay performance is impaired by an mPFC lesion, but learning, over 10-trial blocks, is unaffected. Performance for sham (light) and lesion (dark) groups over blocks of 10 trials for each delay length: a) 2-second delay (two-way rmANOVA, main effect of time, F (15,465)=3.328, ****p<0.0001; main effect of lesion, F (1,31)=8.262, **p = 0.0073; time x lesion interaction, F (15,465)=1.271, p = 0.2162); b) 4-second delay (two-way rmANOVA, main effect of time, F (15,465)=5.788, ****p<0.0001; main effect of lesion, F (1,31)=13.77, ***p = 0.0008; time x lesion interaction, F (15,465)=0.4330, p = 0.9692); c) 8-second delay (two-way rmANOVA, main effect of time, F (15,465)=5.183, ****p<0.0001; main effect of lesion, F (1,31)=3.75, p = 0.0605; time x lesion interaction, F (15,465)=0.4050, p = 0.9777); d) 16-second delay (two-way rmANOVA, main effect of time, F (15,465)=3.509, ****p<0.0001; main effect of lesion, F (1,31)=1.570, p = 0.2195; time x lesion interaction, F (15,465)=1.982, *p = 0.0151).

With the complicated structure of the task during this stage (i.e., having all four delay lengths randomly interleaved within one day), there was an improvement in performance for both the sham and lesion groups over time. Therefore, the difference in total performance observed between the two groups might have multiple explanations. It could be due to: 1) a difference in learning to cope with the newly introduced, variable delays, or 2) a difference in memory maintenance. To distinguish between these two possibilities, we evaluated the learning from day to day and within a day by analyzing performance in 10-trial blocks for each delay (Figure 2.4). At all delay lengths, a two-way repeated measures ANOVA showed a significant main effect of time ($p<0.0001$ for all delays), indicating learning. In addition, there was a significant main effect of lesion at 2s and 4s, as was seen with the pooled data analysis (p-values: 2s: 0.0073, 4s: 0.0008) and a trend-level effect at 8s ($p=0.0605$), but no effect at 16s ($p=0.2214$). Crucially, there was no time x lesion interaction at the delays that revealed a difference between the groups (p-values: 2s: 0.2162, 4s: 9692, 8s: 9777). This analysis indicates that while there is an impairment in the performance of the lesion animals during the delays, this difference cannot be attributed to a difference in learning during the delay condition, but rather is explained by a difference in memory.

Both the acquisition and delay stages of this task demonstrated an impairment due to the mPFC lesion; however, the acquisition stage clearly represents a difference in learning whereas the delay stage appears to denote a difference in memory or task execution. While we were interested to discover how the performance in these two stages was differentially affected, we also wanted to know how they might be related. To that end, we analyzed each animal's performance during both stages using a linear regression analysis of the total performance at each delay versus the acquisition, as measured by the number of days to reach the criterion (Figure 2.5). This analysis revealed a significant though weak correlation between days to criterion and performance for each of the delays (2s: $R^2=0.2850$, $p=0.0014$; 4s: $R^2=0.3783$,

p=0.0001; 8s: R^2=0.2201, p=0.0059; 16s: R^2=0.2943, p=0.0011). The correlation between days to criterion and delay performance demonstrates that the two stages are related. The R^2 values indicate that 22-37% of the variance in the delay performance can be explained by the days to criterion. Thus, the deficit in learning does not fully account for the difference in delay performance.

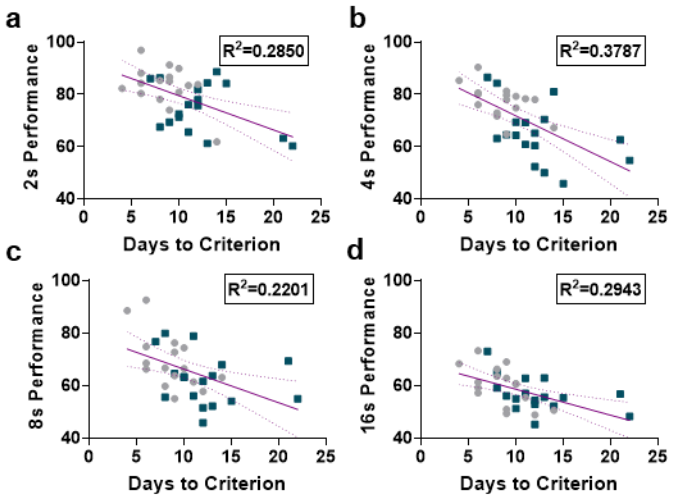

Figure 2.5. Correlations between acquisition and performance at each delay show a linear relationship. Each animal's delay performance, at each of the 4 delays, versus that animal's acquisition performance, measured in days to criterion. At each delay, a linear regression was evaluated across all animals (sham light, lesion dark). All 4 delays demonstrated significant, weak linear relationships with the days to criterion (solid line with 95% confidence intervals in dashed lines). a) At 2-second delay, R^2=0.2850, **p=0.0014; b) at 4-second delay, R^2=0.3787, ****p=0.0001; c) at 8-second delay, R^2=0.2201, **p=0.0059; d) at 16-second delay, R^2=0.2943, **p=0.0011.

2.4 Discussion

2.4.1 The mPFC is required for acquisition and delay performance of an operant-based DNMS working memory task.

In rodents, working memory describes the ability to hold information online for short periods of time and then use it to accomplish a goal. Working memory can be assessed in a variety of different tasks where a delay separates the acquisition of information from the period

in which the information must be used for the correct performance of the task. In this study, we used mice to investigate the role of the mPFC in an operant-based DNMS working memory task similar to one previously shown to be dependent on the striatum (Akhlaghpour et al., 2016) and the hippocampus (Goto & Ito, 2017). Although the mPFC, a structure that has been implicated in many cognitive functions and psychiatric disorders, has previously been shown to be required for other working memory tasks, we wished to validate this structure's importance for the current operant-based task, which offers several advantages including a smaller exploratory component and a higher daily throughput. To that end, we explored the impact of an mPFC lesion on both learning and delay performance in the current operant working memory task in mice.

Our data demonstrate that lesioning the mPFC impaired both acquisition and delay performance in this operant task. During the acquisition of the task, where the trials contained a short (0s) delay between the sample and choice phases, all animals began at a chance level of performance (50% correct). As they continued to train in the task, the lesioned animals were slower to perform the task correctly than the sham animals. All mice eventually learned the task, reaching the criterion of 3 consecutive days above 80% correct performance; however, the lesioned animals took more days to reach this criterion. After all animals reached a similar high level of performance, delays were introduced. As expected, both sham and lesioned animals showed delay-dependent effects on performance, with accuracy dropping as the delay time increased. Additionally, lesioned animals showed impaired performance with the delays relative to sham animals that was most evident for the shorter delays of 2 and 4 seconds, when the sham animals continued to perform at a relatively high level. For the longer delays of 8 and 16 seconds, the sham animals performed very close to chance, likely making it difficult to see any additional deficit in the performance of the lesioned mice.

Other parameters of the task, such as the time taken to complete each trial or the percentage of total rewards collected, which might have reflected a change in mobility or motivation, were unaffected. This result indicates that the deficit in acquisition and delay task performance in the mPFC lesioned mice is not due to them experiencing longer effective delays or being less motivated to earn rewards. Moreover, as learning rates during the delay condition are comparable in lesioned versus non-lesioned mice a deficit in learning cannot explain the deficit observed under the delay condition. This interpretation is supported by the relatively weak correlation in the performances of individual animals during both stages. Thus, the deficit observed in the delay stage can at least partly be explained by a deficit in memory.

2.4.2 There are also costs associated with the DNMS operant task.

This operant DNMS task offers several advantages highlighted throughout this paper, such as shorter trial lengths and a smaller exploratory component. However, there is an associated cost of prolonged training. In the T-maze DNMS task, animals acquire the task within a week whereas in the operant task DNMS task, it took the animals three weeks. In addition, maze tasks heavily depend on locomotor exploration which is a more ethologically relevant behavior for a mouse than lever pressing. Performing the T-maze task, which requires spatial exploration of goal arms likely engages different, but also overlapping, neuronal circuitry than performing the operant task. In this context, it will be interesting to determine whether sample encoding is also dependent on the ventral hippocampal input to the mPFC in the operant DNMS task as it has been observed for the T-maze task (Abbas et al., 2018; Bolkan et al., 2017; Spellman et al., 2015).

2.4.3 Similar findings have been documented in other working memory tasks.

Previous work has demonstrated the importance of the mPFC in maze-based spatial working memory tasks in rodents. These studies showed that a lesion of the mPFC in either

mice or rats impairs the acquisition of a DNMS T-maze task (Granon et al., 1994; Kellendonk et al., 2006), and that acute optogenetic silencing of projections to and from the mouse mPFC impairs performance of the task after delays are introduced (Bolkan et al., 2017). Similarly, delay performance in this task is impaired by an mPFC lesion in rats (Aultman & Moghaddam, 2001). Furthermore, studies disrupting the rat mPFC showed that this region is also important in several other more complicated maze-based working memory tasks, including a figure-eight maze (Yoon et al., 2008) and a radial arm maze (Seamans et al., 1995). These results, combined with those of the current study, demonstrate that the mPFC is an essential structure for the acquisition and performance of various working memory tasks with a non-match-to-sample structure.

Several studies also explored the role of the mPFC in maze-based working memory tasks that instead require delayed alternation. In the delayed alternation T-maze task, the animal starts by selecting one of two arms to visit. In all subsequent trials, the animal must choose the opposite arm from the one previously visited in order to receive a reward. While this task does require working memory, the alternation from trial to trial allows for an alternating strategy that would not work in the DNMS task, where for each trial the sample arm is newly chosen. Despite this difference, Larsen and Divac showed that performance in a delayed alternation T-maze task was impaired following a prefrontal lesion in rats, similar to what has been seen in DNMS T-maze tasks (Larsen & Divac, 1978). Therefore, it appears the mPFC is essential for both DNMS as well as delayed alternation based T-maze working memory tasks.

Other investigators have studied the role of the mPFC in an operant version of a delayed alternation task, finding that an mPFC lesion impairs performance (Dunnett et al., 1999; Rossi et al., 2012). For instance, in Rossi et al, an mPFC lesion in mice impaired both acquisition and delay performance, similar to our findings (Rossi et al., 2012). Of note, their operant task

differed from the delayed alternation T-maze task of Larsen & Divac in several important ways. First, it was less dependent on information collected during exploratory behavior in the arms. Second, the operant sample phase allowed the animal to select a new sample each trial, while the delayed alternation T-maze task described above had one sample to start the entire set of trials, requiring that the animal alternate from arm to arm on each subsequent trial. However, similar to the delayed alternation task described above, the animal could adopt a non-working memory based strategy to solve the task. In this case, after selecting the initial sample lever, the animal could immediately wait in front of the opposite lever until it appeared, effectively overriding the need to utilize working memory during the delay time. Nevertheless, in this task, Rossi et al found that lesioning the mPFC of mice did impair performance. Additionally, in this paradigm, the animal had a fixed amount of time to perform as many trials as possible, and animals with an mPFC lesion performed significantly more trials and made significantly more lever presses. At one level, this contrasts with our findings, as we saw no effect of the mPFC lesion on the time to complete each trial or in the latencies between different actions within a trial. However, given that in the Rossi et al task, the animals could complete as many trials as possible in ninety minutes, the lesioned animals may have been able to attempt more trials than controls because their higher error rate resulted in less time spent consuming rewards. We would not be able to detect this in our experiment given that our daily sessions were based on a fixed number of trials rather than a fixed amount of time.

Altogether, this rich literature suggests that the mPFC is required for working memory as assayed in a variety of different T-maze and operant-based tasks. Our results support this notion by demonstrating the necessity of the region for this operant-based version of the DNMS paradigm.

2.4.4 The mPFC is not necessary for all operant-based cognitive tasks.

While many DNMS tasks, including the one presented in this study, are dependent on the mPFC, this is not necessarily the case for all operant-based tasks where information needs to be maintained over a sustained period of time. For instance, in a different operant-based task where animals need to press the opposite lever from that indicated by a visual cue following a delay, Kahn et al found no effect of a mPFC lesion (Kahn et al., 2012). This apparent conflict with our findings may be explained by several differences between the tasks.

First, in the task presented here, we introduced all delay lengths within a single day, a more complicated trial structure that required an adjustment period, whereas Kahn et al tested one delay length over three days before switching to the next delay length. Our data do not indicate that the impairment we see is due to a difference in learning during the delay stage; however, it is possible that the DNMS task is simply more difficult than the Kahn et al task and therefore requires the mPFC while the easier task did not.

Second, as with the task described in Rossi et al., in the task described in Kahn et al, the animal could adopt the alternate strategy of waiting in front of the correct lever immediately following the presentation of the light cue, negating the need to use any working memory. Given that the animals in Kahn et al were heavily trained on the task, having completed 6 weeks of training followed by a 3 week-long sustained attention test before beginning the delayed version of the task, it is possible that they adopted this more efficient strategy by the time the working memory test began.

Third, the difference between our results may arise because the cued information is passively given in the Kahn et al task, where our task requires the animal to move to press the cued lever. Several studies have shown that locomotion can enhance neural activity and learning in response to visual stimuli, indicating that the involvement of movement in the sample

encoding phase of our task may lead to a difference in the cognitive processing of this phase of the trial (Dadarlat & Stryker, 2017; Kaneko et al., 2017; Pakan et al., 2018; Stryker, 2014). Thus, differences in the trial structure between the Kahn et al task and the one presented in this study may be quite substantial on a neural and circuit level, explaining the differences in mPFC dependence.

2.4.5 The mPFC is part of a larger network supporting working memory performance in this task.

Previous studies have used *in vivo* electrophysiology to investigate the roles and relationships of the hippocampus, MD, and mPFC during the different task phases of the DNMS T-maze paradigm (Abbas et al., 2018; Bolkan et al., 2017; Parnaudeau et al., 2013; Spellman et al., 2015). This approach has led to critical new insights into the properties of these circuits, including the directionality of essential projections during different task phases (e.g., vHip-to-mPFC during the encoding phase, MD-to-mPFC during the maintenance phase, and mPFC-to-MD during the choice phase) and the differential roles of specific cell types involved (e.g., parvalbumin vs. somatostatin interneurons). In addition to the mPFC, the DNMS operant task used in this paper has previously been shown to rely on the dorsomedial striatum (Akhlaghpour et al., 2016) and the hippocampus (Goto & Ito, 2017; Goto et al., 2010). With all of the parallels between the T-maze and the operant-based DNMS tasks, we might expect the MD, which is crucial for the maintenance and choice phases of the T-maze, to play a similar role in this operant task.

Given the multi-region network that appears to be involved, an electrophysiological approach similar to what has been done with the T-maze might be used down the line to explore the communication between regions during the DNMS operant task. Some studies already have started to ask these questions in similar tasks (Hyman et al., 2010), but the exact circuitry

involved is still unknown. Furthermore, given the importance of mPFC in task acquisition, physiological recordings should also be done during this period. These studies would allow us to better understand the circuit connectivity involved in the encoding, maintenance, and selection of the correct lever. They might include: 1) *in vivo* electrophysiology to measure local field potentials in the mPFC, hippocampus, dorsomedial striatum, and MD to explore any directionality in coherence of oscillatory activity between the regions during the task; 2) acute optogenetic silencing or activation of specific interneuron populations in the mPFC to elucidate their differential roles; or 3) acute manipulation of projections between the mPFC and the MD, hippocampus, or dorsomedial striatum to understand the specific elements of circuit connectivity required for the task.

In sum, this study demonstrates the importance of the mPFC in an operant-based working memory task. This operant task has several advantages over T-maze DNMS tasks. First, the short task phase allows a large number of trials to be assessed each day, enabling multiple different conditions and manipulations to be introduced on a given day. Additionally, this short task phase allows for temporally precise manipulations and interpretations of task-related neural activity when combined with *in vivo* recordings and imaging studies. In addition, the automated nature of the task allows for multiple animals to run simultaneously in an experimenter-independent environment. With this task, future experiments will be able to delve deeper into questions regarding the neural circuitry and communication contributing to this type of cognitive, prefrontal-dependent behavior.

2.5 Methods

Animals. All experiments were carried out on male C57/Bl6 mice purchased from Jackson Laboratory (Stock #000664). Mice were aged 8 weeks at the start of experiments and housed under a 12-h light-dark cycle in a temperature-controlled environment with food and

water available ad libitum. Mice were group housed with littermates (5 mice/cage). During behavioral training and testing, mice were food-restricted and maintained at 85% of their initial weight. All procedures were done in accordance with guidelines derived from and approved by the Institutional Animal Care and Use Committees at Columbia University and the New York State Psychiatric Institute.

Surgical procedures. Mice were anesthetized with ketamine (10mg/ml) and xylazine (1mg/ml) and head-fixed in a stereotactic apparatus (Kopf). Mice were injected bilaterally into the mPFC with either ibotenic acid (Sigma-Aldrich, I2765), dissolved in ddH_2O at 10 mg/ml, or phosphate buffered saline (PBS), at a volume of 0.25 µl (0.1 µl/min). The ibotenic acid was stored at -20°C, and just prior to the injection was re-dissolved at 37°C. The mPFC coordinates used were: +1.8 AP, ±0.35 ML, -2.5 DV (skull at bregma).

Behavioral apparatus. Eight identical operant-conditioning chambers (ENV-307A; Med Associates, Georgia, VT) were used. The chamber measured 15.24 cm long x 13.34 cm wide x 12.7 cm high. Each chamber was housed in a sound-attenuated box and equipped with two retractable levers (ENV-312-3M) on the front wall (the 13.34 cm side), with one milk dipper between them (ENV-302RM-S, Figure 2.2a). The back wall contained one noseport (ENV-313M) directly opposite to the milk dipper. A 1.0-A house light was positioned directly above the noseport. A computer (COM-106-NV, Intel i5-7400) controlled and recorded all experimental events and responses via an interface (MED-SYST-16e-V). Med-PC V programs were used to administer and record all behavioral tasks.

Behavioral procedures. Two weeks following the ibotenic acid injection, mice were gradually food restricted to 85% of their body weight. Mice were then shaped to the different parts of the operant task. First, the mice were given 2 days of dipper training, during which the mice were presented with the dipper containing 1 drop of evaporated milk (0.01 ml). Each day,

the animals were given the opportunity to obtain 20 rewards in a maximum of 30 min with a random inter-trial interval (ITI), averaging 5 seconds. For the next 3 days, the animals were trained to associate a lever press with a milk reward. Each day, the mice were given a maximum of 60 minutes with each retractable lever, baited with High-Calorie Nutritional Gel (Tomlyn), to receive a maximum of 60 rewarded lever presses on each side. Every second trial, a 10-second ITI was introduced. Next, the mice were given one day during which each lever was presented 30 times in a pseudo-random order to receive a maximum of 60 rewards. For this experiment, pseudo-random refers to a random distribution with the restriction that the same lever cannot be presented for more than 2 consecutive trials. In the final step of shaping, the noseport was introduced. Each trial began with an illuminated noseport. When the noseport was entered, one of the two levers would extend in a pseudo-random order, and a lever press would result in a milk reward, followed by a 5-second ITI. Each day, the animal could perform a maximum of 60 rewarded trials within a maximum of 60 minutes. After 4 days of noseport training, the animals began the acquisition stage of the behavior.

Acquisition was repeated on 19 consecutive days. Throughout the 19 days, the animals were given unlimited time to complete the required trials. Each trial began with the house light being turned on and an illuminated noseport to signal an initial noseport entry. The first noseport entry triggered the start of the sample lever presentation. During the sample phase, only one lever was presented in a pseudo-random order. After the sample lever press, the noseport was immediately re-illuminated (following a 0-second delay) signaling a second noseport entry. Following the second noseport entry, the choice phase began, and both levers were presented. If the animal pressed the opposite lever to the sample lever of that trial (non-match), the trial was recorded as “correct” and a dipper reward was given. If the animal pressed the same lever as the sample, the trial was recorded as “incorrect” and the dipper was not presented. This final step was followed by a 10-second ITI during which the house light was turned off.

During the first 5 days of acquisition, there were 120 trials per day total; 60 trials with each lever presented as the sample. Furthermore, the animal had unlimited time following the sample lever press for the second noseport entry.

For the subsequent 10 days of acquisition (120 trials per day), mice had a 5-second time limit in which to make the second noseport entry. This restriction allowed us to shape the animals' behavior to ensure a standardized length of delay between subjects. If the animal did not make a noseport entry in the time allotted, the trial was aborted and was omitted from the calculations.

Finally, during the last 4 days of acquisition, the number of trials was increased to 160 trials. This allowed the animals to adjust to the longer days before the delays were introduced.

During the acquisition stage, all mice achieved a criterion level of performance, defined as 3 consecutive days above 80% correct.

Following acquisition, the delay stage began. In this stage, each trial had the same structure as during the acquisition stage, with one difference: a delay of 2, 4, 8 or 16 seconds was introduced between the sample lever press and the second noseport illumination. Each day every mouse was presented with a total of 160 trials with 40 trials of each delay condition randomly interspersed. This testing was repeated for 5 days. On the first day of testing, all animals performed poorly even at the shortest (2-second) delay (despite a previous high performance with 0-second delays), demonstrating the need for a short adjustment period to the new task parameters. The data from this adjustment period was therefore excluded, and the last 4 days, when the performance was more consistent, were taken together for analysis.

All behavioral testing was conducted during the light cycle.

Statistics. A two-way repeated measures ANOVA was used to assess significant overall effect of lesion and interactions between lesion and time during the acquisition stage or between lesion and delay length during the delay stage. Two-tailed t-tests were performed to compare the number of days to criterion for the lesioned and sham-lesioned groups, as well as other task characteristics.

Histology. At the end of experimentation, mice were transcardially perfused with PBS followed by 4% PFA. Fixed tissue was then sectioned (40 μm coronal) using a vibratome and mounted on charged slides. The tissue was stained with Cresyl Violet (Sigma-Aldrich C5042) to target Nissl bodies. Eight slices for each animal spanning and extending past the mPFC (from AP +3.2 to -0.5 relative to bregma) were then examined with a brightfield light microscope (Zeiss) to assess the location and extent of the lesion, which was determined based on loss of cell density, accumulation of clumped Nissl staining from dead tissue and contraction of the gray matter (Hunt & Aggleton, 1998) (Figure 2.1c).

Data availability. The data that support the findings of this study are available from the corresponding author upon reasonable request.

Code availability. Med-PC V and Matlab code used for administering the behavior and analysis of the data that support the findings of this study is available from the corresponding author upon reasonable request.

Chapter 3: Adolescent thalamic inhibition leads to long-lasting impairments in prefrontal cortex function†

3.1 Abstract

Impaired cortical maturation is a postulated mechanism in the etiology of neurodevelopmental disorders, including schizophrenia. In sensory cortex, activity relayed by the thalamus during a postnatal sensitive period is essential for proper cortical maturation. Whether thalamic activity also shapes prefrontal cortical maturation is unknown. Here, we show that inhibiting the mediodorsal and midline thalamus during adolescence leads to a long-lasting decrease in thalamo-prefrontal projection density and cortical excitability. Adolescent thalamic inhibition also causes prefrontal-dependent cognitive deficits during adulthood that are associated with disrupted prefrontal cross-correlations and task outcome encoding. In contrast, thalamic inhibition during adulthood has no long-lasting consequences. Strikingly, exciting the thalamus in adulthood during a cognitive task rescues prefrontal cross-correlations, task outcome encoding, and cognitive deficits. These data point to adolescence as a sensitive window of thalamo-cortical circuit maturation. Furthermore, by supporting prefrontal network activity, boosting thalamic activity provides a potential therapeutic strategy for rescuing cognitive deficits in neurodevelopmental disorders.

---

†This chapter is under review at Nature Neuroscience. It has been modified from the pre-print version of this publication, which can be found at: **Benoit, L. J.**, Holt, E. S., Posani, L., Fusi, S., Harris, A., Canetta, S., Kellendonk, C. Adolescent thalamic inhibition leads to long-lasting impairments in prefrontal cortex function, 09 August 2021, PREPRINT (Version 1) available at Research Square https://doi.org/10.21203/rs.3.rs-730508/v1

L.J.B., S.E.S., and C.K. designed the experiments. L.J.B. performed the experiments and analyzed the data. S.E.S. and E.H. assisted in the performance and analysis of the experiments. A.Z.H. assisted in the design, performance, analysis, and interpretation of experiments. L.P. and S.F. assisted in the analysis of experiments. L.J.B., S.E.S., and C.K. interpreted the results and wrote the paper.

3.2 Introduction

Sensitive periods denote developmental time windows of heightened plasticity during which alterations in experience can lead to long-lasting changes in the anatomy and function of the nervous system (Hensch, 2004; Takesian & Hensch, 2013b). Frequently, these windows represent periods in which the refinement of brain circuitry and function is particularly susceptible to changes in neuronal activity. A classic example is in the visual system, where transient developmental monocular deprivation can permanently impair acuity in the deprived eye (Wiesel & Hubel, 1963). This impairment in function persists even after the deprivation in visual input is reversed, as the thalamo-cortical inputs representing the closed eye are permanently disrupted in an activity-dependent manner. While sensitive periods in the circuit refinement of sensory cortices have been well-documented (Caras & Sanes, 2015; de Villers-Sidani et al., 2007; Sun et al., 2019; Wiesel & Hubel, 1963), recent evidence suggests that similar transient changes in activity during postnatal development can have lasting changes in the prefrontal cortex (PFC), an associative cortical area that supports higher cognitive functioning (Bicks et al., 2020; Bitzenhofer et al., 2021a; Canetta et al., 2021; Larsen & Luna, 2018a; Nabel et al., 2020).

Disturbances in PFC function are believed to underlie the cognitive symptoms found in psychiatric disorders, such as schizophrenia. Schizophrenia is thought to have a developmental origin (Insel, 2010; Sakurai & Gamo, 2019; Weinberger & Berman, 1996), and one prominent hypothesis is that during adolescence, a vulnerable period for the development of this disorder, the maturation of the PFC is disrupted (Feinberg & Campbell, 2010). In schizophrenia, recent studies have identified a decreased correlation between activity in the thalamus and the dorsolateral PFC under resting conditions, a finding which may have a structural basis (Katz et al., 1996; Kubota et al., 2013; Marenco et al., 2012). This decreased correlation has also been

measured in patients during cognitive testing (Giraldo-Chica et al., 2017; Mitelman et al., 2005; Pinault & Deschenes, 1998; Woodward et al., 2012), where it has been linked to impairments in functioning. Strikingly, decreased thalamo-prefrontal connectivity was also seen in younger adolescents at high risk for psychosis, and it predicted later illness conversion (Anticevic et al., 2015; Marenco et al., 2012; Woodward & Heckers, 2016a), raising the intriguing possibility that decreased input from the thalamus could be part of the developmental etiology of PFC dysfunction in the disorder (Anticevic et al., 2014a; Anticevic et al., 2015; Cho et al., 2016; Woodward & Heckers, 2016a).

Here, we directly test the hypothesis that input activity from the thalamus during adolescence is important for PFC circuit maturation and that decreasing this input during adolescence will lead to long-lasting impairments in the functioning of the PFC. To address this question, we used a combination of viral genetics and the designer receptor, hM4DGi, to selectively reduce activity of the thalamus during adolescence. Using a Cre/LoxP strategy, hM4DGi expression was restricted to the midline thalamus including the mediodorsal thalamus, an area that projects to the medial PFC (mPFC) in the mouse. We found that transient thalamic inhibition during adolescence led to several persistent changes in adulthood, including (1) deficits in two mPFC-dependent cognitive tasks, (2) decreased excitatory drive onto mPFC pyramidal cells, (3) decreased anatomical thalamo-mPFC input, (4) reduced mPFC neuron cross-correlations, and (5) impaired mPFC neuron encoding of extra-dimensional set shifting task outcomes. In contrast, inhibiting the thalamus for a comparable period during adulthood had no long-lasting effects on excitatory inputs to mPFC cells or behavior. These data point to adolescence as a sensitive time window of thalamo-cortical circuit maturation. Strikingly, enhancing thalamic excitability during adulthood rescued the behavioral deficits and restored the ability of mPFC neurons to encode task outcome in mice that received adolescent thalamic inhibition. Prior studies have suggested that the thalamic inputs act as a non-specific amplifier

supporting prefrontal activity during the delay periods of a working memory task and a contextual switching task (Bolkan et al., 2017; Hsiao et al., 2020; Parnaudeau et al., 2018; Rikhye et al., 2018a; Rikhye et al., 2018b; Saalmann, 2014; Schmitt et al., 2017). Our data suggest that the thalamus plays a broader function in facilitating mPFC activity that is not restricted to delay-containing tasks. Thus, this study demonstrates first the importance of thalamic input activity during adolescence for adult prefrontal cortical circuit function and second offers therapeutic insights into how to reverse cognitive deficits arising from a developmentally altered brain.

3.3 Results

3.3.1 A chemogenetic approach to transiently and chronically reduce thalamic cell activity during development or adulthood

We first aimed to establish that we can inhibit thalamic activity during adolescence and adulthood. Therefore, we stereotactically injected an adeno-associated virus (AAV) carrying a Cre-dependent version of the inhibitory designer receptor, hM4DGi (hereafter referred to as hM4D), into the thalamus of GBX2-CreERT mice (Figure 3.1a). Viral injections were performed at postnatal day P13 and Cre-mediated recombination was induced by tamoxifen injection at P15-16, at a time when GBX2 expression is restricted to the mediodorsal and midline thalamus, thereby limiting viral spread (Figure 3.1b, c). To determine the efficacy of hM4D-mediated inhibition of thalamic neurons, we performed whole-cell patch clamp recordings from thalamic neurons in both adolescent and adult brain slices. Application of the DREADD ligand, clozapine-n-oxide (CNO), led to a hyperpolarization of thalamic neurons consistent with activation of G-protein coupled inward rectifying potassium (GIRK) channels (Figure 3.1d). Thalamic neurons in control animals did not respond to CNO. CNO-application led to comparable effects sizes in adolescent and adult brain slices that were consistent with published results in adult thalamic

neurons (Parnaudeau et al., 2013). Crucially, CNO-application hyperpolarized thalamic neurons in animals that had been exposed to twice daily intraperitoneal (i.p.) CNO injections for two weeks, suggesting that chronic CNO treatment does not lead to hM4D receptor de-sensitization (Figure 3.1d). These data indicate that repeated hM4D activation can continuously inhibit thalamic neuron activity during adolescence and adulthood.

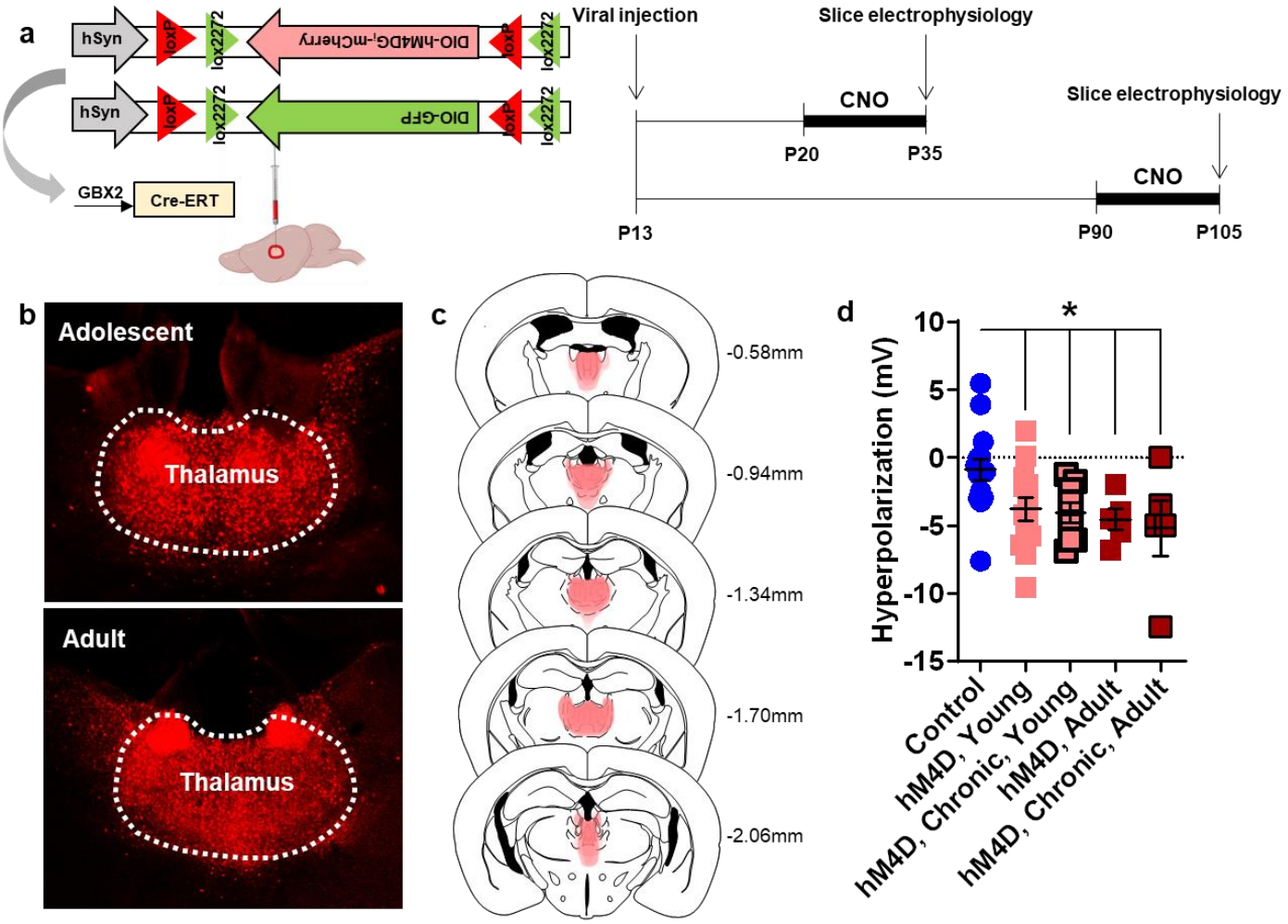

Figure 3.1. A chemogenetic approach to reversibly and chronically inhibit thalamic cells during development or adulthood. (a) Experimental design and timeline. Mice were injected with virus at P13, and whole cell patch clamp recordings were made at P35 or P105 in cells expressing hM4D-mCherry or control, GFP, at baseline and in response to bath application of 10 µM. Animals were either never exposed to CNO prior to perfusion (naïve) or given twice daily 1 mg/kg CNO i.p. injections for two weeks (chronic). (b) Example images illustrating hM4D-mCherry expression in the midline thalamus in adolescent and adult animals. (c) Superimposed traces of hM4D-mCherry viral spread (pink shading) relative to mediodorsal and midline

thalamic nuclei (dashed black lines) in coronal slices. Distance from bregma listed beside each coronal slice. (d) Quantification of CNO-induced hyperpolarization. Control cells at P35 and P105 were pooled because CNO did not show an effect at either age. CNO induced a significant hyperpolarization in both P35 and P105 cells expressing hM4D relative to control cells. Dots indicate individual cell responses and bars indicate mean ± SEM. Control: n=15 cells, 5 animals; hM4D naïve young: n=13 cells, 5 animals; hM4D chronic young: n=8 cells, 3 animals; hM4D naïve adult: n=5 cells, 3 animals; hM4D chronic adult: n=5 cells, 3 animals; 1-way ANOVA, effect of treatment $F(4, 41)=3.203$, $p=0.0223$; Holm-Sidak post-hoc, P35 hM4D naïve vs. Control *$p=0.0480$, P35 hM4D CNO-exposed vs. Control *$p=0.0480$, P105 hM4D naïve vs. Control *$p=0.0480$, P105 hM4D CNO-exposed vs. Control *$p=0.0366$. *$p<0.05$

3.3.2 Thalamic activity in adolescence, but not adulthood, is required for cognitive functioning

We then tested the long-term effects of transient thalamic inhibition during adolescence (P20-50) on prefrontal-dependent cognitive task performance. To this end, CNO (1 mg/kg) was injected twice daily in hM4D and control GFP mice from days P20-50, and the animals were tested forty days later, at P90 (Figure 3.2a). To assess cognition during adulthood, we chose an operant-based Non-Match to Sample (NMS) working memory task (Figure 3.2b), whose acquisition is delayed after a lesion of the mPFC (Benoit et al., 2020) and an odor- and texture-based attentional set shifting task (ASST), in which the extra-dimensional set shifting component of the task (EDSS) is sensitive to mPFC lesions (Figure 3.2c) (Birrell & Brown, 2000; Bissonette et al., 2008). Following adolescent thalamic inhibition from P20-50, we found that the acquisition of the NMS task was impaired in animals expressing hM4D compared with controls (Figure 3.2d). No changes were seen in any other task variables, such as trial length, task latencies, or rewards consumed (Figure 3.4), suggesting that the impairments in performance were not due to a decrease in motivation or mobility.

Similarly, in a second cohort of mice tested in the ASST, we found that the mPFC-dependent EDSS was impaired in animals expressing hM4D compared with controls (Figure 3.2e). Meanwhile, behavior in the non-mPFC-dependent initial acquisition portion of the set

shifting task (IA) was unchanged. No changes were seen in any other task variables, including IA or EDSS task latencies (Figure 3.5).

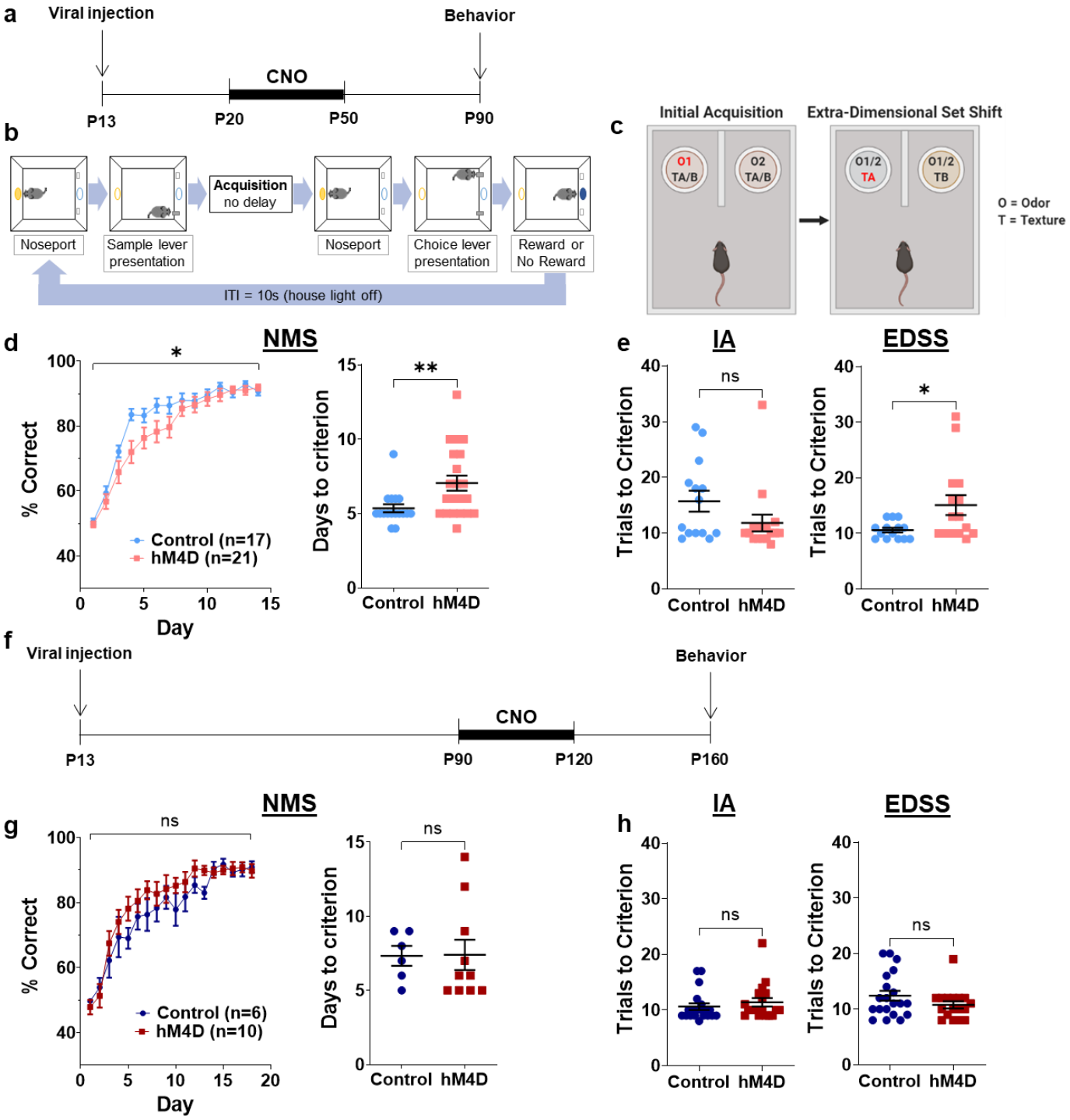

Figure 3.2. Thalamic activity in adolescence, but not adulthood, is required for cognitive behavioral performance. Schematics of (a) the Non-Match to Sample (NMS) task and (b) the attentional set-shifting task (ASST). (c) Adolescent experimental timeline. CNO was administered from P20-50 to mice expressing hM4D or GFP in the thalamus, and behavioral testing was conducted 40 days later, at P90. (d) Adolescent-inhibited hM4D animals take significantly longer to acquire the NMS task (left), taking significantly more days to reach criterion (right). Control: n=17 animals; hM4D: n=21 animals; learning curve: 2-way repeated measures (rm) ANOVA, effect of time $F(4.201,151.2)=102.0$, $p<0.0001$, effect of group $F(1,36)=3.143$, $p=0.0847$, effect of group x time $F(13,468)=2.088$, *$p=0.0137$; days to criterion (3 consecutive days above 70%): Control: (mean ± standard error of the mean, SEM) 5.35±0.27 days, hM4D: 7.05±0.51 days; unpaired t-test: $t=2.746$, $df=36$, **$p=0.0094$. (e) Adolescent-inhibited hM4D animals are no different than controls in the initial acquisition (IA) of the ASST (left, Control: n=14 animals, 15.71±1.88 trials, hM4D: n=16 animals, hM4D: 11.81±1.50 trials; unpaired t-test, $t=1.639$, $df=28$, $p=0.1125$) but take significantly more trials in the extra-dimensional set shift (EDSS) than controls (right, Control: n=14 animals, 10.57±0.42 trials, hM4D: n=15 animals, hM4D: 15.07±1.79 trials; unpaired t-test, $t=2.372$, $df=27$, *$p=0.0251$). (f) Adult experimental timeline, with CNO administered P90-120 and testing at P160. There were no differences in either (g) the acquisition of the NMS task (Control: n=6 animals, hM4D: n=10 animals; learning curve: 2-way rmANOVA, effect of time $F(5.501,77.01)=40.21$, $p<0.0001$, effect of group $F(1,14)=1.462$, $p=0.2467$, effect of group x time $F(17,238)=0.8680$, $p=0.6126$; days to criterion: Control: 7.33±0.67 days, hM4D: 7.40±1.02 days; unpaired t-test, $t=0.04654$, $df=14$, $p=0.9635$) or (h) the IA (Control: n=20 animals, 10.60±0.59 days, hM4D: n=18 animals, 11.39±0.76 trials; unpaired t-test, $t=0.8260$, $df=36$, $p=0.4142$) and EDSS (Control: 12.40±0.89 trials, hM4D: 10.76±0.64 days; unpaired t-test, $t=1.442$, $df=35$, $p=0.1583$) portions of the ASST between adult-inhibited hM4D animals and controls. Learning curves depict mean performance ± SEM for each day. For other plots, dots represent individual animals; lines represent mean ± SEM. *$p<0.05$, **$p<0.01$

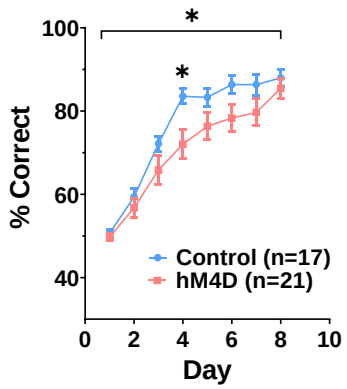

Figure 3.3. Adolescent-inhibited hM4D animals have a significantly worse overall performance during the first 8 days of the NMS task. Post-hoc analyses show that this difference is strongest at day 4. Control: n=17 animals; hM4D=21 animals. 2-way rmANOVA, effect of time $F(3.129,112.7)=87.66$, $p<0.0001$, effect of group $F(1,36)=4.575$, *$p=0.0358$, effect of group x time $F(7,252)=1.546$, $p=0.1523$; Holm-Sidak post-hoc analysis at day 4, *$p=0.0456$. Learning curves depict mean performance ± SEM for each day. *$p<0.05$

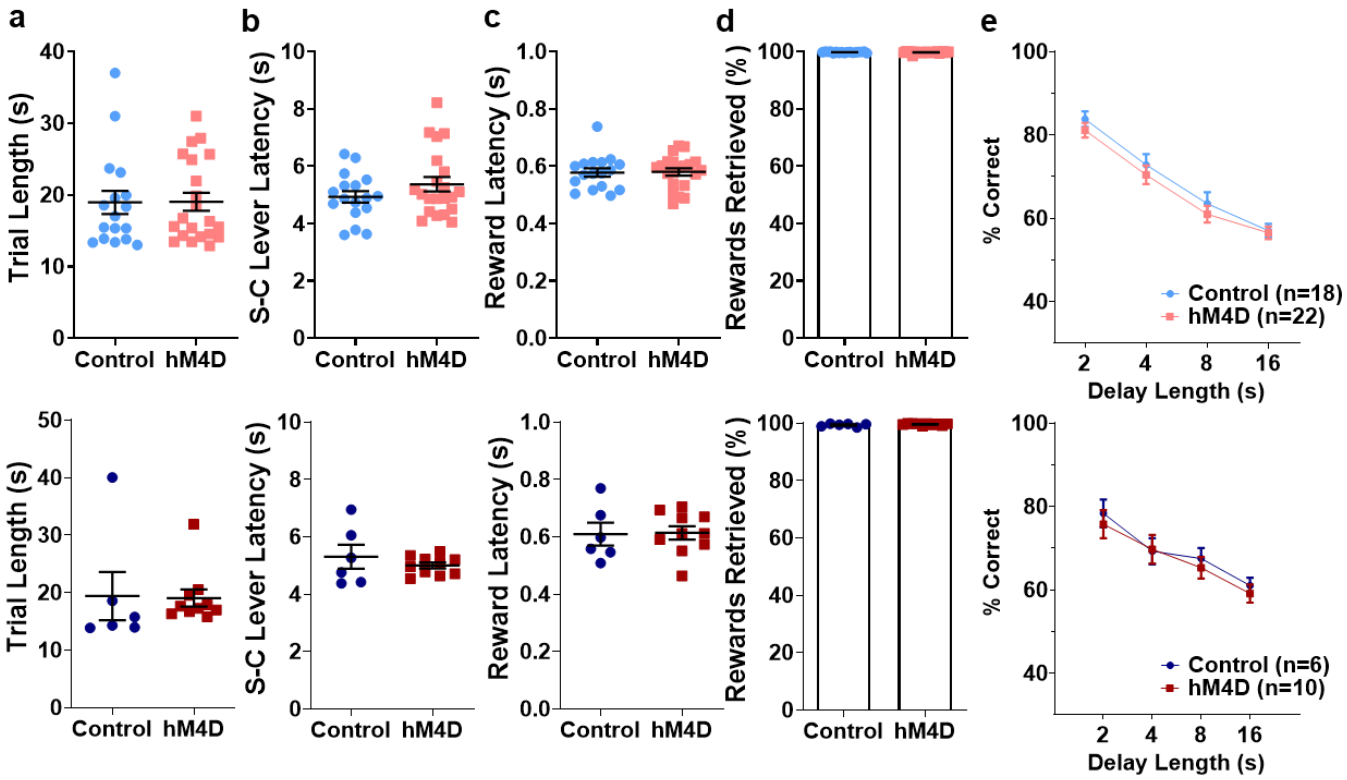

Figure 3.4. Other metrics in the NMS task were unaffected by thalamic inhibition. In the NMS task, no metrics of mobility or motivation were affected by adolescent (top) or adult (bottom) thalamic inhibition, including (a) mean trial length, adolescent: Control: n=17 animals, 18.94±1.61 s, hM4D: n=21 animals, 19.03±1.26 s; unpaired t-test: t=0.04228, df=36, p=0.9665; adult: Control: n=6 animals, 19.41±4.19 s, hM4D: n=10 animals, 19.05±1.50 s; unpaired t-test: t=0.09631, df=14, p=0.9246, (b) mean sample lever press-choice lever press latency, adolescent: Control: 4.932±0.199 s, hM4D: 5.372±0.252 s; unpaired t-test: t=1.321, df=36, p=0.1949; adult: Control: 5.304±0.416 s, hM4D: 4.999±0.102 s; unpaired t-test: t=0.8949, df=14, p=0.3875, (c) mean latency to collect reward, adolescent: Control: 0.5781±0.0143 s, hM4D: 0.5801±0.0125 s; unpaired t-test: t=0.1086, df=36, p=0.9141; adult: Control: 0.6091±0.0396 s, hM4D: 0.6137±0.0233 s; unpaired t-test: t=0.1064, df=14, p=0.9168,and (d) percentage of rewards retrieved, adolescent: Control: 99.78±0.05%, hM4D: 99.71±0.07%; unpaired t-test: t=0.7668, df=36, p=0.4482; adult: Control: 99.36±0.21 s, hM4D: 99.62±0.10 s; unpaired t-test: t=1.199, df=14, p=0.2503. (e) Adolescent (top) and adult (bottom) thalamic inhibition do not change delay performance. There are no differences in performance at any delay length tested (2s, 4s, 8s, 16s). Adolescent: 2-way rmANOVA: effect of group $F(1,38)=0.7487$, $p=0.3923$, effect of delay length $F(2.63, 100.00)=125$, $p<0.0001$, effect of group x delay length $F(3,114)=0.2506$, $p=0.8608$; adult: 2-way rmANOVA: effect of group $F(1,14)=0.1574$, $p=0.6975$, effect of delay length $F(2.50,34.97)=40.65$, $p<0.0001$, effect of group x delay length $F(3.42)=0.3923$, $p=0.7591$. Dots represent individual animals; lines represent mean ± SEM.

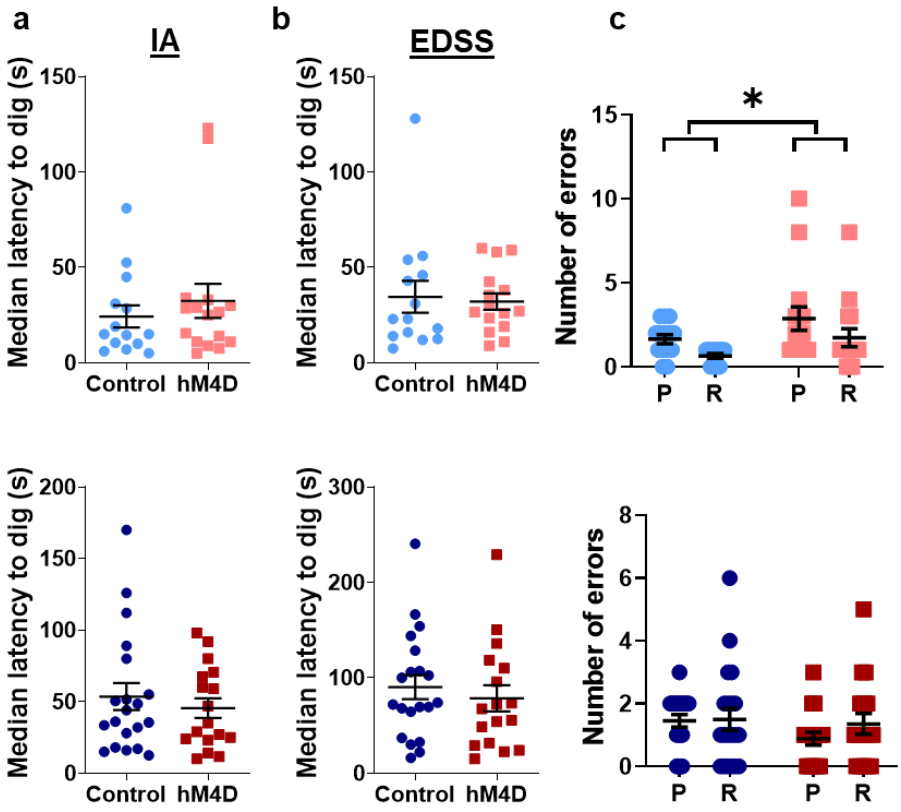

Figure 3.5. Other metrics in the ASST were unaffected by thalamic inhibition. In the ASST, no metrics of mobility or motivation were affected by adolescent (top) or adult (bottom) thalamic inhibition, including median latency to dig during (a) IA (adolescent: Control: n=14 animals, 24.29±5.84 s, hM4D: n=16 animals, 32.47±8.91 s; unpaired t-test: t=0.7448, df=28, p=0.4626; adult: Control: n=20 animals, 53.50±9.41 s, hM4D: n=17 animals, 45.44±6.95 s; unpaired t-test: t=0.6682, df=35, p=0.5084) or (b) SS (adolescent: Control: n=14 animals, 34.57±8.39 s, hM4D: n=15 animals, 32.07±4.32 s; unpaired t-test: t=0.2708, df=27, p=0.7886; adult: Control: n=20 animals, 90.20±12.58 s, hM4D: n=17 animals, 78.44±13.70 s; unpaired t-test: t=0.6323, df=35, p=0.5313). (c) Similarly, the breakdown of types of errors during EDSS, perseverative (P) and random (R), was unaffected. Following adolescent inhibition (top), there was an overall effect of the manipulation, with increased numbers of both perseverative and random errors (2-way rmANOVA, effect of group F(1,27)=4.215, *p=0.0499). Following adult inhibition (bottom), there was no change in either type of error (2-way rmANOVA, effect of group F(1,35)=1.369, p=0.2499). Dots represent individual animals; lines represent mean ± SEM. *p<0.05

To address whether the primary contribution of this behavioral deficit came from the thalamo-mPFC projections, or other thalamic projections, we next targeted only thalamo-mPFC projections during adolescent inhibition. We used a dual virus approach, with a retrogradely-transported viral vector containing Cre recombinase injected into the mPFC and a viral vector containing Cre-dependent hM4D into the thalamus (Figure 3.6a). Using the same behavioral

timeline, we found the same behavioral findings in the ASST, with intact IA and impaired EDSS in the adolescent-inhibited animals (Figure 3.6b, c).

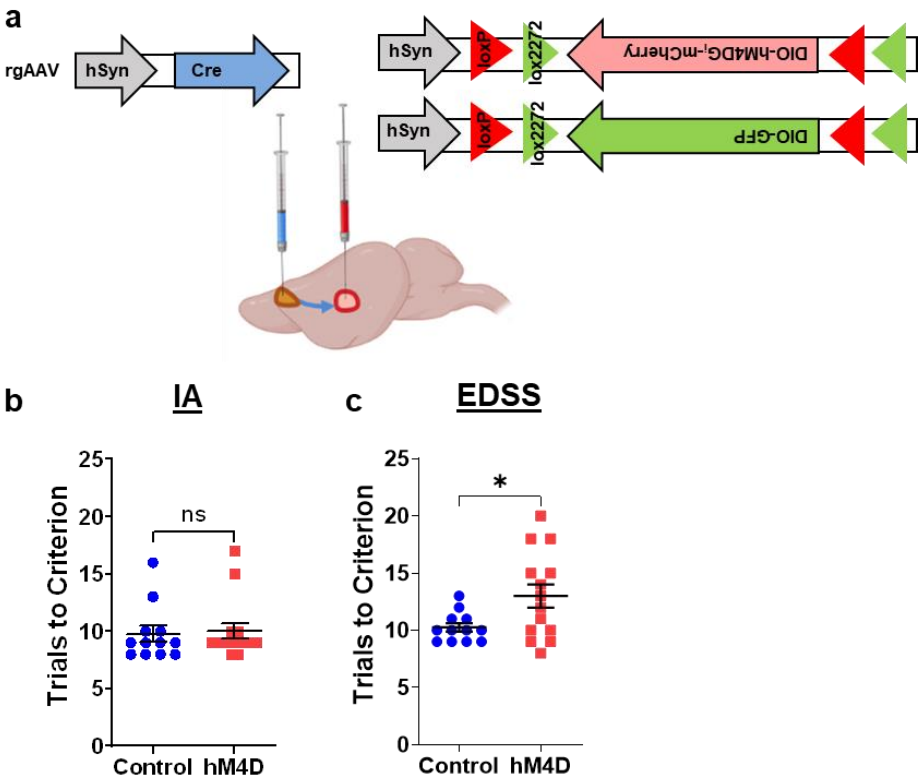

Figure 3.6. Thalamo-mPFC projection activity during adolescence is required for adult cognitive flexibility. (a) Schematic for viral injections to target thalamo-mPFC projections. At P12, one virus was injected into the mPFC containing a retrogradely transported Cre driver, and another virus was injected into the thalamus containing floxed, Cre-dependent hM4D or the control GFP. (b) Adolescent-inhibited hM4D animals are no different than controls in the IA portion of the ASST. Control: n=12 animals, 9.75±0.70 trials; hM4D: n=14 animals, 10.00±0.70 trials; unpaired t-test, t=0.2507, df=24, p=0.8042. (c) Adolescent-inhibited hM4D animals take significantly more trials in the EDSS to reach criterion than controls. Control: 10.25±0.37 trials; hM4D: 13.00±1.02 trials; unpaired t-test, t=2.385, df=24, *p=0.0254. Dots represent individual animals; lines represent mean ± SEM. *p<0.05

These results indicate that adolescent thalamic inhibition results in long-term, persistent consequences to mPFC-dependent cognitive processes. To test whether adolescence is in fact a sensitive period, or whether the circuit is sensitive to transient changes at any age, we also inhibited the thalamus for a comparable time window during adulthood, P90-120, and tested the long-term effects forty days later, at P160 (Figure 3.2f).

While there was an effect of age on performance in the NMS task, with the older P160 animals performing worse than the P90 animals, adult thalamic inhibition affected neither acquisition of the NMS task (Figure 3.2g) nor trials to criterion in the EDSS task (Figure 3.2h), supporting the hypothesis that adolescence is a sensitive period in which changes in thalamic activity influence the development of thalamo-mPFC circuit maturation.

3.3.3 Thalamic activity in adolescence, but not adulthood, is required for prefrontal excitability

To determine whether thalamic inhibition during adolescence leads to long-lasting changes in mPFC circuit function, we used slice physiology to measure spontaneous excitatory and inhibitory activity in mPFC layer II/III pyramidal cells, which receive projections from the thalamus (Figure 3.7a). Following adolescent thalamic inhibition, the frequency of spontaneous excitatory post-synaptic currents (sEPSCs) was reduced, while the sEPSC amplitude was unchanged (Figure 3.7b, c). This change in frequency, but not amplitude, suggests a decrease in the quantity or functionality of pre-synaptic excitatory inputs. In contrast, we found no changes in frequency or amplitude of spontaneous inhibitory post-synaptic currents (sIPSCs) (Figure 3.7b, d) pointing to a selective decrease in excitatory drive onto mPFC neurons.

These effects were again selective to thalamic inhibition during adolescence as we found no changes in excitatory or inhibitory inputs to prefrontal pyramidal cells following chronic thalamic inhibition in adulthood (Figure 3.7f, g). These findings, consistent with the behavioral results, point to adolescence as a sensitive time period during which thalamic activity regulates the development of the mPFC.

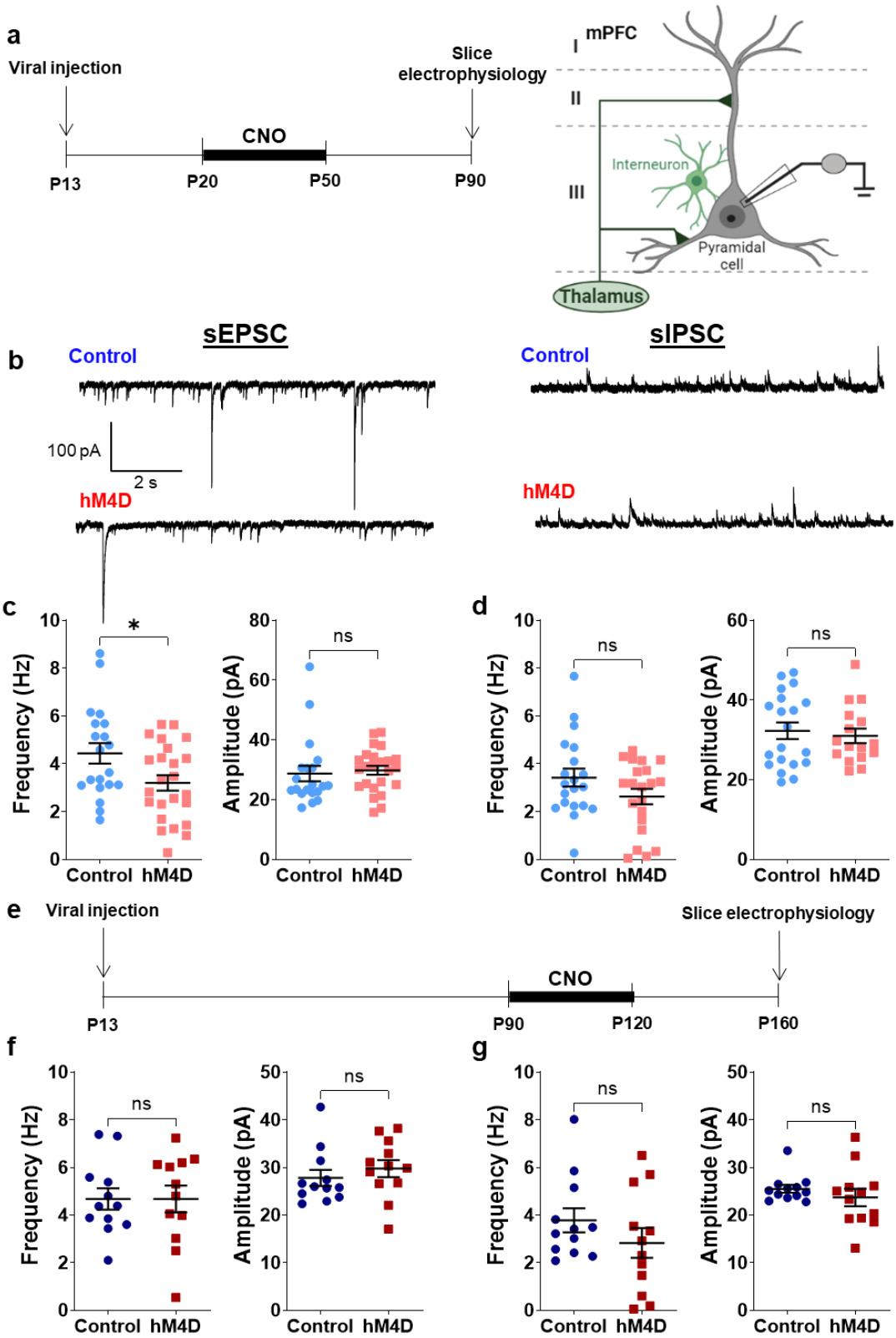
a
Viral injection
Slice electrophysiology
CNO
P13
P20
P50
P90
mPFC
I
II
III
Interneuron
Pyramidal cell
Thalamus
b
sEPSC
sIPSC
Control
hM4D
100 pA
2 s
c
d
Frequency (Hz)
Amplitude (pA)
ns
*
Control
hM4D
e
Viral injection
Slice electrophysiology
CNO
P13
P90
P120
P160
f
g

Figure 3.7. Thalamic activity in adolescence, but not adulthood, is required for mPFC pyramidal excitability in adulthood. (a) Adolescent experimental timeline and schematic. Whole cell patch clamp recordings were made from pyramidal cells in layer II/III of the mPFC from hM4D and control mice. These pyramidal cells receive excitatory inputs from the thalamus as well as inhibitory inputs from local interneurons. (b) Representative traces showing spontaneous excitatory post-synaptic currents (sEPSCs, left) and spontaneous inhibitory post-synaptic currents (sIPSCs, right). (c) sEPSC frequency is significantly reduced following adolescent thalamic inhibition relative to control mice, but sEPSC amplitude is unchanged. Control: n=20 cells, 5 animals; hM4D: n=24 cells, 7 animals; frequency: Control: 4.438±0.429 Hz, hM4D: 3.202±0.325 Hz; unpaired t-test, t=2.337, df=42, *p=0.0243; amplitude: Control: 28.71±2.57 pA, hM4D: 29.82±1.47 pA; unpaired t-test, t=0.3881, df=42, p=0.6999. (d) sIPSC frequency and amplitude are also unchanged. Control: n=20 cells, 5 animals; hM4D: n=21 cells, 7 animals; frequency: Control: 3.421±0.376 Hz, hM4D: 2.627±0.323 Hz; unpaired t-test, t=1.606, df=39, p=0.1163; amplitude: Control: 32.29±2.08 pA, hM4D: 31.03±1.84 pA; unpaired t-test, t=0.4450, df=34, p=0.6592. (e) Adult experimental timeline. (f) sEPSC and (g) sIPSC frequency and amplitude are unchanged following adult thalamic inhibition. Control: n=12 cells, 3 animals; hM4D: n=12 cells, 3 animals; sEPSC: n=12 Control cells, n=12 hM4D cells; frequency: Control: 4.674±0.448 Hz, hM4D: 4.675±0.561 Hz; unpaired t-test, t=0.001936, df=22, p=0.9985; amplitude: Control: 27.78±1.68 pA, hM4D: 29.75±1.78 pA; unpaired t-test, t=0.8048, df=22, p=0.4296; sIPSC: n=12 Control cells, n=12 hM4D cells; frequency: Control: 3.775±0.506 Hz, hM4D: 2.825±0.625 Hz; unpaired t-test, t=1.181, df=22, p=0.2501; amplitude: Control: 25.49±0.82 pA, hM4D: 23.69±1.82 pA; unpaired t-test, t=0.9030, df=22, p=0.3763. Dots represent individual animals; lines represent mean ± SEM. *p<0.05

3.3.4 Adolescent thalamic activity is required to maintain thalamic projection density to the mPFC

We next aimed to discover whether decreased subcortical anatomical inputs may contribute to the decrease in sEPSC frequency measured in the mPFC following adolescent thalamic inhibition. To test this question, we injected a retrogradely transported fluorescent protein, GFP, into the mPFC of adult mice that had experienced adolescent thalamic inhibition. Three weeks later, we used stereology to calculate the density of retrogradely labelled neurons in the thalamus, as well as in the basolateral amygdala (BLA, Figure 3.8a), an additional region that projects to layer II/III of the mPFC. After outlining the regions using DAPI staining, we found a decrease in the density of cells projecting from the thalamus to the mPFC (Figure 3.8c). In contrast, we found no change in the density of cells projecting from the BLA (Figure 3.8d), suggesting that there is no global competition between subcortical regions projecting to the

mPFC, as has previously been seen in early postnatal lesion studies (Guirado et al., 2016). The difference in thalamic projections is maintained when the thalamus/BLA ratio is taken (Figure 3.8e), indicating that there is not an artificial effect caused by different injected viral volumes across animals and groups. We saw no change in overall cell density within the thalamus based on DAPI-positive cell counts (Figure 3.9), suggesting a loss of thalamic inputs to the mPFC rather than thalamic cells.

3.3.5 Enhancing thalamic excitability in the adult animal rescues the cognitive impairments induced by adolescent thalamic inhibition

The anatomical changes suggest that the circuit alterations are persistent. Previous work has shown that exciting the thalamus can enhance performance in prefrontal-dependent cognitive tasks including in a working memory and a 2-alternative forced choice task (Bolkan et al., 2017; Schmitt et al., 2017). Moreover, it has been suggested that the thalamus may act as a non-specific amplifier of mPFC activity during the delay periods of those behaviors (Bolkan et al., 2017; Hsiao et al., 2020; Rikhye et al., 2018a; Rikhye et al., 2018b; Schmitt et al., 2017). Even though our task does not include delays in which the trial-specific information must be kept online, we aimed to discover whether activation of the remaining thalamic inputs would still improve behavior and whether this amplification can overcome the developmental circuit abnormalities.

Therefore, we enhanced thalamic activity during the set shifting task using a stabilized step-function opsin (SSFO, Figure 3.10a). To correct the impaired EDSS behavior, we activated the SSFO with a 5 second pulse (473nm, 4mW) before the start of the EDSS portion of the task (Figure 3.10b). Because the SSFO will slowly inactivate over time, we repeated the 5 s pulse during the intertrial interval (ITI) every 30 minutes while the animal was engaged in the task.

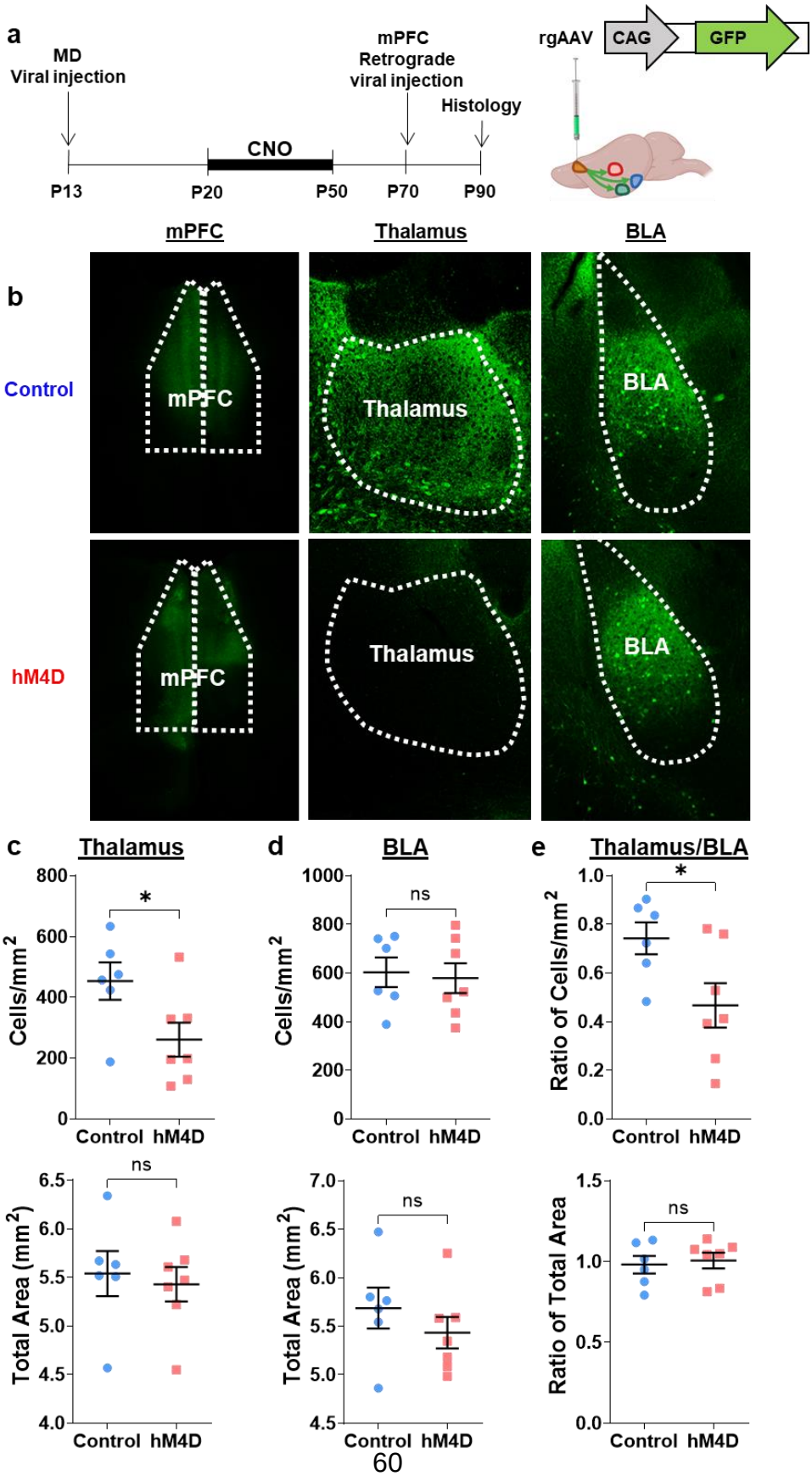
a
MD
Viral injection
CNO
mPFC
Retrograde
viral injection
Histology
P13
P20
P50
P70
P90
rgAAV
CAG
GFP
b
mPFC
Thalamus
BLA
Control
hM4D
c
Thalamus
Cells/mm2
Total Area (mm2)
d
BLA
e
Thalamus/BLA
Ratio of Cells/mm2
Ratio of Total Area
Control
hM4D
*
ns

Figure 3.8. Adolescent thalamic activity is required to maintain the density of projections to the mPFC from the thalamus, but not from the BLA. (a) Experimental timeline and schematic. At P70, a retrograde tracer, GFP, was injected into the mPFC, before perfusion 3 weeks later. (b) Representative confocal images illustrating GFP staining in the mPFC (left), thalamus (middle), and basolateral amygdala (BLA, right) in control (top) and hM4D (bottom) animals. Outlines were determined using DAPI staining. (c) Stereology was conducted using DAPI staining for outlines of regions and GFP staining for cell counting. Quantification of GFP-positive cell density showed a significant decrease in thalamo-mPFC projecting cells in adolescent-inhibited hM4D animals compared to controls (top, Control: n=6 animals, 453.2±61.3 cells/mm^2, hM4D: n=7 animals, 260.3±56.1 cells/mm^2; unpaired t-test, t=2.326, df=11, *p=0.0401). Stereological estimates showed no difference in overall thalamic area (bottom, Control: 5.539±0.232 mm^2, hM4D: 5.429±0.178 mm^2; unpaired t-test, t=0.3834, df=11, p=0.7087). (d) Stereology in the BLA showed no differences in either GFP-positive cell density (top, Control: 602.4±61.1 cells/mm^2, hM4D: 578.5±61.0 cells/mm^2; unpaired t-test, t=0.2749, df=11, p=0.7885) or BLA area (bottom, Control: 5.687±0.211 mm^2, hM4D: 5.432±0.163 mm^2; unpaired t-test, t=0.9713, df=11, p=0.3523). (e) The ratio of thalamic to BLA projection cell densities showed a significant reduction in adolescent-inhibited hM4D animals compared to controls (top, Control: 0.742±0.065, hM4D: 0.467±0.091; unpaired t-test, t=2.376, df=11, *p=0.0368) but no change in region area (bottom, Control: 0.981±0.055, hM4D: 1.006±0.049; unpaired t-test, t=0.3471, df=11, p=0.7351). Dots represent individual animals; lines represent mean ± SEM. *p<0.05

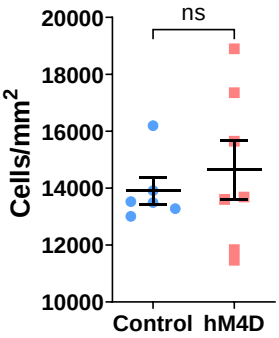

Figure 3.9. Thalamic DAPI staining shows no differences in overall cell density in the thalamus for control or hM4D animals. Control: n=6 animals, 13902±474 cells/mm^2, hM4D: n=7 animals, 14642±1051 cells/mm^2; unpaired t-test, t=0.6050, df=11, p=0.5575. Dots represent individual animals; lines represent mean ± SEM.

We performed a crossover experiment where each animal performed the ASST twice, with and without SSFO activation, ten days apart. We replicated the behavioral deficit in the adolescent thalamus-inhibited animals when the SSFO was not active, and found that increasing thalamic excitability via SSFO activation during EDSS was sufficient to rescue the behavior of adolescent thalamic inhibition animals to control levels (Figure 3.10d). The effects of SSFO activation did not persist from the first day of testing to the second testing day, and

repeating the experiment did not influence behavior (2-way rmANOVA; effect of light $F(1,46)=6.302$, $p=0.0156$, effect of run day $F(1,46)=2.512$, $p=0.1199$, effect of light x day run $F(1,46)=1.364$, $p=0.2488$). These data give an important mechanistic insight: even though the sensitive period in the circuit occurs in adolescence, thalamo-mPFC circuitry can still be acutely manipulated in adulthood to rescue the behavioral deficits.

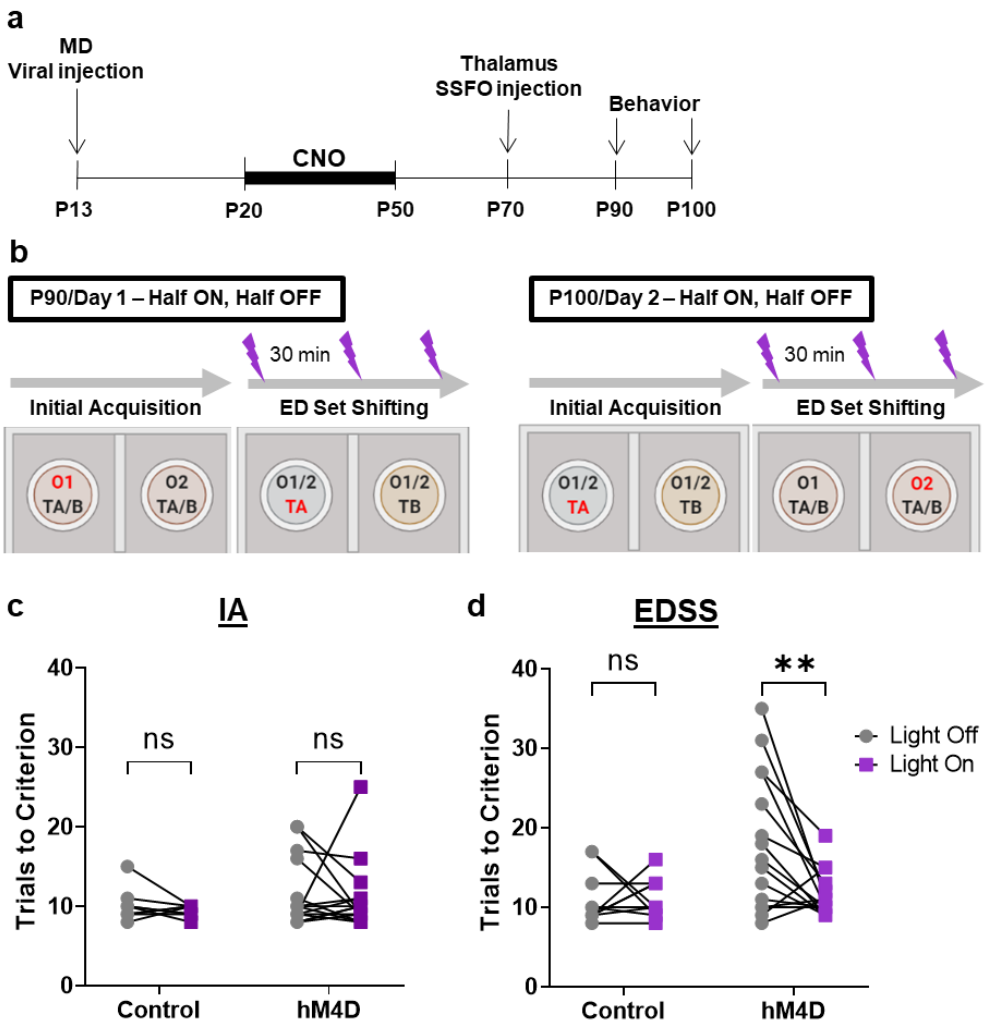

Figure 3.10. Acute thalamic activity enhancement rescues the ASST behavioral deficit following adolescent thalamic inhibition. (a) Experimental timeline. At P70, a stabilized step-function opsin (SSFO) was injected into the thalamus along with optrodes. Behavioral testing was done at P90 and P100. (b) Schematic for behavior. For the light ON animals, the SSFO was stimulated before the EDSS and again every 30 min during the inter-trial interval (ITI) until completion of the task. Animals were randomly assigned to two groups: (1) light ON (SSFO activation) on Day 1 at P90 and light OFF on Day 2 at P100; (2) light OFF on Day 1 at P90 and

light ON on Day 2 at P100. (c) There is no significant difference in IA performance between the control or hM4D light OFF groups (2-way rmANOVA; effect of group $F(1,23)=2.407$, $p=0.1344$, effect of light $F(1,23)=0.3319$, $p=0.5702$, effect of group x light $F(1,23)=0.001148$, $p=0.9733$; Holm-Sidak post-hoc: Control Light OFF vs. hM4D Light OFF $p=0.4425$). Further, all groups showed equivalent trials to criterion during the IA (Holm-Sidak post-hoc: Control Light OFF vs. ON $p=0.8925$, hM4D Light OFF vs. ON $p=0.8925$). (d) hM4D light OFF animals take significantly more trials to reach criterion during EDSS compared with control light OFF animals. Acute SSFO stimulation (light ON) during the EDSS rescued the behavior in the adolescent-inhibited hM4D animals but had no effect on control animals (2-way rmANOVA; effect of group $F(1,23)=5.407$, $p=0.0292$, effect of light $F(1,23)=5.002$, $p=0.0353$, effect of group x light $F(1,23)=5.002$, $p=0.0353$; Holm-Sidak post-hoc: Control Light OFF vs. ON $p>0.9999$, hM4D Light OFF vs. ON $^{**}p=0.0035$; Light OFF Control vs. hM4D $^{**}p=0.0046$, Light ON Control vs. hM4D $p=0.8197$). Dots represent individual animals, lines connecting performance with light OFF and light ON. Control: n=10; hM4D: n=15. $^{**}p<0.01$

3.3.6 Oscillatory activity does not explain the behavioral deficits and rescue

In sum, developmental thalamic inhibition leads to altered prefrontal circuit function, which results in impaired EDSS behavior. This deficit is then rescued by acute thalamic activation. To better understand the network mechanisms driving these findings, we examined several metrics of mPFC activity during the behavior: local field potential (LFP) activity, single unit cellular activity, and neural ensemble activity.

Prior work from our group, using the same set shifting task, identified an increase in the power of gamma frequency (40-90 Hz) oscillations in the mPFC before correct, but not incorrect, choices during the EDSS behavior (Canetta et al., 2021). Moreover, this correct trial induced gamma signal was attenuated in mice that performed poorly in this set shifting task following developmental inhibition of their prefrontal parvalbumin (PV) expressing interneurons (Canetta et al., 2021). Similarly, other studies have also highlighted the importance of mPFC interneuron activity and the associated changes in task-related gamma power in proper EDSS behavior (Canetta et al., 2016b; Cho et al., 2015; Cho et al., 2020; Goodwill et al., 2018; Mukherjee et al., 2019b).

Consistent with our prior results (Canetta et al., 2021), we found that mPFC gamma power was increased specifically before the decision in correct trials compared with power in

incorrect trials of control animals (Figure 3.11a, d). However, this difference in correct vs incorrect gamma power was still observed after adolescent inhibition of the MD, albeit with a smaller-appearing effect size (Figure 3.11b, d). Moreover, thalamic SSFO activation had no significant effect on mPFC gamma power (Figure 3.11c, d). These results suggest that changes in gamma power do not explain the deficit in the behavioral performance in mice that experience adolescent thalamic inhibition.

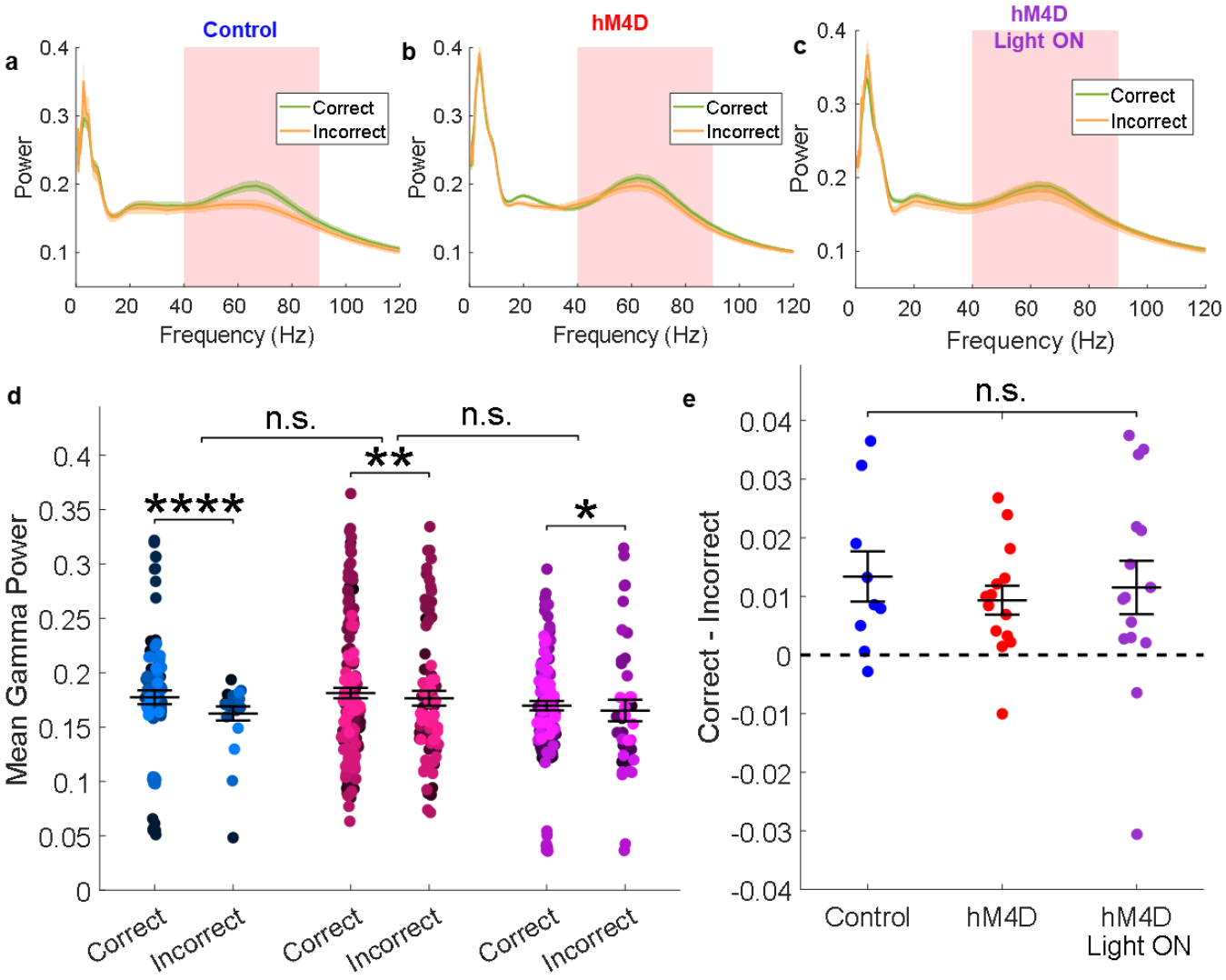

Figure 3.11. Adolescent thalamic activity is not required for the mPFC gamma signature during the EDSS, which is not changed by acute thalamic activation. (a) Control animal without SSFO activation (Light OFF) mPFC normalized power (artificial units, A.U.) as a function of frequency during the 6 seconds preceding the decision point during the EDSS during correct

trials (green), and incorrect trials (orange). Red shading indicates 40-90 Hz (gamma). Lines and shading indicate mean ± SEM. (b) As in (a), but for adolescent-inhibited hM4D Light OFF animals. (c) As in (a), but for adolescent-inhibited hM4D animals that have acute SSFO activation during EDSS (Light ON). (d) Mean gamma power (40-90 Hz) is significantly increased in correct vs incorrect trials for all three groups, and this pattern is not significantly different across groups. Control Light OFF: left, blue; hM4D Light OFF: center, pink; hM4D Light ON: right, purple. Control Light OFF: n=9 animals, 88 correct trials, 23 incorrect trials, Correct: 0.1774±0.0064; Incorrect: 0.1625±0.0066; linear mixed effects model: fixed effect (Trial Type), ****p=5.1208e-05; hM4D Light OFF: n=14 animals, 177 correct trials, 89 incorrect trials, Correct: 0.1813±0.0048; Incorrect: 0.1765±0.0068; linear mixed effects model: fixed effect (Trial Type), **p=0.0014916; hM4D Light ON: n=15 animals, 137 correct trials, 41 incorrect trials, Correct: 0.1697±0.0043; Incorrect: 0.1652±0.0099; linear mixed effects model: fixed effect (Trial Type), *p=0.015341. Linear hypothesis F-test to compare differences: Control vs. hM4D: p=0.3092; hM4D vs. hM4D Light ON: p=0.7607. Lines and error represent mean ± SEM. Dots represent individual trials for each animal (colors of the dots). (e) Mean difference in gamma power between correct and incorrect trials by animal shows no differences across groups, all groups having an increased gamma power for correct over incorrect trials. Control Light OFF: 0.0134±0.0043; hM4D Light OFF: 0.0093±0.0025; hM4D Light ON: 0.0115±0.0045; 1-way ANOVA, F(2,35)=0.2329, p=0.7935. Lines and error represent mean ± SEM. Dots represent individual animal mean difference. *p<0.05, **p<0.01, ****p<0.0001

Other cognitive tasks are known to generate thalamo-cortical oscillations in the beta frequency range (12-30 Hz) (Bolkan et al., 2017; Parnaudeau et al., 2018; Parnaudeau et al., 2013). In the ASST, we recorded an increase in beta power during the trial compared to the inter-trial interval (ITI, Figure 3.12a). This beta activation was equivalent across all trial types (Figure 3.12e) and was not affected by the developmental manipulation (Figure 3.12b). In addition, we found no changes in a variety of other physiological metrics, including thalamo-mPFC coherence in the beta frequency range across trial types (Figure 3.12c, d, f) and phase-locking between mPFC cell firing and thalamic beta oscillatory activity (Figure 3.13).

Altogether, these data show that changes in oscillatory activity cannot explain the behavioral deficit in mice that experienced developmental thalamic inhibition. As a result, we next analyzed the activity of cells and neural ensembles in the mPFC.

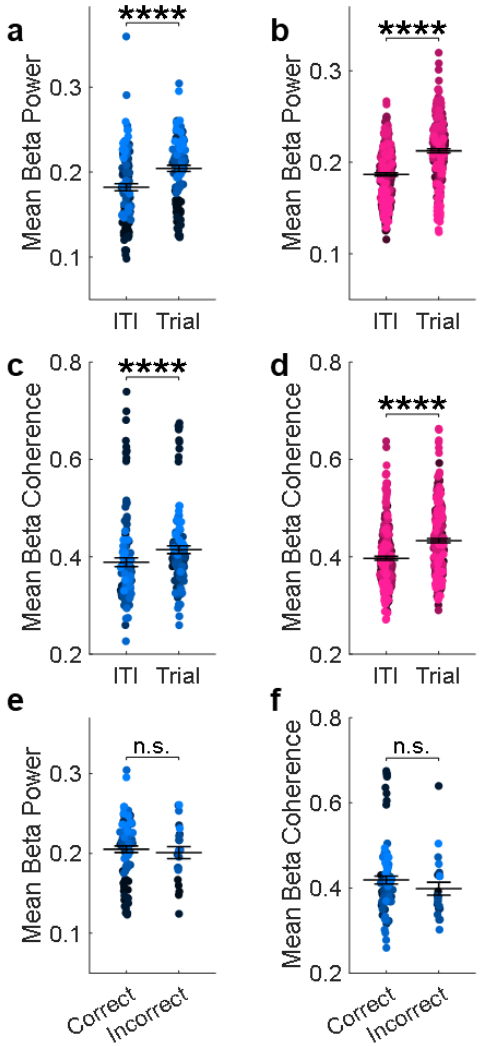

Figure 3.12. Thalamic beta oscillatory activity is engaged during the ASST. Mean thalamic beta (12-30 Hz) power is specifically enhanced during the EDSS trials compared to the ITI for (a) control (n=10 animals, ITI: 0.1822±0.0042; Trial: 0.2044±0.0036; linear mixed effects model: fixed effect (Trial), p=3.2642e-16) and (b) hM4D (n=15 animals, ITI: 0.1866±0.0018; Trial: 0.2124±0.0022; linear mixed effects model: fixed effect (Trial), p=2.0872e-41) animals. (c) As in (a) except for mean beta (12-30 Hz) mPFC-thalamic coherence (ITI: 0.3890±0.0090; Trial: 0.4146±0.0080; linear mixed effects model: fixed effect (Trial), p=2.0137e-07). (d) As in (b) except for mean beta mPFC-thalamic coherence (0.3968±0.0041; Trial: 0.4331±0.0044; linear mixed effects model: fixed effect (Trial), p=6.7099e-19). (e) Mean thalamic beta power (88 correct trials, 23 incorrect trials, Correct: 0.2052±0.0041; Incorrect: 0.2011±0.0075; linear mixed effects model: fixed effect (Trial Type), p=0.18827) and (f) beta mPFC-thalamic coherence (Correct: 0.4188±0.0092; Incorrect: 0.3984±0.0152; linear mixed effects model: fixed effect (Trial Type), p=0.72808) are unchanged across trial types in controls. Dots represent individual trials for each animal (colors of the dots). Lines and error represent mean ± SEM. ****p<0.0001

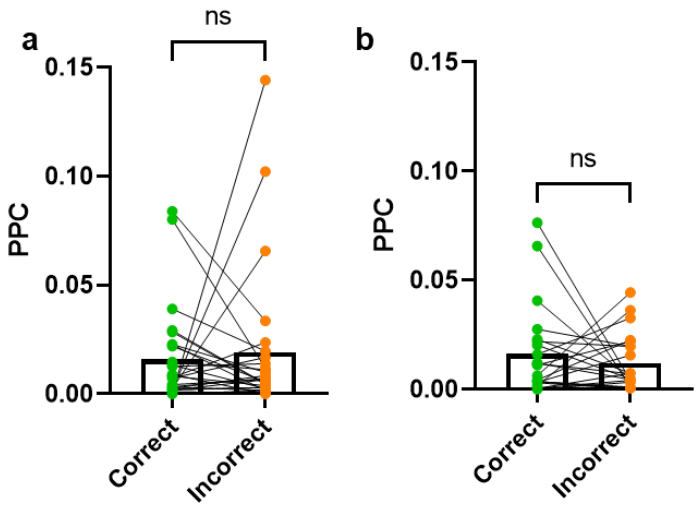

Figure 3.13. Adolescent thalamic inhibition has no effect on phase locking between thalamic oscillatory activity and mPFC single unit firing during the ASST. Pairwise phase consistency (PPC) values show no differences between phase-locking of mPFC cell firing and thalamic beta oscillatory activity in (a) control (n=6 animals, 27 cells, Correct PPC: 0.01575±0.00420; Incorrect: 0.01904±0.00642; paired t-test: t=0.4114, df=26, p=0.6841) or (b) hM4D (n=7 animals, 22 cells, Correct: 0.01623±0.00441; Incorrect: 0.01205±0.00561; paired t-test: t=0.7443, df=21, p=0.4649) animals. Dots represent individual cells, with lines connecting each cell's correct and incorrect PPC value.

3.3.7 Adolescent thalamic activity is required for adult mPFC neurons to encode task outcome

To determine whether thalamic inhibition may alter encoding of information within the mPFC, we analyzed the firing rates of single units in the mPFC. Most mPFC units showed task-modulated activity with cells showing either enhanced or decreased activity during the EDSS task trials compared with the ITI (Figure 3.14). However, overall single unit firing rates (FR) were not altered by either the developmental manipulation and or the SSFO rescue (Figure 3.15b). This was true during the ITI, over the course of the trial, in the pre-decision, and in the post-decision periods, when looking at either raw FR (Figure 3.17) or FR that were normalized to ITI activity (Figures 3.18, 3.19). Furthermore, FR did not significantly vary between different trial types, such as correct trials and incorrect trials (Figure 3.15c). Again, this was true throughout the different epochs of the trial (Figures 3.17, 3.18, 3.19). Thus, individual FR do not

predict trial outcomes in control animals, and this metric was not affected by either developmental thalamic inhibition or acute thalamic activation. These findings were consistent, even when selecting only the task-modulated cells, or other subcategories, such as cells that increased their firing rates during the trial or cells that decreased their firing during the trial.

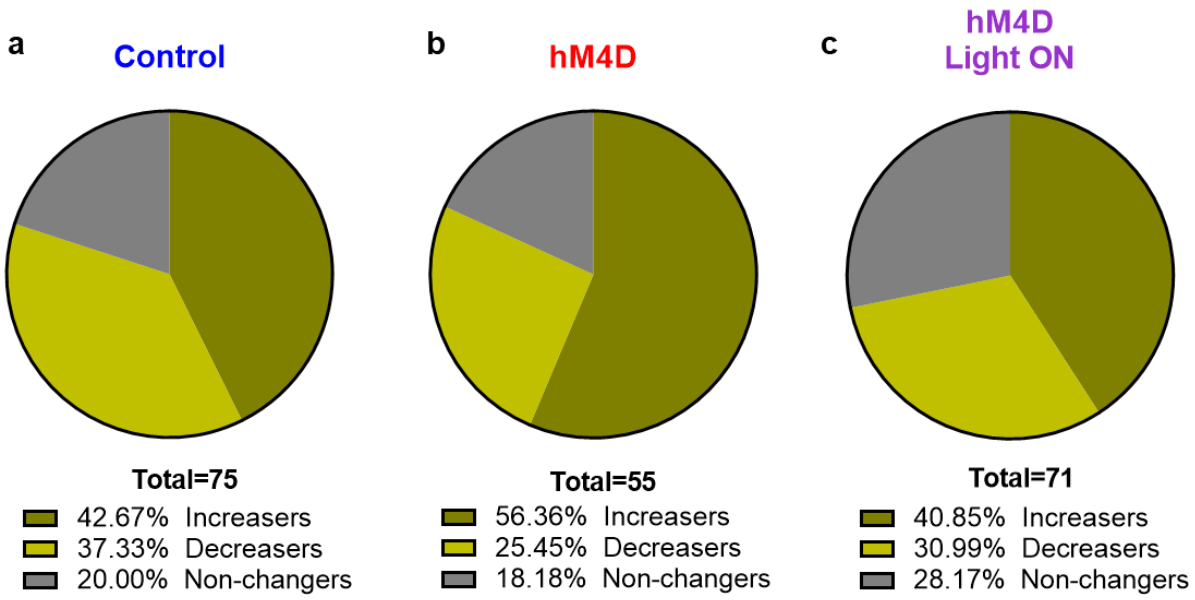

Figure 3.14. Breakdown of cells by their firing rates show that most are modulated during EDSS trials. Breakdown of cells by behavior during the trial compared to the inter-trial interval (ITI), with cells that have a significantly increased firing rate during the trial (increasers), decreased firing rate (decreasers), or unchanged firing rate compared to the ITI (non-changers). This shows a majority of cells modulated during EDSS trials, with (a) 80% modulated in control animals, (b) 81.82% modulated in adolescent-inhibited hM4D animals, and (c) 71.83% modulated in hM4D animals during EDSS thalamic activation.

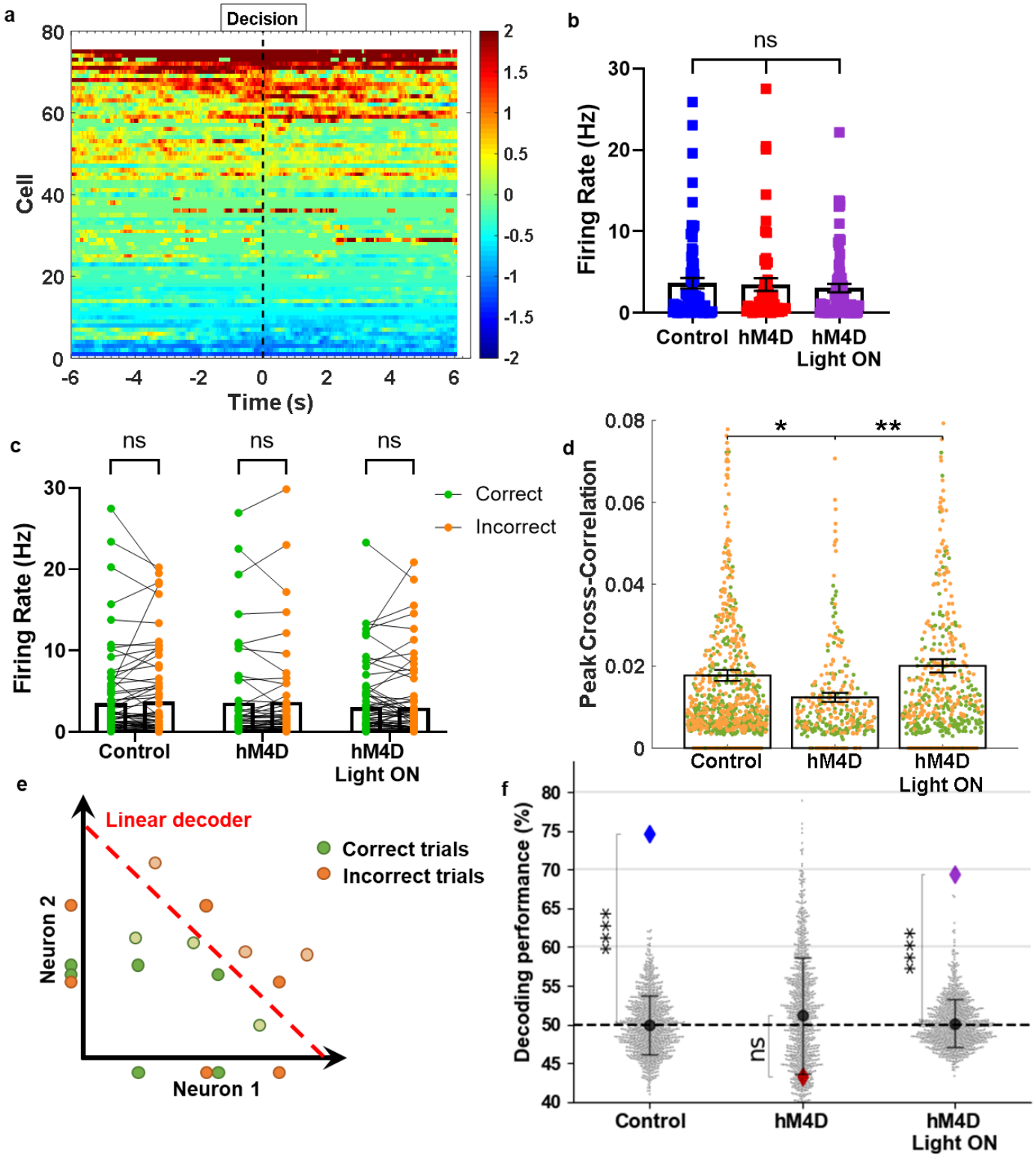

Figure 3.15. Adolescent thalamic activity is required for mPFC cellular encoding of ASST trial outcome. (a) Control Light OFF cell mean firing rate (FR) during EDSS, z-scored,

normalized to the ITI. Time in s represents time before and after the decision point (dashed black line). Color scale represents z-score for each time bin. (b) FR during the trial across the different experimental conditions showed no changes in population activity. Control Light OFF: n=8 animals, 75 cells, 3.650±0.639 Hz; hM4D Light OFF: n=12 animals, 55 cells, 3.487±0.777 Hz; hM4D Light ON: n=13 animals, 71 cells, 3.058±0.516 Hz; 1-way ANOVA, F(2,194)=0.2493, p=0.7796. Dots represent individual cells; lines represent mean ± SEM. (c) FR during correct rule and incorrect rule trials for cells from control Light OFF animals (left), adolescent-inhibited hM4D Light OFF animals (center), and thalamic-activated hM4D animals (right) show no differences in FR for different trial types. Dots represent individual cells, lines connecting FR for correct and incorrect trials. Control Light OFF: FR during Correct: 3.570±0.647 Hz, Incorrect: 3.744±0.630 Hz; paired t-test: t=0.6546, df=71, p=0.5148; hM4D Light OFF: Correct: 3.607±0.859 Hz, Incorrect: 3.676±0.873 Hz; paired t-test: t=0.3174, df=48, p=0.7523; hM4D Light ON: Correct: 3.058±0.519 Hz, Incorrect: 3.023±0.550 Hz; paired t-test: t=0.1539, df=70, p=0.8781. (d) Peak cross-correlation values for each pair of cells within an animal during correct (green) and incorrect (orange) trials across experimental conditions shows decreased cross-correlations in adolescent-inhibited hM4D Light OFF animals compared to both control Light OFF and rescued thalamic activation animals. This graph has been truncated along the y-axis to better demonstrate the mean and SEM. The complete distribution, along with the firing patterns of the truncated cells, in Figure 3.16. Control Light OFF: n=6 animals, 73 cells, 507 cell pairs, 0.0177±0.0430; hM4D Light OFF: n=9 animals, 52 cells, 181 cell pairs, 0.0124 ±0.0212; hM4D Light ON: n=11 animals, 69 cells, 327 cell pairs, 0.0201±0.0414; linear mixed effects model, fixed effect of group: Control Light OFF vs. hM4D Light OFF: *p=0.041622; hM4D Light OFF vs. hM4D Light ON: **p=0.0090838. Bars with error represent mean ± SEM. Individual dots represent cell pair correlations for each trial outcome type. (e) Schematic of the linear decoder. For a hypothetical pair of neurons, neither cell's firing rate alone shows a strong difference between correct and incorrect trial firing (dots along the x and y axes). However, when plotted together, it is possible to train a linear decoder (red dashed line) to discriminate between trial outcomes. With this training, we can then test the decoder on additional trials (lightly shaded circles). In this example, the linear decoder performs at 100%. (f) Decoding trial outcome using FR during the EDSS. Decoder performance is significantly above chance for control Light OFF animals, at chance for hM4D Light OFF animals, and rescued by acute thalamic activation. Actual decoder performance in colored diamonds (Control Light OFF: blue; hM4D Light OFF: red; hM4D Light ON: purple). Shuffled trial outcomes show chance decoder performance, mean ± standard deviation (black circles and error bars) and individual shuffles (grey circles). Control Light OFF: n=4 animals, 60 cells, 1000 shuffles, actual performance: 74.71%, shuffled performance: 49.95±3.75%, ****p=3.9604e-11; hM4D Light OFF: n=7 animals, 45 cells, 1000 shuffles, actual performance: 43.25%, shuffled performance: 51.13±7.49%, p=0.2926; hM4D Light ON: n=9 animals, 61 cells, 1000 shuffles, actual performance: 69.41%, shuffled performance: 50.15±3.08%. *p<0.05, **p<0.01, ****p<0.0001

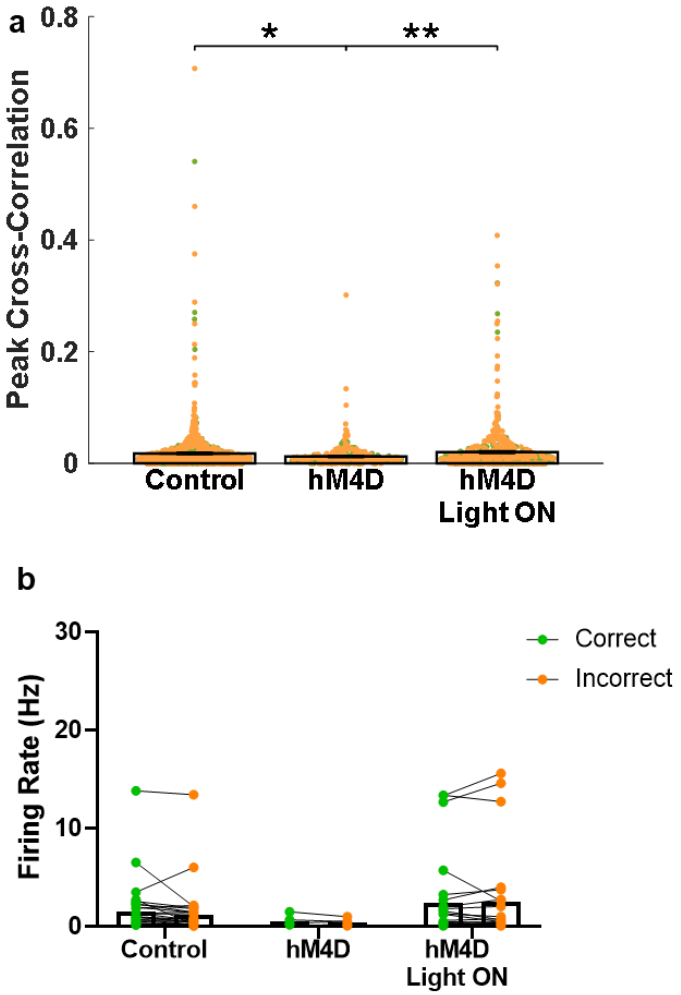

Figure 3.16. Peak cross-correlation values for all cell pairs. (a) Un-truncated plot with peak cross-correlations from all cell pairs for control, hM4D, and hM4D light ON groups. Statistics are as represented in the truncated version in Figure 3.15. Bars and error represent mean ± SEM. (b) Firing rates of cells that had a peak cross-correlation above 0.08 (the cut-off used for the graph in Figure 3.15). These cells do not show a particular pattern of firing across correct and incorrect trials. Each dot represents cell firing rate for each trial type, lines connecting each cell's FR for correct and incorrect trials. Control: n=33 cells with peak cross-correlation above 0.08 from 6 animals; hM4D: n=6 cells from 3 animals; hM4D Light ON: n=26 cells from 5 animals.

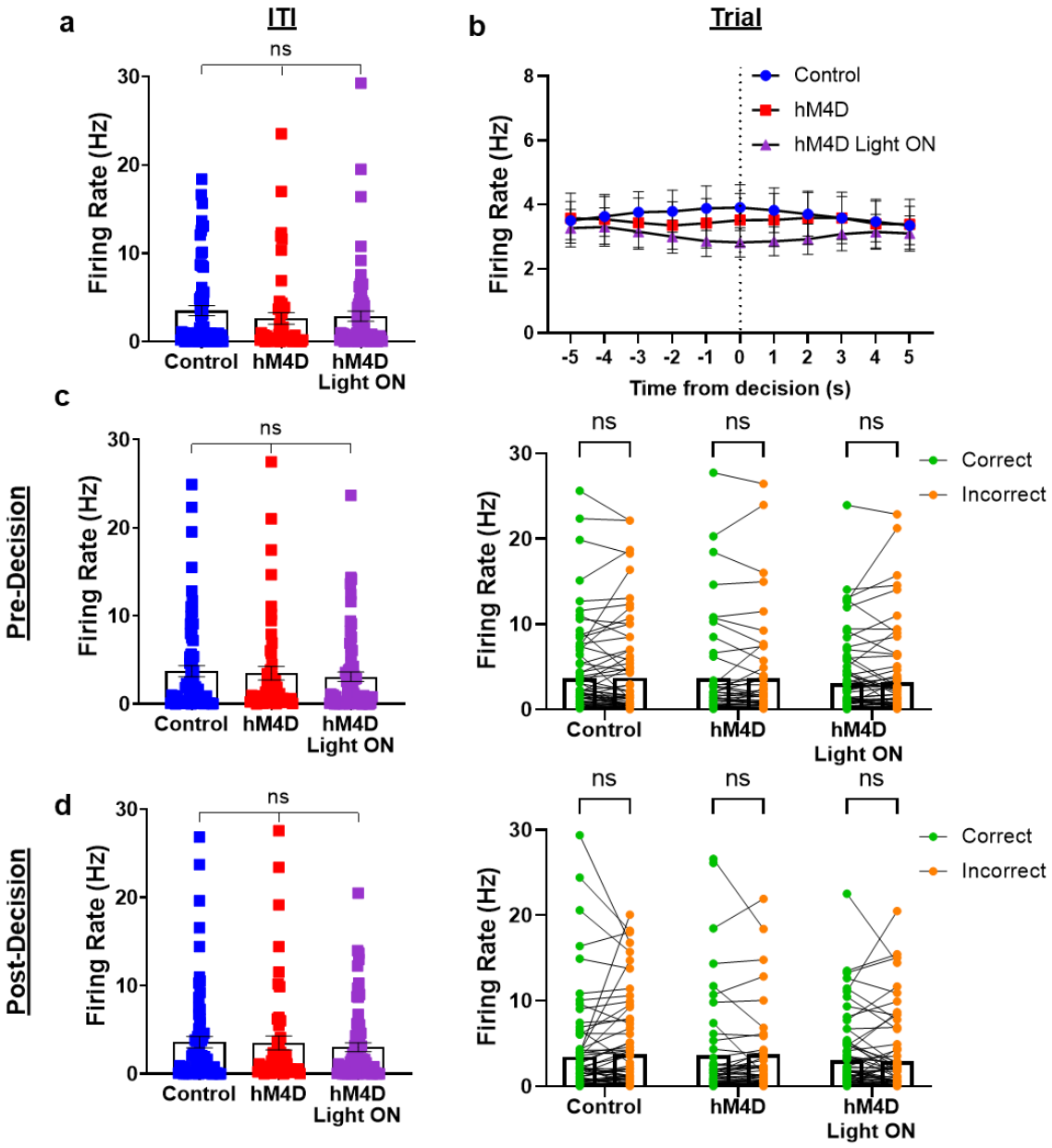

Figure 3.17. Raw firing rates during different phases of EDSS trials. Raw firing rates show no differences between groups across different epochs of the EDSS: (a) during the ITI (1-way ANOVA, F(2,194)=0.5915, p=0.5545), (b) over the course of the trial (overlapping 2s bins, with x-axis labels depicting the middle of each bin; 2-way rmANOVA, effect of group F(2,194)=0.2743, p=0.7604; dots and lines represent mean ± SEM), during the (c) pre-decision (all trials: 1-way ANOVA, F(2,194)=0.2492, p=0.7797; correct vs. incorrect trials: 2-way rmANOVA, effect of group F(2,189)=0.2507, p=0.7785, effect of trial type F(1,189)=0.1220, p=0.7273, effect of group x trial type F(2,189)=0.02524, p=0.9751; Holm-Sidak post-hoc correct vs. incorrect, Control: p=0.9962; hM4D: p>0.9999; hM4D Light ON: p=0.9707) and (d) post-decision (all trials: 1-way ANOVA, F(2,194)=0.2433, p=0.7843; correct vs. incorrect trials: 2-way rmANOVA, effect of group F(2,189)=0.3826, p=0.6826, effect of trial type F(1,189)=0.2501,

p=0.6176, effect of group x trial type F(2,189)=0.5463, p=0.5800; Holm-Sidak post-hoc correct vs. incorrect, Control: p=0.6988; hM4D: p=0.9761; hM4D Light ON: p=0.9475) periods, both across trial types (left) and between correct and incorrect trials (right). Dots represent individual cells; lines either represent mean ± SEM or connect correct and incorrect trials.

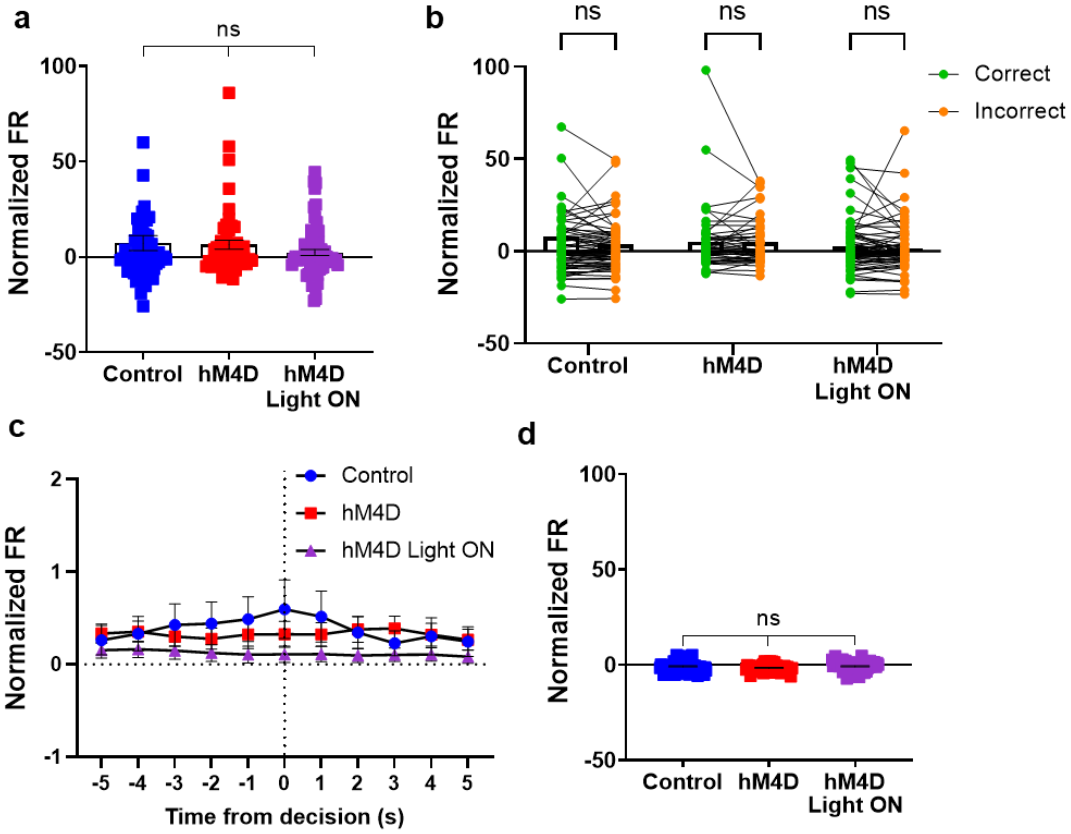

Figure 3.18. Normalized firing rates across different EDSS trial types and phases. Firing rates normalized to the ITI show no differences between groups across different epochs of the EDSS: (a) during the trial (1-way ANOVA, F(2,194)=0.8801, p=0.4164), (b) between correct and incorrect trials (2-way rmANOVA, effect of group F(2,189)=0.7554, p=0.4712, effect of trial type F(1,189)=1.521, p=0.2189, effect of group x trial type F(2,189)=0.7342, p=0.4812; Holm-Sidak post-hoc correct vs. incorrect, Control: p=0.2067; hM4D: p=0.9981; hM4D Light ON: p=0.9848), (c) over the course of the trial (overlapping 2s bins, with x-axis labels depicting the middle of each bin; 2-way rmANOVA, effect of group F(2,194)=0.9097, p=0.4044; dots and lines represent mean ± SEM), and (d) during the ITI (1-way ANOVA, F(2,194)=2.533, p=0.0821). Dots represent individual cells; lines either represent mean ± SEM or connect correct and incorrect trials.

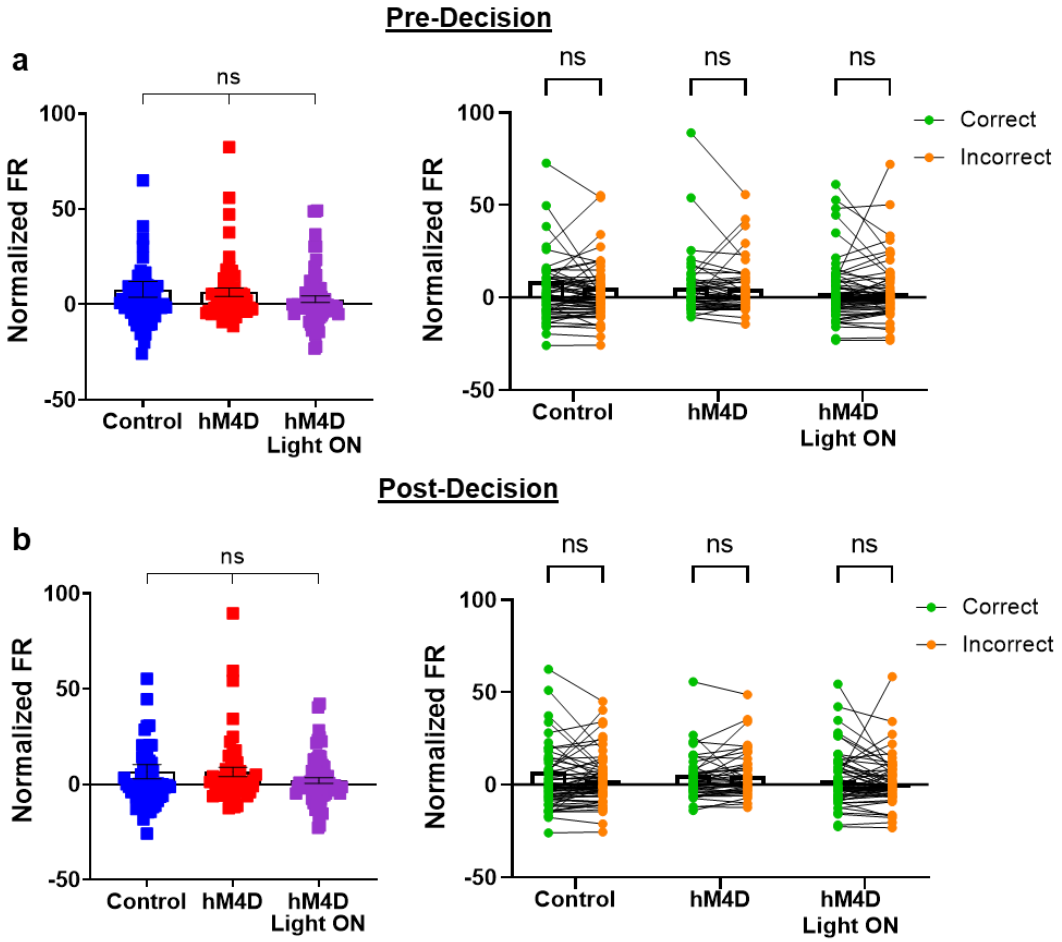

Figure 3.19. Normalized firing rates during different phases of EDSS trials. Firing rates normalized to the ITI show no differences between groups across different epochs of the EDSS: during the (a) pre-decision (all trials: 1-way ANOVA, $F(2,194)=0.8216$, $p=0.4413$; correct vs. incorrect trials: 2-way rmANOVA, effect of group $F(2,189)=0.6661$, $p=0.5149$, effect of trial type $F(1,189)=0.5679$, $p=0.4520$, effect of group x trial type $F(2,189)=0.4469$, $p=0.6403$; Holm-Sidak post-hoc correct vs. incorrect, Control: $p=0.5151$; hM4D: $p=0.9983$; hM4D Light ON: $p>0.9999$) and (b) post-decision (all trials: 1-way ANOVA, $F(2,194)=0.9407$, $p=0.3921$; correct vs. incorrect trials: 2-way rmANOVA, effect of group $F(2,189)=0.9687$, $p=0.3815$, effect of trial type $F(1,189)=1.702$, $p=0.1936$, effect of group x trial type $F(2,189)=0.6456$, $p=0.5255$; Holm-Sidak post-hoc correct vs. incorrect, Control: $p=0.2171$; hM4D: $p=0.9994$; hM4D Light ON: $p=0.9347$) periods, both across trial types (left) and between correct and incorrect trials (right). Dots represent individual cells; lines either represent mean ± SEM or connect correct and incorrect trials.

Behavioral outcomes may also be understood by analysis of multi-neuronal activity in the mPFC (Narayanan & Laubach, 2009; Stefanini et al., 2020; Yuste, 2015). Previous studies have highlighted the benefits of analyzing firing rates across multiple neurons to better elucidate

task behaviors, contexts, and outcomes (Stefanini et al., 2020). We therefore chose to analyze the mPFC cell activity as a neural ensemble.

First, we were interested in the correlation between the firing of cells. We therefore analyzed cross-correlations between the firing of each cell, finding a peak correlation during the EDSS trials for each pair of cells. Adolescent thalamic inhibition reduced peak cross-correlations, and they were recovered following acute thalamic SSFO activation (Figure 3.15d).

We also employed a linear decoder to elucidate differences in firing for trials that have different outcomes at the network-level (Figure 3.14e). Taking the firing rates for all cells in an experimental group across all trials, we trained a linear decoding algorithm using 50% of all trials for each cell to predict whether the behavioral outcome would yield a correct or incorrect trial. We then tested the decoder on the other 50% of trials to determine whether we could predict trial outcome based on cell firing rates. To determine chance performance, we employed the same decoding algorithm using randomly shuffled trial outcomes, repeated 1000 times (Bernardi et al., 2020). Employing this decoder on the control group showed a resulting performance that was significantly better than chance, at 74.71% accuracy (Figure 3.14f). This finding is eliminated following adolescent thalamic inhibition, where the decoder was no better than chance at 43.25% accuracy. Crucially, acute thalamic enhancement rescued the decoder performance to 69.41% accuracy.

Of note, no subset of neurons contributed more to the decoder performance, with an even distribution across the populations in all three groups (Figure 3.20a, b). Similarly, the decoding performance discrepancies across groups are visible with randomly selected subgroups of neurons. The pattern can be seen with as few as 5 neurons (Figure 3.20c). Moreover, the control decoding performance was not seen when applied to trials in the IA

portion of the ASST (Figure 3.20d), indicating the specificity of the role of the mPFC during the EDSS.

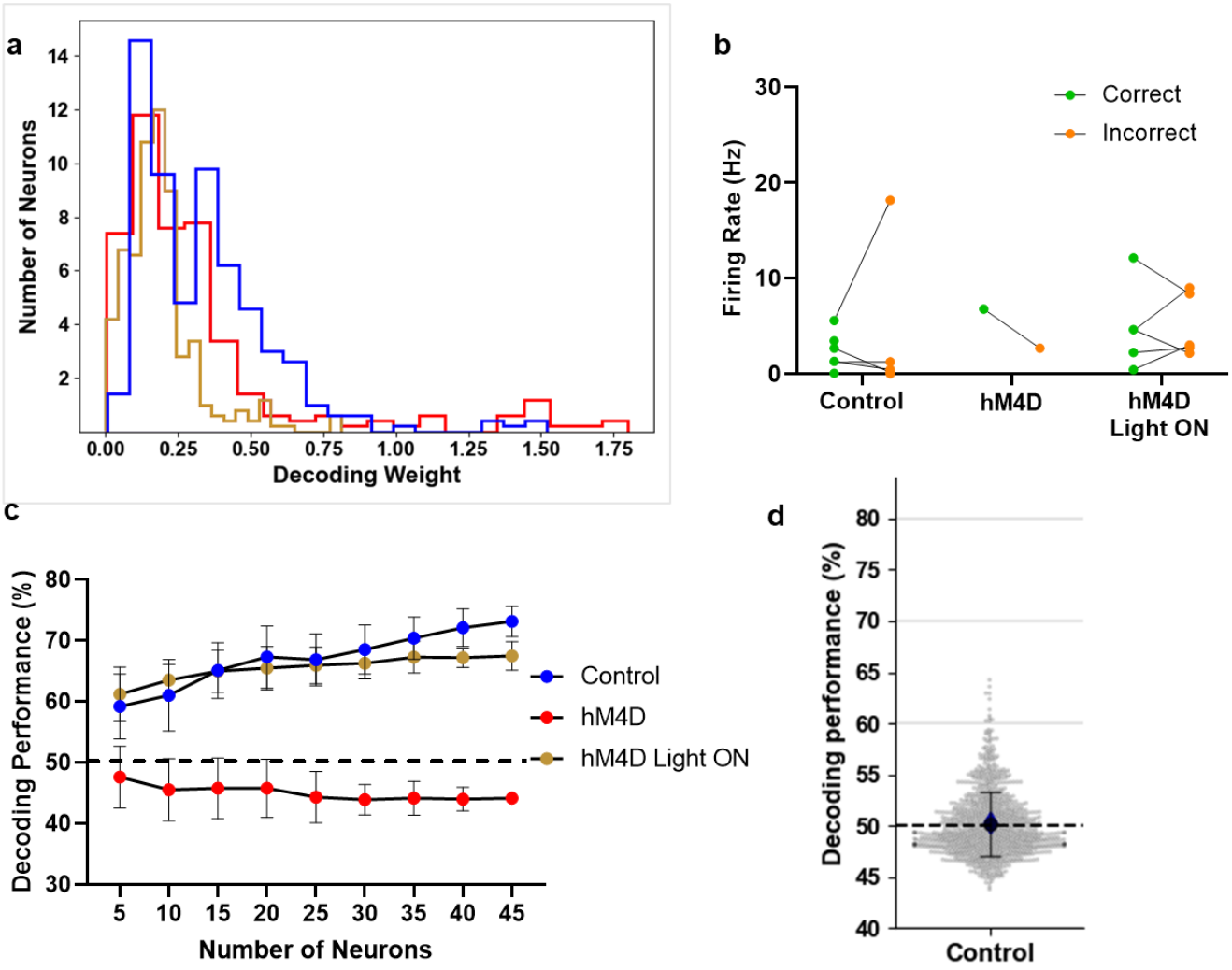

Figure 3.20. The decoding performance does not depend on a particular subset of cells. (a) Histogram of control (blue), hM4D (red), and hM4D Light ON (gold) cell decoding weights show the distribution of the contributions across cells is unchanged across groups, with few cells in each group contributing more than the general population. (b) Firing rates of cells that had a significantly elevated decoding weight relative to the shuffled data. There are very few cells (<10% for each group) that contribute significantly more than when shuffled, and further, these cells do not show a particular pattern of firing across correct and incorrect trials. Each dot represents cell firing rate for each trial type, lines connecting each cell's FR for correct and incorrect trials. Control: n=7 cells from 3 animals; hM4D: n=1 cell from 1 animal; hM4D Light ON: n=5 cells from 2 animals. (c) The decoder performance was calculated using randomly selected subgroups of neurons, repeated 25 times for each multiple of 5 neurons. Each point represents mean performance for the 25 repetitions of random selection, with error bars representing standard deviation. Significant separation between hM4D and both Control and

hM4D Light ON groups is already seen with 5 neurons. Chance performance at 50% shown with the dashed black line. 2-way rmANOVA Holm-Sidak post-hoc for each chunk, analysis with 5 neurons: Control vs. hM4D: $p<0.0001$, Control vs. hM4D Light ON: $p=0.1557$, hM4D vs. hM4D Light ON: $p<0.0001$. (d) Decoding performance (blue diamond) is no better than chance for control animals during the IA portion of the ASST. Black dot and lines represent mean and standard deviation of shuffled decoding performance; grey circles represent individual shuffles. n=3 animals, 47 cells, 1000 shuffles; actual performance: 50.35%, shuffled performance: 50.13±3.14%, $p=0.9438$.

Together, these findings show that adolescent thalamic inhibition disrupts prefrontal encoding of EDSS task outcome in adulthood while decreasing correlated activity between prefrontal neurons. This disruption can be rescued by acute thalamic activation during adulthood.

3.4 Discussion

3.4.1 Adolescence is a sensitive period for the development of thalamo-mPFC circuitry

Thalamic input activity has been shown to be important for sensory cortex maturation, including the visual cortex (Caras & Sanes, 2015; de Villers-Sidani et al., 2007; Takesian & Hensch, 2013b; Wiesel & Hubel, 1963). More recent studies have also begun to explore how neuronal activity shapes the development of higher cognitive structures, such as the medial prefrontal cortex (mPFC) (Bitzenhofer et al., 2021a; Canetta et al., 2021; Larsen & Luna, 2018a). Primarily, these studies have focused on changes to intrinsic components of mPFC circuitry, such as interneuron or layer II/III pyramidal neuron activity (Bicks et al., 2020; Bitzenhofer et al., 2021b; Canetta et al., 2021), or the effects of changes to frontal activity on other cortical regions (Nabel et al., 2020). Some have also highlighted similarities between mechanisms found in sensory sensitive periods and mPFC adolescent development, including BDNF expression, NMDA receptor changes, and the formation of perineuronal nets (Baker et al., 2017; Flores-Barrera et al., 2014; Hill et al., 2012; Larsen & Luna, 2018b). This paper is the

first to explore whether afferent input from the thalamus shapes cortical maturation and whether inhibition of thalamic activity leads to long-lasting changes in mPFC function and behavior.

We found that thalamic inhibition during adolescence leads to persistent impairments in mPFC circuit function and cognitive behaviors in adulthood. Specifically, we observed impairments in two mPFC-dependent behavioral tasks assessing the acquisition of a non-match to sample rule and attentional set shifting. These changes were associated with a decrease in cortical excitability. We determined that adolescence is a sensitive period because the impairments in behavior and excitability were not observed following a comparable thalamic inhibition during adulthood. These results indicate that excitatory activity from the thalamus during adolescence is essential for mPFC and thalamo-mPFC development. This mirrors the findings in sensory sensitive periods, where thalamo-cortical inputs are compromised following sensory deprivation, ultimately leading to cortical restructuring (Fagiolini & Hensch, 2000a; Hensch, 2004; Wiesel & Hubel, 1963).

3.4.2 Adolescence is a key period of cortical maturation

While sensitive periods in sensory systems often occur during very early postnatal development (Caras & Sanes, 2015; de Villers-Sidani et al., 2007; Wiesel & Hubel, 1963), we found that adolescence is a sensitive period for mPFC and thalamo-mPFC development. Adolescence is known to be a period of vulnerability in the development of psychiatric disorders such as schizophrenia in humans (Insel, 2010; Morgunova & Flores, 2021; Sakurai & Gamo, 2019; Weinberger & Berman, 1996). Moreover, functional imaging studies have shown that thalamo-prefrontal hypoconnectivity, a finding in patients with schizophrenia, is already present in young adolescents at clinical high risk for the disorder (Anticevic et al., 2015; Giraldo-Chica et al., 2017; Marenco et al., 2012; Mitelman et al., 2005; Pinault & Deschenes, 1998; Woodward & Heckers, 2016a; Woodward et al., 2012). We chose to inhibit thalamic activity in mice during the

P20-50 window because it is known that the mPFC and thalamo-cortical projections are maturing during this time (Bitzenhofer et al., 2020; Caballero et al., 2014; Caballero et al., 2020; Chini & Hanganu-Opatz, 2021; Delevich et al., 2021; Goodwill et al., 2018; Konstantoudaki et al., 2018; Miyamae et al., 2017a; Paus et al., 2008; Yang et al., 2014b). In rodents, the volume of the mPFC peaks around P24 after which point it decreases, reflecting a period of dendritic pruning in mPFC pyramidal neurons, which peaks around P30 (Marmolejo et al., 2012; Pattwell et al., 2016; Van Eden & Uylings, 1985; Zuo et al., 2005). It has been postulated that this volumetric change and pruning could result in part from refinement of thalamo-cortical synaptic contacts during this period (Ferguson & Gao, 2014). Furthermore, one hypothesis originally presented by Feinberg states that in schizophrenia aberrant activity-dependent pruning during adolescence may lead to persistent changes in prefrontal circuit function (Feinberg & Campbell, 2010). Although we did not study the effects of thalamic inhibition on cortical pruning, we show that decreased thalamic input activity is important for cortical circuit maturation. Future studies should address how much altered pruning contributes to the anatomical and slice physiological changes described here.

In addition to dendritic pruning, the mPFC also undergoes changes in myelination and interneuron development, which together promote emergent changes in network activity and behavioral functionality (Caballero et al., 2014; Paus et al., 2008; Uhlhaas & Singer, 2011). Therefore, the P20-50 window represents a possible period of heightened thalamo-cortical projection refinement in normal development, which may in turn affect multiple other components of prefrontal development.

Our work does not explain how thalamic inhibition immediately alters mPFC or thalamo-mPFC function during adolescence, as we focused on the long-term consequences measured in the adult animal. Recent work has investigated the mechanisms at play during adolescence in

control cortical function (Nabel et al., 2020). Other studies have explored homeostatic plasticity in sensory systems following changes in activity (Wen & Turrigiano, 2021; Wu et al., 2021). They found that different forms of plasticity (e.g. changes in intrinsic excitability and synaptic excitation and inhibition) occur at different developmental stages. However, these effects on plasticity were only analyzed within 1 or 2 days after the change in activity or during the developmental period, and the persistence of these effects remains unknown. Future studies will address the mechanisms involved in adolescent development of the thalamo-mPFC circuit in controls as well as immediate plasticity mechanisms in the mPFC that are induced by thalamic inhibition during adolescence.

3.4.3 Adolescent thalamic inhibition impairs thalamo-cortical projections

Thalamic projections to the mPFC are a crucial source of excitatory input to mPFC pyramidal cells. Following adolescent thalamic inhibition, we found reduced mPFC pyramidal excitability in adulthood. Due to the reduction in spontaneous excitatory post-synaptic current frequency, but not amplitude, we hypothesized that this change was primarily driven by a reduction in pre-synaptic inputs and that decreased inputs from the thalamus may contribute to this change.

We were able to confirm this hypothesis through retrograde labelling. Adolescent thalamic inhibition led to a reduction in thalamo-mPFC projection cell density. However, this intervention had no effect on mPFC-projecting cells from other subcortical regions, such as the BLA, indicating specificity to thalamo-cortical projections. This result is distinct from what has been observed after early developmental subcortical lesions, which showed a compensatory increase in BLA-mPFC projections following early postnatal (P7) ventral hippocampal lesions (Guirado et al., 2016). We believe this thalamo-mPFC projection reduction is due to a decrease in axonal arborization rather than thalamic cell numbers because DAPI staining in the thalamus

was unchanged. Moreover, before adolescence, the thalamus has already undergone a period of heightened apoptosis around P13, further supporting the notion that inhibiting the thalamus during adolescence comes primarily at a period of thalamo-cortical synaptic refinement (Ferguson & Gao, 2014; Rios & Villalobos, 2004). Since we used bilateral injections of retrograde virus to investigate the impact of developmental thalamic inhibition on cortical projections, we were unable to determine whether there were any changes to cortico-cortical contralateral projections. Future studies could examine whether intra-cortical connectivity is also affected.

We demonstrated that non-specific acute thalamic activation in adulthood following adolescent thalamic inhibition was sufficient to rescue the behavioral cognitive deficit. However, we also found that this restored cognitive ability was not long-lasting as there was no residual effect 10 days following the thalamic activation. Thus, it is unlikely that a one-time thalamic activation is sufficient to regrow the lost thalamic inputs. Rather, it simply boosted activity of the remaining thalamic projections, further pointing to a non-specific role for these inputs.

3.4.4 Task-evoked oscillatory activity cannot explain the behavioral outcomes

Our previous studies have shown the importance of task-induced gamma for predicting behavioral performance during EDSS and that this signal can be persistently disrupted following adolescent inhibition of mPFC PV interneurons (Canetta et al., 2021). Here, we also found that mPFC gamma power was correlated with behavioral performance in control animals, with elevated gamma in correct trials compared with incorrect trials, but this pattern was not affected by adolescent thalamic inhibition. Consistent with the unchanged gamma power in developmental thalamic inhibition mice, we did not find any deficits in cortical inhibition in adult mice that experienced adolescent thalamic inhibition, as we had observed following adolescent

PV inhibition (Canetta et al., 2021). This suggests that the long-term consequences of adolescent thalamic inhibition may not necessarily involve cortical PV interneurons.

Beta oscillatory activity has also previously been identified in thalamo-prefrontal manipulations, often in the context of working memory behaviors (Bolkan et al., 2017; Parnaudeau et al., 2013). While we did find task-induced beta oscillations, these were not correlated with behavioral outcome in controls and were not affected by adolescent thalamic inhibition.

Altogether, these data suggest that, despite reduced thalamic inputs to the mPFC, oscillatory measures of the thalamo-mPFC circuitry cannot explain the deficits observed during the EDSS behavior following adolescent thalamic inhibition. Thus, while these oscillations may be necessary for the proper execution of this task, they are not the only mechanism at play.

3.4.5 The thalamus supports local mPFC encoding of behavioral trial outcomes

To determine whether adolescent thalamic inhibition disrupts single unit activity in the adult animal, we examined average mPFC cell firing rates during EDSS trials but found no changes in individual neuron firing rates across different trial types or throughout the trial. However, recent theories suggest that multiple neurons can form ensembles that determine functional properties and outcomes, in ways beyond single neuron firing (Stefanini et al., 2020; Yuste, 2015).

When we studied the cross-correlations between cell pairs, we found that cross-correlations were disrupted following adolescent thalamic inhibition. This disruption was rescued by acute thalamic activation, pointing to a role of thalamic inputs in enhancing mPFC cellular communication. The cell-cell cross-correlations found in both correct and incorrect trials likely reflects the fact that the animals are learning throughout the task, receiving feedback during both types of trials. We hypothesize that the enhanced cross-correlation in control animals

allows the animals to incorporate this feedback during both correct and incorrect trials. By contrast, following adolescent thalamic inhibition, the decreased cross-correlation across both trial types speaks to the animals' inability to incorporate information during both correct and incorrect trials.

To further explore the effects on population encoding, we trained a linear decoding algorithm using a subset of trials to predict the EDSS trial outcome based on mPFC neuronal ensemble activity. Using this decoder, we were able to accurately predict trial outcome in control animals, but the decoding ability was entirely lost, down to chance levels, following adolescent thalamic inhibition. Of note, this inability to decode does not indicate that there is no information present in the activity. There are several technical reasons why we may see a chance level decoder performance, including a high level of noise. It is also possible that the hM4D animals are using a different circuit to ultimately perform the task due to inadequate thalamo-cortical circuitry, which could explain why the mPFC cell activity no longer helps to predict trial outcome. Importantly, mPFC neurons regained the ability to encode task outcome after thalamic stimulation, suggesting that thalamic excitation rescues outcome encoding and task performance.

Other thalamo-cortical circuits, namely in motor circuitry, have shown a task-specific role for both thalamic and cortical activity (Guo et al., 2017). In addition, modifying activity of different mPFC cell types have also demonstrated task-specific roles for mPFC cellular subpopulations (Kamigaki & Dan, 2017). Meanwhile, thalamic input to the mPFC has been hypothesized to non-specifically amplify or sustain local mPFC connectivity and encoding (Rikhye et al., 2018a; Rikhye et al., 2018b; Schmitt et al., 2017). Further analysis of previous work done in a T-maze working memory task shows that acute thalamic suppression leads to a mild, but significant, decrease in mPFC cell cross-correlations (Figure 3.21) (Bolkan et al., 2017). This study points

to a role of the thalamus as a non-specific amplifier of mPFC cellular encoding during this cognitive flexibility task in two major ways. First, adolescent thalamic inhibition disrupted thalamo-mPFC projections in adulthood, which coincides with both reduced mPFC cellular cross-correlations and disrupted mPFC task outcome encoding. Second, non-specific thalamic activation, even in the context of fewer thalamic projections, during the EDSS was sufficient to restore these cross-correlations and outcome-specific mPFC activity.

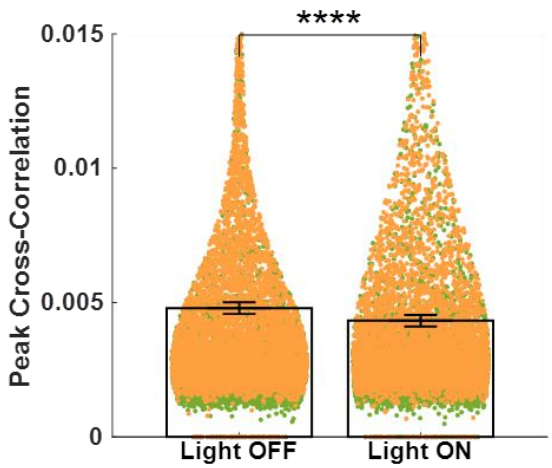

Figure 3.21. Acute thalamic inhibition during a working memory T-maze task decreases peak cross-correlation values in the mPFC. Peak cross-correlation values for pairs of mPFC single units during the delay period of a working memory T-maze task for correct (green) and incorrect (orange) trials, as described in Bolkan et al 2017 (Bolkan et al., 2017). Acute thalamo-mPFC inhibition (Light ON) during the delay shows decreased cross-correlations compared with the same cell pairs at baseline (Light OFF). n=9 animals, 891 cells, 5254 cell pairs; Light OFF: 0.0048±0.0002; Light ON: 0.0043±0.0002; linear mixed effects model, fixed effect of group: Light OFF vs. ON: ****p=3.587e-17. Bars with error represent mean ± SEM. Individual dots represent cell pair correlations for each trial outcome type. This graph has been truncated along the y-axis to better demonstrate the mean and SEM.

Prior studies have found that hyper-activation of mPFC neuronal populations can have detrimental effects, reflecting an inverted U-shaped pattern of mPFC neuronal activity and functional outcomes (Tanaka, 2008; Taylor et al., 2007). By enhancing thalamic activity, we found improved behavioral performance in the adolescent-inhibited animals and no change in performance in the control animals. Thus, thalamic SSFO activation, which facilitates activity of thalamic neurons that are engaged in the task, does not lead to the over-stimulation of mPFC

neurons that direct mPFC activation might. This finding further supports the theory of the thalamus as a facilitator of mPFC ensemble activity as this manipulation may modulate activity of a subset of mPFC neurons without increasing overall mPFC activity. This is also consistent with our finding that thalamic SSFO activation does not increase mPFC activity overall, with no increase in firing rate.

The mPFC itself has been intensively studied in cognitive flexibility tasks, such as the ASST. Some studies have pointed to the post-decision period as a crucial point for the mPFC during the EDSS (Cho et al., 2020; Spellman et al., 2021). While we found mPFC encoding throughout the trial, the decoder performed better when using post-decision versus pre-decision period firing activity within a trial, indicating that the mPFC may indeed be particularly important in the period following the choice.

3.4.6 The mPFC and the thalamus are interconnected in cognition

Many of the analyses and interpretations in this study have focused on the impact of adolescent thalamic inhibition on adult mPFC functioning. However, separating mPFC function from thalamic function in the context of cognition is almost impossible as the two regions are reciprocally connected. Thus, changing activity in one part of the circuit will change activity in the other part of the circuit. Indeed, in schizophrenia, prefrontal-dependent cognitive deficits are also linked to the thalamus and its reciprocal connectivity to the PFC (Giraldo-Chica et al., 2017; Mitelman et al., 2005; Pinault & Deschenes, 1998; Woodward et al., 2012).

In agreement with this tenet, we found that adolescent thalamic inhibition and cognitive deficits were linked with reduced thalamo-mPFC projections. Moreover, thalamo-mPFC projection-specific inhibition during adolescence led to similar behavioral deficits as GBX2-driven thalamic inhibition, pointing to the importance of these projections in cognitive function. However, the impact of adolescent thalamic inhibition did not extend to all aspects of thalamic

function. Beta and gamma oscillations in the thalamus were unaffected by adolescent thalamic inhibition. In addition, we found no changes in power in the epsilon band (>100 Hz), a metric for multi-unit activity (Belluscio et al., 2012; Keller et al., 2016; Park et al., 2021; Scheffer-Teixeira et al., 2013) (Figure 3.22).

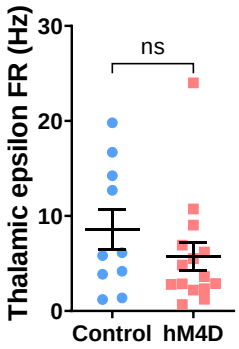

Figure 3.22. Adolescent thalamic inhibition does not impact thalamic multi-unit activity in the ASST. Mean thalamic epsilon firing rates during EDSS trials for each animal show no significant differences in thalamic activity for control or adolescent-inhibited hM4D animals. Control: n=10 animals, 8.606±2.114 Hz; hM4D: n=15 animals, 5.726±1.499 Hz; unpaired t-test, t=1.144, df=23, p=0.2643. Dots represent individual animals; lines represent mean ± SEM.

While our preliminary analysis of thalamic function showed no effects, it is possible that, in addition to mPFC and thalamo-mPFC differences, other changes intrinsic to the thalamus may still contribute to the behavioral deficits. However, it should also be noted that the exact role of the thalamus in these cognitive behaviors remains an area of debate (Block et al., 2007; Ferguson & Gao, 2018; Ouhaz et al., 2021; Schmitt et al., 2017). Therefore, future studies should probe thalamic function more directly during cognitive testing following adolescent thalamic inhibition.

3.4.7 Acute thalamic enhancement following developmental inhibition offers great promise for therapeutic interventions

Following thalamic inhibition during adolescence, we found persistent anatomical changes in thalamic projections to the mPFC. Nevertheless, we were able to rescue the

behavioral deficits by acutely enhancing activity in the thalamic in the adult mouse, even though this manipulation is unlikely to reverse the anatomical changes. We and others have previously shown that enhancing thalamic excitability during the delay of a prefrontal-dependent working memory and a 2AFC task enhanced performance in both tasks (Bolkan et al., 2017; Schmitt et al., 2017), while inhibiting the thalamus impaired mPFC-dependent contextual switching (Rikhye et al., 2018a). Our data suggest that the thalamus plays a broader function in amplifying mPFC activity that is not restricted to delay-containing cognitive processes. This result offers a major insight into potential therapeutic interventions in this circuit, as it indicates that even with persistent changes in circuit anatomy, a relatively non-specific thalamic excitation may still be able to improve behavior. Human imaging studies have pointed to the importance of the thalamo-prefrontal connectivity in cognitive functioning (Giraldo-Chica et al., 2017; Mitelman et al., 2005; Pinault & Deschenes, 1998; Woodward et al., 2012). In patients with schizophrenia, deficits in cognition have been related to hypoconnectivity between the thalamus and PFC, which is already seen in young adolescents before their diagnosis (Anticevic et al., 2015; Marenco et al., 2012; Woodward & Heckers, 2016a). Given the relevance of thalamo-prefrontal circuitry in psychiatric disorders like schizophrenia, this study offers key mechanistic insights into the etiology of, and potential therapies for, these disorders.

3.5 Methods

Animal Husbandry. All animal procedures were done in accordance with guidelines derived from and approved by the Institutional Animal Care and Use Committees at Columbia University and the New York State Psychiatric Institute. Animals were housed under a 12 h light-dark cycle in a temperature-controlled environment with food and water available ad libitum, unless otherwise noted. Heterozygous GBX2-CreERT (Jackson Labs, Stock #022135) males, back-crossed for at least 5 generations, were bred with C57/Bl6 females (Jackson Labs,

Stock #000664) to produce offspring that were used in all experiments. At postnatal day 10 (P10), tail samples were collected from offspring to genotype (Transnetyx, Inc). At P13, GBX2-CreERT heterozygous offspring were used for viral injections. These mice were housed in cages with the mother and littermates. At P15 and P16, all offspring were given intraperitoneal (i.p.) injections of tamoxifen (Sigma-Aldrich, T5648), dissolved in corn oil, at 75 mg/kg. All offspring were weaned at P28, and GBX2-CreERT heterozygotes were kept for experiments and group housed with same-sex littermates (5 mice/cage).

For thalamic inhibition, mice were given i.p. injections of clozapine-N-oxide (CNO), dissolved in 0.9% saline, at 1 mg/kg, twice per day. All mice were given CNO, regardless of viral vector or group. These injections took place every day P20-50 for adolescent inhibition and P90-120 for adult inhibition.

At P70, mice used for cell density studies were injected with virus, and mice used for *in vivo* optogenetic neurophysiology recordings during behavioral experiments were virally injected and implanted with optrodes. Implanted mice were subsequently housed in cages of 2-3 mice/cage.

All behavioral testing and *in vivo* recordings were done 40 days after the last CNO injection in adult mice (>P90). During behavioral training and testing, mice were food-restricted and maintained at 85% of their initial weight.

For the dual virus approach, C57/Bl6 males and females were bred together and all pups were used for the experiment. Surgeries were conducted at P13, and mice were given i.p. injections of JHU37160 (an alternative hM4D ligand to CNO (Bonaventura et al., 2019)), dissolved in 0.9% saline, at 0.01 mg/kg, twice per day. Again, all mice were given the ligand, regardless of viral vector or group. These injections took place every day P20-50.

Surgical procedures. For the viral injections at P13, mice were anesthetized with ketamine (4 mg/ml) and xylazine (0.6 mg/ml) and head-fixed in a stereotactic apparatus (Kopf). Mice were injected bilaterally in the midline thalamus with AAV5-hSyn-DIO-hM4D-mCherry (Addgene #44362) or a control virus, either AAV5-hSyn-DIO-EGFP (Addgene #50457) or AAV5-hSyn-DIO-mCherry (Addgene #50459) at a volume of 0.25 µl (0.1 µl/min).

For the dual virus approach surgeries at P13, mice were injected bilaterally in the midline thalamus as above, with AAV5-hSyn-DIO-hM4D-mCherry or the control, AAV5-hSyn-DIO-EGFP. They were also injected bilaterally in the mPFC with rgAAV-hSyn-Cre-WPRE-hGH (Addgene #105553) at a volume of 0.25 µl (0.1 µl/min).

The juvenile midline thalamus coordinates used were: -1.0 AP, ±0.25 ML, -3.0 DV (skull at bregma), and the juvenile mPFC coordinates used were: -0.92 AP, ±0.13 ML, -1.45 DV (skull at bregma).For the cell density study surgeries at P70, mice were anesthetized with ketamine (10 mg/ml) and xylazine (1 mg/ml) and head-fixed in a stereotactic apparatus (Kopf). Mice were injected bilaterally into the mPFC with retrograde AAV-CAG-GFP (Addgene #37825) at a volume of 0.25 µl (0.1 µl/min). The mPFC coordinates used were: +1.8 AP, ±0.35 ML, -2.5 DV (skull at bregma).

For the *in vivo* optogenetic neurophysiology experiments, mice were anesthetized with isoflurane and head-fixed in a stereotactic apparatus (Kopf). All mice were injected bilaterally into the midline thalamus with AAV5-CaMKII-hChR2(C128S/D156A)-EYFP (University of North Carolina Vector Core) at a volume of 0.4 µl (0.1 µl/min). The midline thalamus coordinates used for the viral injection were: -1.2 AP, ±0.35 ML, -3.2 DV (skull at bregma). During the same procedure, mice were also implanted with an optrode, consisting of a 36-channel narrow electronic interface board (Neuralynx, Bozeman, MT), a single stereotrode bundle, additional local field potential (LFP) wires, and 2 flat tipped, ferrule-coupled optical fibers (0.22 NA, 200 µm

diameter). Stereotrodes for recording spikes were made from 13 µM tungsten fine wire (California Fine Wire, Grover Beach, CA) and were coupled to one 50 µM tungsten wire for recording LFPs. This stereotrode bundle was then unilaterally targeted to the left mPFC. Another 50 µM tungsten wire was glued to the left optical fiber, extending 450 µm below the bottom of the fibers. Both fibers and the wire were implanted into the midline thalamus. For signal processing, skull screws placed over the cerebellum and olfactory bulb served as ground and reference, respectively, while spikes were referenced to a local mPFC stereotrode wire. Coordinates were as follows: mPFC: +1.85 AP, -0.35 ML, -1.4 DV (brain); midline thalamus: -1.2 AP, ±0.3 ML, -2.7 DV (brain).

All coordinates are in mm relative to bregma (AP, ML) and skull or brain surface (DV) where specified.

Behavioral procedures. All behavioral tasks were conducted during the light cycle. At P90, mice were gradually restricted to 85% of their body weight.

Non-Match to Sample working memory task: The task was conducted as previously described in Benoit et al, 2020 (Benoit et al., 2020). Eight identical operant-conditioning chambers (ENV-307A; Med Associates, Georgia, VT) were used. The chamber measured 15.24 cm long x 13.34 cm wide x 12.7 cm high. Each chamber was housed in a sound-attenuated box and equipped with two retractable levers (ENV-312-3M) on the front wall (the 13.34 cm side), with one milk dipper between them (ENV-302RM-S). The back wall contained one noseport (ENV-313M) directly opposite to the milk dipper, which delivers 1 drop of evaporated milk (0.01 ml). A 1.0 A house light was positioned directly above the noseport. A computer (COM-106-NV, Intel i5-7400) controlled and recorded all experimental events and responses via an interface (MED-SYST-16e-V). Med-PC V programs were used to administer and record the task. Mice were shaped to the different parts of the operant task. They were first given 2 days of

habituation to the milk dipper, followed by 7 days of training to associate a lever press with a milk reward. Lastly, they were given 5 days of noseport training before beginning the acquisition stage of the behavior.

During acquisition, each trial began with the house light being turned on and an illuminated noseport to signal an initial noseport entry. The first noseport entry triggered the start of the sample lever presentation. During the sample phase, only one lever was presented in a pseudo-random order. After the sample lever press, the noseport was immediately re-illuminated (following a 0 second delay) signaling a second noseport entry. Following the second noseport entry, the choice phase began, and both levers were presented. If the animal pressed the opposite lever to the sample lever of that trial (non-match), the trial was recorded as "correct," and a dipper reward was given. If the animal pressed the same lever as the sample, the trial was recorded as "incorrect," and the dipper was not presented. This final step was followed by a 10 second inter-trial interval (ITI) during which the house light was turned off.

Acquisition was repeated every day with 120 trials per day; 60 trials with each lever presented as the sample, in a pseudo-random order. For this experiment, pseudo-random refers to a random distribution with the restriction that the same condition cannot be presented for more than 2 consecutive trials. Beginning on day 6 of acquisition, mice had a 5-second time limit in which to make the second noseport entry. This restriction allowed us to shape the animals' behavior to ensure a standardized length of delay between subjects. If the animal did not make a noseport entry in the time allotted, the trial was aborted and was omitted from the calculations. For the final 3 days of acquisition, the total number of trials was increased to 160 trials. Throughout the experiment, mice were given unlimited time to complete the required trials.

During the acquisition stage, all mice achieved a criterion level of performance, defined as 3 consecutive days above 70% correct.

Attentional Set Shifting cognitive flexibility task: The task was conducted as previously described in Canetta et al, 2016 (Canetta et al., 2016a). Mice were first habituated to the testing arena on day 1. On days 2-3, they were trained to dig in both bedding media (corn cob and paper pellet, both unscented) to obtain a food reward. Once the animals dug reliably when presented with both types of bedding, testing began. For each trial, mice were placed at the opposite end from 2 terra cotta pots containing different odor/medium combinations. For initial acquisition (IA), mice needed to learn that the cinnamon scent, not the paprika scent, predicted a Honey Nut Cheerio reward, irrespective of the bedding media. For the first 5 trials, mice could explore both pots until they found the reward, but the trial was only scored as correct if the animal initially chose the correct pot. From the 6^{th} trial onward, once the mouse began digging in a pot, the entrance to the area containing the other pot was closed off. Criterion was reached when the mouse made eight of ten consecutive correct choices. If the mouse did not meet criterion in 30 trials, the animal did not advance to the next stage (one animal from the adolescent manipulation hM4D group did not meet the IA criterion). If the mouse did reach criterion, extra-dimensional set shifting (EDSS) began. In the EDSS portion of the task, the animal needed to learn that the type of bedding medium (paper pellets, not corn cobs) predicted the Honey Nut Cheerio reward, irrespective of odor. Criterion was reached when a mouse made eight of ten consecutive correct choices.

For optogenetic experiments, mice completed the task twice, 10 days apart. Animals were randomized to receive the light ON or OFF on Run Day 1 or Run Day 2 during the EDSS portion of the task. For Run Day 1, the rules in the IA and the EDSS were as described above, with odor (cinnamon rewarded) predicting the reward in the IA and texture (paper rewarded)

predicting the reward in the EDSS. For Run Day 2, the rule in the IA was the same as the EDSS for Run Day 1, with paper rewarded. The rule in the EDSS for Run Day 2 was odor predicting the reward, with paprika rewarded. For the EDSS on the second run, mice that previously had the light ON for Run Day 1 had the light OFF and vice versa. There was no effect of Run Day on overall performance; therefore, the light conditions could be pooled across runs for analysis.

Optogenetic Parameters. In optogenetic stabilized step-function opsin (SSFO) experiments, for the light ON run, a 5 s blue light pulse (473 nm, 4 mW) was used for opsin activation prior to the first EDSS trial. The light was delivered via flat tipped 200 µm diameter, 0.22 NA fiber optics. To ensure continued opsin activation throughout the EDSS trials, the 5 s pulse was repeated between trials every 30 min.

Slice Electrophysiology. Whole-cell current and voltage clamp recordings were performed in layer 2/3 mPFC pyramidal cells and midline thalamic cells. Recordings were obtained with a Multiclamp 700B amplifier (Molecular Devices) and digitized using a Digidata 1440A acquisition system (Molecular Devices) with Clampex 10 (Molecular Devices) and analyzed with pClamp 10 (Molecular Devices). Following decapitation, 300 µM slices containing mPFC or midline thalamus were incubated in artificial cerebral spinal fluid (ACSF) containing (in mM) 126 NaCl, 2.5 KCl, 2.0 $MgCl_2$, 1.25 NaH_2PO_4, 2.0 $CaCl_2$, 26.2 $NaHCO_3$, and 10.0 D-Glucose, bubbled with oxygen, at 32°C for 30 minutes before being returned to room temperature for at least 30 minutes prior to use. During recording, slices were perfused in ACSF (with drugs added as detailed below) at a rate of 5 mL/min. Electrodes were pulled from 1.5 mm borosilicate-glass pipettes on a P-97 puller (Sutter Instruments). Electrode resistance was typically 3-5 MΩ when filled with internal solution consisting of (in mM): 130 K-Gluconate, 5 NaCl, 10 HEPES, 0.5 EGTA, 2 Mg-ATP, and 0.3 Na-GTP (for thalamic recordings; pH 7.3, 280

mOsm) or 130 mM Cs-Gluconate, 10 HEPES, 2 MgCl2, 0.2 EGTA, 2.5 MgATP, 0.3 NaGTP, and 5 Lidocaine N-ethyl bromide (for pyramidal cell recordings; pH 7.3, 280 mOsm).

Midline thalamic recordings: Animals were sacrificed at P35 or P105 after either receiving CNO for 2 weeks or not. hM4D (mCherry-tagged) or GFP-infected thalamic cells were identified by their fluorescence at 40x magnification under infrared and diffusion interference contrast microscopy using an inverted Olympus BX51W1 microscope coupled to a Hamamatsu C8484 camera. Intrinsic and active membrane properties (resting membrane potential, input-output firing frequency curve) were recorded in current clamp using the K-Gluconate intracellular solution detailed above before and after 10 µM CNO was bath applied to the slice.

mPFC recordings: Animals were sacrificed for recordings at P90 for the adolescent manipulation or P160 for the adult manipulation. mPFC pyramidal cells were visually identified based on their shape and prominent apical dendrite at 40x magnification under infrared and diffusion interference contrast microscopy using an inverted Olympus BX51W1 microscope coupled to a Hamamatsu C8484 camera. Spontaneous excitatory post-synaptic currents (sEPSCs) were recorded in voltage clamp at a holding potential of -55 mV and spontaneous inhibitory post-synaptic currents (sIPSCs) were recorded in voltage clamp at a holding potential of +10 mV. 60 seconds of the current recording for each condition was analyzed. Recordings were filtered with an eight-pole low-pass Bessel filter, and sEPSCs and sIPSCs were detected using MiniAnalysis (Synaptosoft). All event data was averaged by cell.

In vivo electrophysiology. *In vivo* electrophysiology recordings were performed while the animals were performing the attentional set shifting task. Field potential signals from the mPFC and midline thalamus were referenced against a screw implanted in the anterior portion of the skull above the olfactory bulb. Recordings were amplified, band-pass filtered (1-1000 Hz LFPs; 600-6000 Hz spikes) and digitized using a Digital Lynx system (Neuralynx). LFPs were

collected at 2kHz, while spikes were detected by online thresholding, collected at 32 kHz, and sorted off-line. TTLs were manually inserted to record the timing of relevant events (e.g., trial start, decision point, trial end).

Histology. Adult mice were deeply anesthetized with 100 mg/kg ketamine and 5 mg/kg xylazine (i.p.). For *in vivo* electrophysiology experiments, electrolytic lesions were induced at each recording site by passing current (50 µA, 30 s) through electrodes prior to perfusion. All animals were perfused with phosphate-buffered saline (PBS) followed by 4% paraformaldehyde in PBS. Brains were dissected out and post-fixed in 4% PBS overnight before being transferred to 1% PBS for long-term storage. Brains were sectioned serially at 40 µm for cell density studies, and 50 µm for all other experiments, on a vibratome (Leica, Buffalo Grove, IL, USA). The following primary antibodies were used: mCherry (rabbit-anti-dsred; Takara Bio, Mountainview, CA, USA; 632496, 1:250) or green fluorescent protein (GFP; Abcam, Cambridge, UK, ab13970, 1:1000). Primary antibody incubation was 48 hours at 4˚C. Alexa Fluor-conjugated secondary antibodies (Invitrogen, 1:1000) were used for secondary detection. Stained tissue slices were then mounted on slides with Vectashield mounting medium containing DAPI (Vector Labs). Viral expression was confirmed from mCherry or GFP staining, and locations of recording site lesions were confirmed under DAPI.

Stereology was used to assess retrogradely-labeled cell numbers in the midline thalamus and BLA in adult developmental manipulation and control animals for the cell density studies using StereoInvestigator software (MBF Biosciences, Williston, VT, USA). Every 3rd slice was used, and regions were traced using DAPI staining. During image acquisition and quantification, the investigator was blind to the treatment.

LFP and single-unit analysis. Neuralynx files containing LFP and spike data were imported into Matlab with Neuralynx MATLAB import/export package v 4.10.

LFP samples were notch filtered using the MATLAB Chronux package to remove 60 cycle noise (http://chronux.org/; rmlinesmovingwinc.m). Mechanical artifacts were eliminated by removing samples whose voltage was more than 3 standard deviations from the entire signal mean. The cleaned signal was then root-mean-squared. Power and coherence were calculated using the wavelet transformation package in MATLAB. These values were averaged over the relevant time windows (e.g., 6 s before the decision point). Frequency ranges were as follows: 40-90 Hz for gamma, 12-30 Hz for beta.

Single units were automatically clustered using Klustakwik (Ken Harris) based on spike sorting of the first two principal components, peak voltage and energy from each stereotrode channel. Clusters were then accepted, merged or removed based on isolation distance, visual inspection of feature segregation, inter-spike interval distribution, cross-correlation in spike timing for simultaneously recorded units, and stability across the recording session. From recordings during the optogenetic experiment, we isolated 75, 55, and 69 single units from the control, hM4D, and hM4D light ON groups, respectively.

To analyze the phase-locking of single cells in the mPFC with the LFP in the thalamus in the beta range, we calculated the pairwise phase comparison (PPC) (Vinck et al., 2010) of mPFC spikes to thalamic LFP. The LFP signal was first digitally bandpass-filtered (12-30 Hz) using a zero-phase-delay filter (filter0, K. Harris and G. Buzsaki), and the Hilbert transform of the bandpass-filtered signal was calculated to obtain the oscillatory phase. The magnitude of the phase-nonuniformity of spike times relative to the filtered LFP oscillation was then calculated for the 6 s before the decision point in correct and incorrect trials. Of note, we chose the period before the decision point given our previous findings in that window (Canetta et al., 2021). However, we found similar results when looking in the 6 s period after the decision point or the

full 12 s window. In order to avoid spuriously high or low PPC values, only units that fired at least 50 spikes in each condition were used.

Statistics. Statistical analysis and graph preparation for all data was done with Prism 9 software (Graphpad Software, San Diego, CA, USA) or custom scripts in MATLAB (Mathworks, Natick, MA, USA) and Python. One-way ANOVA, two-way repeated measures ANOVA, and unpaired or paired two-tailed t-tests were used to analyze slice physiology, behavior, cell density, and single unit firing rates. For the slice physiology acute CNO experiment, Holm-Sidak post-hoc analyses were used to compare the hyperpolarization upon bath application of CNO for all hM4D groups to the control. For the optogenetic behavior, Holm-Sidak post-hoc analyses were used to compare light off vs. light on outcomes.

To analyze differences in gamma power for each group, we fit linear mixed models with gamma power as outcome. The random effect was animal, and the fixed effect was either trial (ITI vs. trial) or trial outcome type (correct vs. incorrect). Power as a function of frequency was plotted by averaging the gamma power across the 6 s before the decision point. Mean power or coherence was calculated for those 6 s for the range of 40-90 Hz for gamma, or 12-30 Hz for beta. Of note, we chose the period before the decision point given our previous findings in that window (Canetta et al., 2021). However, we found similar results when looking in the 6 s period after the decision point or the full 12 s window.

For all cells for each experimental group, firing for all cells were binned into 50 ms windows. These firing rates were then smoothed by taking the average firing rate of the surrounding 5 bins (i.e., 250 ms). These smoothed firing rates were then used in the subsequent analyses, where indicated.

To represent z-scored firing rates, the mean and standard deviation was calculated for the firing rate for all EDSS ITI time bins. The smoothed firing rates for each time bin for the 12 s

surrounding the decision in each trial were calculated using the ITI mean and standard deviation. The mean z-score was then taken across all trials for each time bin.

Mean firing rates were taken for each cell across the 12 s surrounding the decision of each trial. Mean firing rates were calculated first for all trials. Then, the mean firing rate was taken for each trial outcome type (correct vs. incorrect). Paired t-tests were used to compare the firing rates across trial types.

For cross-correlations, firing rates were binned into 50 μs windows. For each trial, the 12 s surrounding the decision point was taken, and the spike train for each trial was concatenated with the trains for that cell and trial outcome type. The firing for each spike train was normalized to overall firing rate, and the Matlab function, xcorr, was then applied to all pairs of cells within each animal, using a maximum lag time of ±80 ms. The peak cross-correlation value for each cell pair was used in the analysis, with each cell pair having a peak cross-correlation during correct and incorrect trials. We then fit a linear mixed model with peak cross-correlation as outcome, fixed effects of group (control, hM4D, hM4D Light ON) and trial outcome type (correct vs. incorrect), and random effects of animal and cell. Of note, because the analysis requires cell pairs, certain animals were removed from the analysis if they had only one isolated cell (Control: 2 eliminated animals; hM4D: 3; hM4D Light ON: 2).

Decoder. The linear decoder was custom-written using Python. The smoothed firing rates for the 12 s around the decision (described above) were used for each trial, and the trial outcome (i.e., correct or incorrect) was also used in the decoder. The analysis was done using the trials from the EDSS (Figure 3.15f) or the IA portion of the task (Figure 3.20d). Of note, certain animals were removed from the analysis if they had fewer than 2 neurons or fewer than 2 of each trial outcome (EDSS: Control: 4 eliminated animals; hM4D: 5; hM4D Light ON: 4; IA: Control: 5).

The neural decoder algorithm was based on linear classifiers trained on pseudo-simultaneous population activity created by combining 50 ms-binned neural patterns recorded from different animals performing the same behavioral task. The decoding algorithm was cross-validated and tested against a null model with shuffled trial condition labels.

Cross-validation: We computed the decoding performance using a 20-fold cross validation (CV) scheme.

For each CV fold, we randomly selected half of the trials of each condition and used them to build pseudo-simultaneous (PS) activity (see below) which was used to train a Support Vector Machine (SVM) with a linear kernel to classify PS patterns into one of the two conditions.

Similarly, the remaining half of the trials were used to build PS activity that was used to test the trained SVM. The decoding performance was then assessed as the mean accuracy on the test set over the CV folds.

Pseudo-population: To build pseudo-populations, we randomly selected 50 ms binned neural patterns from training and testing trials of all animals and concatenated them to form a larger pseudo-simultaneous neural pattern. To obtain the training and testing data sets used in the cross-validation scheme, this procedure was repeated 10 x N times per condition, where N is the total number of neurons.

n-timebins decoding: To increase the signal to noise ratio of the decoder, we used a procedure where the decoder is trained to classify groups of n time bins sampled from the two conditions (n=1 corresponding to standard single time-bin decoding). In practice, this was done when building pseudo-population activity by randomly sampling n different time bins for each individual animal to build a single pseudo-simultaneous time bin. Unless specified otherwise, we used n=5.

Null model and *p*-value: All decoding performance values were tested against *M* repetitions of a null model by shuffling the condition labels of individual trials. After each shuffle of the labels, the exact same decoding procedure described above was repeated on the shuffled data. Unless specified otherwise, we used *M*=1000. The *p*-value associated to the decoding performance was computed by comparing the performance of the shuffled model to the performance of the data.

Implementation: The analysis was performed in Python3 by using the *decodanda* package and the *sklearn* implementation of SVM classifier.

Data availability. The data that support the findings of this study are available from the corresponding author upon reasonable request.

Code availability. Med-PC V, MATLAB, and Python code used for administering the behavior and analysis of the data that support the findings of this study is available from the corresponding author upon reasonable request.

Chapter 4: Conclusions and Future Directions

4.1 General Conclusions

Here, I have described experiments performed to explore the importance of adolescence in the development of the medial prefrontal cortex (mPFC), the mediodorsal nucleus of the thalamus (MD), and the MD-mPFC circuit. To accomplish this, I first summarized the previous literature on this topic in Chapter 1. Next, in Chapter 2, I outlined work done to develop a new, operant-based working memory task that is mPFC-dependent, high throughput, and has a relatively small exploratory component. In Chapter 3, I used this behavioral paradigm, among others, to discover the impact of adolescent thalamic inhibition on long-term functioning of the MD-mPFC circuit. I employed an innovative technique combining viral genetics and pharmacogenetics to transiently reduce activity in the MD and midline thalamus during specific time windows.

Using this model, I tested the effects of adolescent thalamic inhibition on adult functioning and found deficits in mPFC-dependent cognitive behavioral performance, mPFC cell excitability, MD-mPFC anatomical projection density, mPFC encoding of trial information, and mPFC single cell cross-correlational activity. The same intervention during adulthood had no long-term consequences, indicating that adolescence is a sensitive period, in which changes to thalamic input activity has persistent effects on the MD-mPFC circuit. Notably, acute thalamic enhancement during the cognitive behavior rescued the behavioral deficit as well as the mPFC cellular encoding and cross-correlational activity (Figure 4.1).

This work highlights the importance of thalamic activity during the adolescent period for subsequent adult functioning of the mPFC and the MD-mPFC circuit. Moreover, the rescue of

behavior and mPFC activity from acute thalamic activation points to the potential for effective treatments of cognitive dysfunction, even after a developmental insult.

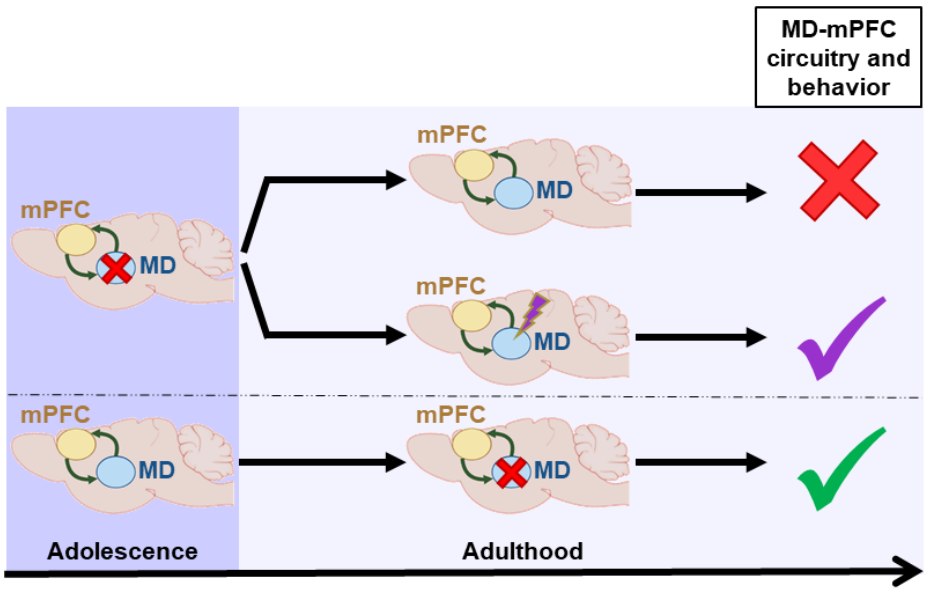

Figure 4.1. Model for adolescence as a sensitive period in the development of the MD-mPFC circuit. Transient MD inhibition during adolescence leads to persistent impairments in MD-mPFC dependent behaviors and circuitry. However, acute activation of the MD during behavior in adulthood can rescue these behavioral and physiological deficits. Meanwhile, transient MD inhibition during adulthood has no long-term consequences on MD-mPFC circuitry. These results point to a model in which adolescence is a sensitive period in the development of the MD-mPFC circuit, but acute interventions can still restore functioning during adulthood.

In this chapter, I will explore the implications of these findings and discuss future avenues of research in this field.

4.2 Behavioral tasks to study the mPFC and MD

4.2.1 An operant-based working memory task to study mPFC functioning

In Chapter 2, I described a newly developed operant-based delayed non-match to sample (DNMS) working memory task for mice, which has several advantages over the previously used maze-based tasks. First, this new operant task allows us to test mPFC functioning in a cognitive task that includes a smaller exploratory component and relies less on

spatial information than classical maze-based tasks. Second, animals can complete many more trials per day in the operant task compared with maze tasks due to the shorter trial lengths and smaller rewards, which provides the possibility of testing multiple different interventions over the course of a single session. Finally, with operant boxes, an experimenter can run several animals simultaneously, with very limited experimenter-induced bias during the behavioral task. Importantly, despite the differences between this operant task and the traditional maze-based tasks, this task is still mPFC-dependent, with impaired performance following an mPFC lesion, as described in Chapter 2 (Benoit et al., 2020).

The role of specific mPFC circuits in this operant task remains to be elucidated. In one maze-based task, the T-maze, MD-mPFC inputs are necessary for delay period maintenance, while vHip-mPFC inputs are essential for sample period encoding (Bolkan et al., 2017; Spellman et al., 2015), but it is unknown whether both inputs are required for this operant task. Acute inhibition of MD-mPFC or vHip-mPFC projections would address this question, allowing for further characterization of the operant task and a more thorough basis for comparing it to maze-based tasks.

The operant DNMS task has two main stages: (1) the acquisition stage, with no delay between the sample and choice lever presentations, and (2) the delay stage, with delays of 2s, 4s, 8s, and 16s between the sample and choice. While the mPFC lesion explored in Chapter 2 showed deficits in both stages of the task, the developmental manipulation from Chapter 3 only caused deficits in the first acquisition stage, but no changes in the second delay stage (Figure 3.4).

One explanation for the milder behavioral phenotype found after the developmental inhibition is that it may have less of an impact on adult mPFC function than an excitatory lesion. Following adolescent thalamic inhibition, mPFC pyramidal cells demonstrate a reduction in the

frequency of sEPSCs, a finding that can be explained (at least in part) by a reduction in the density of MD-mPFC projections. However, we observed no evidence of changes in other mPFC circuits, with no differences in the densities of BLA-mPFC or vHip-mPFC projections (Figure 3.8) or changes in sIPSCs of mPFC pyramidal cells (Figure 3.7). There may be additional changes to mPFC circuitry, such as changes in cortico-cortical projections or recurrent excitation within the cortex. These are two metrics that we did not evaluate but should be explored down the line. Even so, the mPFC circuitry is likely less disrupted following adolescent thalamic inhibition than following the mPFC lesion, which causes gross anatomical changes and cell death, likely implicating many additional mPFC-related circuits (Figure 2.1). It is therefore possible that adolescent thalamic inhibition leaves enough mPFC function intact for the animals to perform the delay stage of the task, while the excitotoxic lesion may not.

Furthermore, due to the structure of the task, all animals progress from the first to the second stage at the same time. Because of natural animal variability, some animals reach the criterion in the first stage more quickly than others. As a result, to maximize consistency across animals, all mice were trained in the acquisition stage until every animal reached a high performance, with many animals performing at a high level for several days after reaching the criterion. This overtraining, in combination with having more aspects of mPFC circuitry intact, may have aided the development of an alternative strategy for performing the task by the end of the acquisition stage, resulting in unimpaired performance during the delay stage. Of course, the lesioned animals may have also developed a strategy using circuits that do not involve the mPFC, but the adolescent-inhibited animals would have had more options given the milder mPFC disruption. The nature of an additional circuit would still need to be identified, with a major question about whether some residual mPFC function is required for its proper functioning.

Overall, the operant DNMS task is still a new behavioral paradigm, and future work should explore the numerous potential circuits that could be involved in proper task execution. In addition to the MD-mPFC or vHip-mPFC inhibition experiments described above, other experiments could include manipulation of other aspects of mPFC circuitry, such as interneuron or layer-specific disruptions. Furthermore, *in vivo* recordings of mPFC and MD activity during the task would give important insights into the mechanisms at play during each trial and over the course of learning.

4.2.2 The role of the MD and MD-mPFC projections in Attentional Set Shifting

In addition to the working memory task, in Chapter 3, we also tested the effects of adolescent thalamic inhibition on adult cognitive flexibility. The behavioral paradigm that has frequently been used to assess this function is called the Attentional Set Shifting Task (ASST), which is a modified version for rodents of the Wisconsin Card Sorting Test (WCST), used in humans. Our data clearly show that adolescent thalamic inhibition, which disrupts MD-mPFC projections and task-specific mPFC cellular activity, impairs the extra-dimensional set shift (EDSS) portion of the task, but not the initial acquisition (IA) portion. Moreover, acute thalamic activation during the EDSS entirely rescued both the behavioral deficit and the mPFC cellular activity. Thus, I hypothesize that the behavioral deficit is due to impaired mPFC or MD-mPFC function, which can be rescued by enhanced thalamic activity.

Consistent with this, many studies have shown that this phenotype (i.e., intact IA and impaired EDSS) is typical of mPFC disruption (Birrell & Brown, 2000; Bissonette et al., 2008; Canetta et al., 2016b). The ASST findings following thalamic manipulations are less clear. In one study, MD lesions also led to disruptions to EDSS (Ouhaz et al., 2021). Similar findings were seen upon MD inactivation via bupivacaine infusions in another cognitive flexibility task (Block et al., 2007), and enhancement of MD-mPFC activity improved rule switching behavior

(Schmitt et al., 2017). However, in another study, pharmacogenetic inhibition of MD-mPFC projections led to disruptions to IA but no changes in EDSS (Ferguson & Gao, 2018). Because of slight variations that can exist in these types of behavioral paradigms, future experiments should include a repeat of the ASST, as performed in Chapter 3, in adults upon acute inhibition of the MD or MD-mPFC projections.

Moreover, other cognitive tasks have shown that beta oscillatory activity in the MD plays an important role in thalamo-mPFC connectivity and task performance (Bolkan et al., 2017; Parnaudeau et al., 2018; Parnaudeau et al., 2013). While there were no disruptions to MD beta activity or MD-mPFC beta coherence during the ASST following adolescent thalamic inhibition (Figure 3.12), these measures should also be explored during the ASST upon acute thalamic inhibition.

4.3 Effects of adolescent thalamic inhibition on circuit properties

4.3.1 mPFC circuitry

The work described in Chapter 3 focuses on the changes to mPFC cells and MD-mPFC projections caused by adolescent thalamic inhibition. We found decreased sEPSC frequency in mPFC layer II/III pyramidal cells, with no changes to either sEPSC amplitude or sIPSCs. Adolescent thalamic inhibition also resulted in reduced MD-mPFC projections and no changes to BLA-mPFC or vHip-mPFC projections. In addition, we found that mPFC cell-cell cross-correlations and task-specific ensemble activity were disrupted during the ASST. For a deeper understanding of the effects on mPFC circuitry, additional analyses should be performed. These could include slice recordings to measure spontaneous activity of mPFC pyramidal cells in the deep layers V and VI as well as mPFC interneurons, including PV cells (which are discussed in more depth below). Other experiments could investigate functional thalamo-mPFC connectivity using optogenetics during slice recordings, as has been done previously in non-manipulated

mice (Canetta et al., 2020). In this way, it would be possible to determine the strength of synaptic projections from the MD onto interneurons and pyramidal cells across mPFC layers. Moreover, the mPFC is also reciprocally connected to the contralateral side as well as other cortical regions. Previous work has demonstrated the importance of both local and long-range cortical projections during adolescent development in proper cortico-cortical projection maturation (Nabel et al., 2020). Further exploration of these cortical inputs and projections via anatomical tracing and slice electrophysiology would inform the impact on this aspect of mPFC circuitry.

4.3.2 Thalamic cells

In addition to the impact of thalamic inhibition on the mPFC, whether there are also persistent changes to the cells within the thalamus has yet to be explored. We found no differences in the overall cellular density in the MD (Figure 3.9), nor did we see changes in MD activity during the ASST behavioral testing, including local field potential oscillatory activity in the beta (Figure 3.12) and gamma ranges (Figure 3.11) and multi-unit activity as deduced from power in the epsilon band (Figure 3.22). However, MD neurons may still be compromised at the functional level. To address this possibility, first, slice electrophysiological studies of adult MD cells to measure cell-intrinsic properties and sEPSCs would provide insight into the functioning of the MD cells and mPFC-MD projections following adolescent thalamic inhibition. Second, *in vivo* single unit recordings in the MD during the ASST could reveal changes to MD cellular function during impaired cognitive performance.

Together, these analyses of mPFC and thalamic cellular populations would greatly add to our understanding of the circuit-level consequences of adolescent thalamic inhibition.

4.4 Dividing the MD and midline thalamic cellular populations

In Chapter 3, we explored two possible approaches for expressing the inhibitory DREADD, hM4D, in the thalamus during adolescence: 1) using the GBX2-Cre line, which affects MD-mPFC projections, central MD cells (which project to the orbitofrontal cortex (OFC)), and other midline thalamic cells (Figure 3.1b); and 2) using the dual virus approach, by injecting a retrogradely transported Cre into the mPFC and a Cre-dependent hM4D into the MD to target only mPFC-projecting cells (Figure 3.6a). The dual virus approach recapitulates the cognitive deficit in the ASST found with the GBX2-Cre approach, indicating that this behavioral deficit is due to compromised mPFC and thalamo-mPFC functioning (Figure 3.6c). However, the GBX2-Cre approach may also affect thalamo-OFC circuitry, which has been associated with deficits in reversal learning (Boulougouris et al., 2007; Schoenbaum et al., 2002). Therefore, it would be important to explore the impact of GBX2-driven thalamic inhibition on OFC-dependent behaviors, such as reversal learning.

Moreover, future work could compare recordings of the MD in slice or during the ASST with these two approaches to thalamic inhibition. Any differences would highlight the role of these additional MD projections and may indicate another avenue of exploration into the adolescent development of other MD circuits.

4.5 Mechanisms and timing in the sensitive period

4.5.1 Narrowing and expanding the sensitive period window

In our manipulations, we inhibited thalamic activity for 30 days, from P20-50. The goal of this long disruption was to encompass several important milestones in the development of the MD and the mPFC. However, as noted in Chapter 1, there are different processes occurring

throughout this period. Therefore, future experiments should aim to narrow this window and discover the mechanisms at play over the course of the 30 days.

A first set of experiments could test the long-term consequences of thalamic inhibition on mPFC and MD functioning during subsections of the window (e.g., P20-35 and P35-50). As outlined in Chapter 3, we know that this manipulation has no effect after P90, but we should also explore the periods directly surrounding P20-50, including P0-20 and P50-70. Prior work has looked at the effects of transient manipulations during the gestational period (Canetta et al., 2016b; Lodge & Grace, 2009), and one study has also looked at the effects of transient mPFC manipulations in the P7-11 period (Bitzenhofer et al., 2021a). As a result, we might expect the earlier window to be susceptible to transient changes.

As for the later window, one study found long-term impacts of a transient increase in mPFC PV activity from P60-70 (Mukherjee et al., 2019a). However, this manipulation was done in a genetic developmental risk factor mouse model with impaired interneuron function, leaving uncertainty about whether this later plasticity would be seen in control mice. Indeed, other studies also found that it was possible to induce plasticity at later ages (>P45) in visual cortex by modulating interneuron activity in animals with reduced GABA levels, but in control animals, this was only possible during the visual sensitive period (P15-20) (Fagiolini et al., 2004; Fagiolini & Hensch, 2000b). Moreover, as outlined in Chapter 1, there are fewer changes taking place in the MD and mPFC development after adolescence. Nevertheless, it would be important to determine whether the P50-70 period is also susceptible to transient changes in thalamic activity.

The nature of the changes caused by manipulations during these different windows may vary depending on the developmental processes occurring at the time of the manipulation. Therefore, it will be essential to employ a host of different metrics to evaluate the long-term

impacts of transient thalamic inhibition during these different windows on adult functioning. These should include the same techniques described above, such as slice electrophysiological recordings of mPFC and thalamic cells, anatomical tracings of thalamo-mPFC projections, and *in vivo* recordings of the mPFC and thalamus during cognitive behaviors.

4.5.2 Characterization of the mechanisms during development

Moreover, further exploration of the processes during inhibition at the time of the manipulation will also give important insights into the mechanisms that are disrupted. In Nabel et al, the authors evaluated circuit dynamics during control conditions over the pre-adolescent, adolescent, and adult periods (Nabel et al., 2020). This work offered important insights into the developmental trajectory of anterior cingulate cortex projections onto the primary visual cortex. It also demonstrated that it is possible to successfully record both *ex vivo* and *in vivo* from adolescent animals. Similarly, adolescent thalamo-mPFC circuit development will be better understood by characterization of the projections during the developmental stages, such as at P20, P35, and P50.

This work should include several different techniques to understand multiple aspects of circuit development. First, slice electrophysiological recordings of mPFC and thalamic cells would reveal changes in the spontaneous activity, offering insights into the progression of inhibitory and excitatory synaptic inputs. Second, anatomical tracings to quantify thalamo-mPFC projection cell density, synaptic density, and the arborization of the projections would indicate the temporal development of outgrowth and pruning. Third, *in vivo* recordings of the mPFC and the MD during cognitive behaviors as well as at baseline would demonstrate how encoding of task relevant information changes with circuit maturation.

These recordings should be done under control conditions and during adolescent thalamic inhibition throughout the developmental period. Together, this work will expand our

understanding of the role of adolescence during the development of the thalamo-mPFC circuit in control animals and will demonstrate the direct impact of developmental perturbations as they occur.

4.6 The role of amygdalar and hippocampal projections

Here, I have focused on the thalamic inputs to the mPFC. The reasons for this choice are outlined in Chapter 1 and include evidence on cognitive functioning and schizophrenia across humans and animal models that implicate the MD and the MD-mPFC reciprocal circuit. Crucially, the developmental timelines of the MD and the mPFC both point to the importance of adolescence and the potential of the MD leading mPFC development during this period. However, as noted above, both the amygdala and the hippocampus also project to the mPFC and are disrupted in patients with schizophrenia. As a result, future work could also explore the long-term consequences of transient disruptions to either of these inputs.

There is an extensive body of literature exploring the long-term consequences of neonatal vHip lesions (NVHL), a developmental model for studying schizophrenia, which demonstrates changes in mPFC functioning that extends to its other subcortical projections (Guirado et al., 2016; O'Donnell, 2012). However, due to the permanent nature of lesions, this work does not identify the impact of the vHip disruption in specific time windows. The proposed experiments using transient DREADD inhibition during different postnatal time windows would therefore enrich our understanding of different periods in the development of these other mPFC inputs.

4.6.1 The Competition Hypothesis

Experiments exploring the consequences of transient disruptions to the hippocampus and amygdala would also offer evidence toward a “competition hypothesis.” As was mentioned

in Chapter 1, the projections from the amygdala, hippocampus, and thalamus all converge onto the same mPFC layer II/III pyramidal cells (Little & Carter, 2012). In sensory sensitive periods, a reduction in activity from one input (e.g., the left eye) can lead to a compensatory increase in projections from another input (e.g., the right eye) (Hensch, 2004; Hubel & Wiesel, 1970; Wiesel, 1982). Therefore, we originally hypothesized that a decrease in activity from the thalamic inputs to the mPFC may lead to a compensatory increase in projections from the hippocampus or the amygdala. In other words, the thalamus, hippocampus, and amygdala could all be competing for territory on the mPFC pyramidal cells, and with a retraction of thalamic inputs, the hippocampal and amygdalar inputs could take over.

However, our data so far do not support this hypothesis. There were no differences in mPFC projection cell densities from the BLA or vHip (Figure 3.8). A previous NVHL study in rats found that the early vHip lesion led to an increase in BLA-mPFC projection density (Guirado et al., 2016). The differences found between our data and this study could have several explanations: (1) the vHip-mPFC and BLA-mPFC projections may engage in competition in a way that does not involve the MD-mPFC projections; (2) the window for this competition may occur at a different time point than our transient manipulation; or (3) the decrease in activity may not be a strong enough manipulation to cause the systemic changes that are caused by the lesion.

These different hypotheses could be addressed with transient, pharmacogenetic inhibition of hippocampal or amygdalar inputs to the mPFC during different time windows and subsequent testing of all inputs to the mPFC.

4.7 PV interneurons in the mPFC receive MD innervation

Within the cortex, I have focused on the primary cellular population in the mPFC: pyramidal cells. They receive projections from the MD, as well as the other subcortical inputs

described above. However, the MD also projects onto the second major mPFC cellular population: interneurons. Specifically, MD projections target PV-expressing interneurons (Canetta et al., 2020; Delevich et al., 2015). Thus, thalamic or thalamo-mPFC inhibition should affect both mPFC pyramidal and PV cells.

As noted in Chapter 3, adolescent thalamic inhibition has no long-lasting impact on either mPFC pyramidal sIPSCs or gamma oscillations, both of which are mediated by PV cells (Cardin et al., 2009; Hu et al., 2014; Markram et al., 2004; Sohal et al., 2009). This is in contrast to other recent work which targeted mPFC PV cells directly during a similar time period (Canetta et al., 2021). In that study, adolescent PV inhibition led to changes in cognitive behavioral performance that mirrored the effects of adolescent thalamic inhibition, but the recordings *ex vivo* and *in vivo* found deficits in PV dysfunction, including reduced sIPSC frequency in pyramidal cells and disruption to gamma oscillations, two measures that are not affected after adolescent thalamic inhibition.

While the circuit dysfunction causing the behavioral phenotype may be specific to the manipulation, there may be more direct metrics of PV function that could be affected by thalamic inhibition. The slice electrophysiology experiment to record from PV interneurons mentioned above could reveal the impact of adolescent thalamic inhibition on spontaneous firing in PV cells. Similarly, retrograde labeling of cells projecting to the PV cells would indicate if the reduction in MD-mPFC projections affects projections onto PV cells and pyramidal cells differentially.

Furthermore, enhancing PV activity in adolescent-inhibited mice may reverse or impact the cognitive deficits. The same study that inhibited PV cells during adolescence found that acute PV activation during the ASST rescued the behavioral and gamma deficits (Canetta et al., 2021). Moreover, other genetic models that disrupt interneuron activity and cognitive flexibility

were also rescued by PV stimulation in the gamma frequency range (Cho et al., 2020). While thalamic inhibition caused no significant changes in gamma oscillatory activity during the task, it is possible that PV activation could still improve behavioral performance and mPFC cellular encoding by engaging this circuit suggesting a second mechanism, in addition to boosting thalamic activity, that could be exploited therapeutically.

In line with this idea, clonazepam, a benzodiazepine which facilitates interneuron activity, was shown to restore gamma activity and behavioral deficits in the genetic interneuron model (Cho et al., 2015; Cho et al., 2020). Given the potential translational implications of this intervention, it would also be very informative to study the use of clonazepam as a rescue for behavioral deficits after transient thalamic inhibition.

4.8 Re-opening the sensitive period

In Chapter 3, after anatomical and physiological changes to mPFC circuitry caused by adolescent thalamic inhibition, we found that non-specific thalamic activation was sufficient to rescue the cognitive behavioral deficit and mPFC cellular encoding. Previous work showed that an optogenetic rescue of interneuron activity during this task in the previously mentioned genetic model not only rescued the behavior during the stimulation, but also persisted a week later (Cho et al., 2015). While we were interested to discover whether thalamic activation would also have continued effects, we found that the rescue did not persist 10 days after the intervention. This suggests that a one-time thalamic activation is not sufficient to induce enough plasticity to restore the MD-mPFC projections, leaving the structural deficits unchanged. However, it is still unknown if chronic thalamic activation could have more persistent effects.

Moreover, it will be crucial to discover whether there are other interventions that will be more long-lasting. Prior work in sensory sensitive periods has explored mechanisms for re-opening or extending the sensitive period in visual cortex (Hensch & Bilimoria, 2012). Several

studies have explored the possibility of influencing the sensitive period facilitators (such as interneuron maturation or BDNF) or brakes (such as myelination or perineuronal nets) (Hensch & Bilimoria, 2012). Because of the clear translational implications, there has been a great deal of interest in the possibility of manipulating excitatory/inhibitory balance or GABA transmission with already available pharmacogenetic drugs, including benzodiazepines (Hensch et al., 1998) and the antidepressant fluoxetine (Vetencourt et al., 2008).

Studies with benzodiazepines have thus far been limited to extending the sensitive period in control animals or opening the sensitive period in adulthood in genetically modified animals, with no possibility of re-opening the sensitive period after inhibition has matured (Fagiolini et al., 2004; Fagiolini & Hensch, 2000b). Meanwhile, chronic fluoxetine has been shown to restore plasticity in adult rats, via manipulation of the excitatory/inhibitory balance in the visual cortex (Vetencourt et al., 2008). This re-opened sensitive period in the visual cortex was also observed with environmental enrichment (Sale et al., 2007) and food restriction, perhaps due to increased serum corticosterone levels (Spolidoro et al., 2011).

Indeed, environmental factors are crucial in determining plasticity in the brain. In NVHL models, cognitive training during adolescence is sufficient to rescue behavioral impairments in the adult (Lee et al., 2012). Given the importance of cognitive enrichment, stress, or socioeconomic status in psychiatric disorders and brain development (Markham & Greenough, 2004; Tooley et al., 2021), future work could aim to manipulate environmental factors to re-open the mPFC sensitive period and reverse the impairments caused by adolescent thalamic disruption.

4.9 Implications for patients with schizophrenia

As described in Chapter 1, functional imaging studies have long implicated the thalamo-PFC circuitry in patients with schizophrenia and cognitive dysfunction (Anticevic et al., 2014a;

Giraldo-Chica et al., 2017). Moreover, young adolescents at clinical high risk for the disorder already demonstrate impaired connectivity between the thalamus and the PFC, with severity linked to subsequent diagnosis (Anticevic et al., 2015). Other studies have also identified adolescence as a vulnerable period in the development of schizophrenia and other disorders, during which environmental exposures can be risk factors (Arseneault et al., 2002; Gomes & Grace, 2017). Thus, early disruptions to the MD-PFC circuit may be partially responsible for the persistent changes seen in adult patients with these disorders.

Therefore, a better understanding of the mechanisms of MD-PFC development during adolescence and the impact of changes to this process will greatly advance our pursuit for early diagnosis and treatment of psychiatric disorders like schizophrenia. This work could lead to the identification of early markers of cognitive impairments and psychiatric disorders, which would allow for early diagnosis, even before the onset of symptoms, and create opportunities for preventative interventions, which would greatly improve long-term patient outcomes. Moreover, treatments for any disorder with cognitive dysfunction could be developed to target, and even reverse, the developmental processes that cause these symptoms. Together, earlier diagnosis and improved treatment options will offer great promise for patients with psychiatric disorders.

References

Abbas, A. I., Sundiang, M. J. M., Henoch, B., Morton, M. P., Bolkan, S. S., Park, A. J., . . . Gordon, J. A. (2018). Somatostatin Interneurons Facilitate Hippocampal-Prefrontal Synchrony and Prefrontal Spatial Encoding. *Neuron, 100*(4), 926-939 e923. doi:10.1016/j.neuron.2018.09.029

Akhlaghpour, H., Wiskerke, J., Choi, J. Y., Taliaferro, J. P., Au, J., & Witten, I. B. (2016). Dissociated sequential activity and stimulus encoding in the dorsomedial striatum during spatial working memory. *Elife, 5*. doi:10.7554/eLife.19507

Alcaraz, F., Fresno, V., Marchand, A. R., Kremer, E. J., Coutureau, E., & Wolff, M. (2018). Thalamocortical and corticothalamic pathways differentially contribute to goal-directed behaviors in the rat. *Elife, 7*. doi:10.7554/eLife.32517

Anomal, R., de Villers-Sidani, E., Merzenich, M. M., & Panizzutti, R. (2013). Manipulation of BDNF signaling modifies the experience-dependent plasticity induced by pure tone exposure during the critical period in the primary auditory cortex. *PLoS One, 8*(5), e64208.

Anticevic, A., Cole, M. W., Repovs, G., Murray, J. D., Brumbaugh, M. S., Winkler, A. M., . . . Glahn, D. C. (2014a). Characterizing thalamo-cortical disturbances in schizophrenia and bipolar illness. *Cereb Cortex, 24*(12), 3116-3130. doi:10.1093/cercor/bht165

Anticevic, A., Haut, K., Murray, J. D., Repovs, G., Yang, G. J., Diehl, C., . . . Cannon, T. D. (2015). Association of Thalamic Dysconnectivity and Conversion to Psychosis in Youth and Young Adults at Elevated Clinical Risk. *JAMA Psychiatry, 72*(9), 882-891. doi:10.1001/jamapsychiatry.2015.0566

Anticevic, A., Tang, Y., Cho, Y. T., Repovs, G., Cole, M. W., Savic, A., . . . Xu, K. (2014b). Amygdala connectivity differs among chronic, early course, and individuals at risk for developing schizophrenia. *Schizophr Bull, 40*(5), 1105-1116. doi:10.1093/schbul/sbt165

Arion, D., Corradi, J. P., Tang, S., Datta, D., Boothe, F., He, A., . . . Lewis, D. A. (2015). Distinctive transcriptome alterations of prefrontal pyramidal neurons in schizophrenia and schizoaffective disorder. *Molecular Psychiatry, 20*(11), 1397-1405. doi:10.1038/mp.2014.171

Arseneault, L., Cannon, M., Poulton, R., Murray, R., Caspi, A., & Moffitt, T. E. (2002). Cannabis use in adolescence and risk for adult psychosis: longitudinal prospective study. *BMJ, 325*(7374), 1212-1213. Retrieved from https://www.ncbi.nlm.nih.gov/pubmed/12446537

Aultman, J. M., & Moghaddam, B. (2001). Distinct contributions of glutamate and dopamine receptors to temporal aspects of rodent working memory using a clinically relevant task. *Psychopharmacology (Berl), 153*(3), 353-364. doi:10.1007/s002130000590

Baho, E., & Di Cristo, G. (2012). Neural activity and neurotransmission regulate the maturation of the innervation field of cortical GABAergic interneurons in an age-dependent manner. *Journal of Neuroscience, 32*(3), 911-918.

Baker, K. D., Gray, A. R., & Richardson, R. (2017). The development of perineuronal nets around parvalbumin gabaergic neurons in the medial prefrontal cortex and basolateral amygdala of rats. *Behav Neurosci, 131*(4), 289-303. doi:10.1037/bne0000203

Balmer, T. S., Carels, V. M., Frisch, J. L., & Nick, T. A. (2009). Modulation of perineuronal nets and parvalbumin with developmental song learning. *Journal of Neuroscience, 29*(41), 12878-12885.

Barbas, H., & Zikopoulos, B. (2007). The prefrontal cortex and flexible behavior. *Neuroscientist, 13*(5), 532-545. doi:10.1177/1073858407301369

Barnes, A. (2004). Race, schizophrenia, and admission to state psychiatric hospitals. *Adm Policy Ment Health, 31*(3), 241-252. doi:10.1023/b:apih.0000018832.73673.54

Barr, W., Ashtari, M., Bilder, R., Degreef, G., & Lieberman, J. (1997). Brain morphometric comparison of first-episode schizophrenia and temporal lobe epilepsy. *The British Journal of Psychiatry, 170*(6), 515-519.

Bavelier, D., Levi, D. M., Li, R. W., Dan, Y., & Hensch, T. K. (2010). Removing brakes on adult brain plasticity: from molecular to behavioral interventions. *Journal of Neuroscience, 30*(45), 14964-14971.

Beaulieu, C. (1993). Numerical data on neocortical neurons in adult rat, with special reference to the GABA population. *Brain Research, 609*(1), 284-292. doi:https://doi.org/10.1016/0006-8993(93)90884-P

Belluscio, M. A., Mizuseki, K., Schmidt, R., Kempter, R., & Buzsaki, G. (2012). Cross-frequency phase-phase coupling between theta and gamma oscillations in the hippocampus. *J Neurosci, 32*(2), 423-435. doi:10.1523/JNEUROSCI.4122-11.2012

Benetti, S., Mechelli, A., Picchioni, M., Broome, M., Williams, S., & McGuire, P. (2009). Functional integration between the posterior hippocampus and prefrontal cortex is impaired in both first episode schizophrenia and the at risk mental state. *Brain, 132*(9), 2426-2436. doi:10.1093/brain/awp098

Benoit, L. J., Holt, E. S., Teboul, E., Taliaferro, J. P., Kellendonk, C., & Canetta, S. (2020). Medial prefrontal lesions impair performance in an operant delayed nonmatch to sample working memory task. *Behav Neurosci*. doi:10.1037/bne0000357

Bernardi, S., Benna, M. K., Rigotti, M., Munuera, J., Fusi, S., & Salzman, C. D. (2020). The Geometry of Abstraction in the Hippocampus and Prefrontal Cortex. *Cell, 183*(4), 954-967 e921. doi:10.1016/j.cell.2020.09.031

Berretta, S. (2012). Extracellular matrix abnormalities in schizophrenia. *Neuropharmacology, 62*(3), 1584-1597. doi:https://doi.org/10.1016/j.neuropharm.2011.08.010

Bickford, M. (2016). Thalamic Circuit Diversity: Modulation of the Driver/Modulator Framework. *Frontiers in Neural Circuits, 9*(86). doi:10.3389/fncir.2015.00086

Bicks, L. K., Yamamuro, K., Flanigan, M. E., Kim, J. M., Kato, D., Lucas, E. K., . . . Morishita, H. (2020). Prefrontal parvalbumin interneurons require juvenile social experience to establish adult social behavior. *Nat Commun, 11*(1), 1003. doi:10.1038/s41467-020-14740-z

Bigl, V., Woolf, N. J., & Butcher, L. L. (1982). Cholinergic projections from the basal forebrain to frontal, parietal, temporal, occipital, and cingulate cortices: a combined fluorescent tracer and acetylcholinesterase analysis. *Brain Res Bull, 8*(6), 727-749. Retrieved from https://www.ncbi.nlm.nih.gov/pubmed/6182962

Birrell, J. M., & Brown, V. J. (2000). Medial frontal cortex mediates perceptual attentional set shifting in the rat. *J Neurosci, 20*(11), 4320-4324. Retrieved from https://www.ncbi.nlm.nih.gov/pubmed/10818167

Bissonette, G. B., Martins, G. J., Franz, T. M., Harper, E. S., Schoenbaum, G., & Powell, E. M. (2008). Double dissociation of the effects of medial and orbital prefrontal cortical lesions on attentional and affective shifts in mice. *J Neurosci, 28*(44), 11124-11130. doi:10.1523/JNEUROSCI.2820-08.2008

Bitzenhofer, S. H., Pöpplau, J. A., Chini, M., Marquardt, A., & Hanganu-Opatz, I. L. (2021a). A transient developmental increase in prefrontal activity alters network maturation and causes cognitive dysfunction in adult mice. *Neuron, 109*(8), 1350-1364.e1356. doi:10.1016/j.neuron.2021.02.011

Bitzenhofer, S. H., Pöpplau, J. A., Chini, M., Marquardt, A., & Hanganu-Opatz, I. L. (2021b). A transient developmental increase in prefrontal activity alters network maturation and causes cognitive dysfunction in adult mice. *Neuron*. doi:10.1016/j.neuron.2021.02.011

Bitzenhofer, S. H., Popplau, J. A., & Hanganu-Opatz, I. (2020). Gamma activity accelerates during prefrontal development. *Elife, 9*. doi:10.7554/eLife.56795

Bjorklund, A., Divac, I., & Lindvall, O. (1978). Regional distribution of catecholamines in monkey cerebral cortex, evidence for a dopaminergic innervation of the primate prefrontal cortex. *Neurosci Lett, 7*(2-3), 115-119. doi:10.1016/0304-3940(78)90153-2

Black, J. E., Kodish, I. M., Grossman, A. W., Klintsova, A. Y., Orlovskaya, D., Vostrikov, V., . . . Greenough, W. T. (2004). Pathology of layer V pyramidal neurons in the prefrontal cortex of patients with schizophrenia. *American Journal of Psychiatry, 161*(4), 742-744.

Block, A. E., Dhanji, H., Thompson-Tardif, S. F., & Floresco, S. B. (2007). Thalamic-prefrontal cortical-ventral striatal circuitry mediates dissociable components of strategy set shifting. *Cereb Cortex, 17*(7), 1625-1636. doi:10.1093/cercor/bhl073

Bodatsch, M., Brockhaus-Dumke, A., Klosterkötter, J., & Ruhrmann, S. (2015). Forecasting Psychosis by Event-Related Potentials—Systematic Review and Specific Meta-Analysis. *Biological psychiatry, 77*(11), 951-958. doi:https://doi.org/10.1016/j.biopsych.2014.09.025

Boksa, P. (2012). Abnormal synaptic pruning in schizophrenia: Urban myth or reality? *J Psychiatry Neurosci, 37*(2), 75-77. doi:10.1503/jpn.120007

Bolkan, S. S., Stujenske, J. M., Parnaudeau, S., Spellman, T. J., Rauffenbart, C., Abbas, A. I., . . . Kellendonk, C. (2017). Thalamic projections sustain prefrontal activity during working memory maintenance. *Nat Neurosci, 20*(7), 987-996. doi:10.1038/nn.4568

Bonaventura, J., Eldridge, M. A. G., Hu, F., Gomez, J. L., Sanchez-Soto, M., Abramyan, A. M., . . . Michaelides, M. (2019). High-potency ligands for DREADD imaging and activation in rodents and monkeys. *Nature Communications, 10*(1), 4627. doi:10.1038/s41467-019-12236-z

Boulougouris, V., Dalley, J. W., & Robbins, T. W. (2007). Effects of orbitofrontal, infralimbic and prelimbic cortical lesions on serial spatial reversal learning in the rat. *Behavioural Brain Research, 179*(2), 219-228.

Bowie, C. R., Leung, W. W., Reichenberg, A., McClure, M. M., Patterson, T. L., Heaton, R. K., & Harvey, P. D. (2008). Predicting schizophrenia patients' real-world behavior with specific neuropsychological and functional capacity measures. *Biol Psychiatry, 63*(5), 505-511. doi:10.1016/j.biopsych.2007.05.022

Breier, A., Schreiber, J. L., Dyer, J., & Pickar, D. (1991). National Institute of Mental Health longitudinal study of chronic schizophrenia: prognosis and predictors of outcome. *Archives of general psychiatry, 48*(3), 239-246.

Brown, A. S., & Derkits, E. J. (2010). Prenatal infection and schizophrenia: a review of epidemiologic and translational studies. *The American journal of psychiatry, 167*(3), 261-280. doi:10.1176/appi.ajp.2009.09030361

Buckley, P. F., Miller, B. J., Lehrer, D. S., & Castle, D. J. (2009). Psychiatric comorbidities and schizophrenia. *Schizophr Bull, 35*(2), 383-402. doi:10.1093/schbul/sbn135

Buzsáki, G., & Wang, X.-J. (2012). Mechanisms of gamma oscillations. *Annu Rev Neurosci, 35*, 203-225.

Caballero, A., Flores-Barrera, E., Cass, D. K., & Tseng, K. Y. (2014). Differential regulation of parvalbumin and calretinin interneurons in the prefrontal cortex during adolescence. *Brain Struct Funct, 219*(1), 395-406. doi:10.1007/s00429-013-0508-8

Caballero, A., Flores-Barrera, E., Thomases, D. R., & Tseng, K. Y. (2020). Downregulation of parvalbumin expression in the prefrontal cortex during adolescence causes enduring prefrontal disinhibition in adulthood. *Neuropsychopharmacology, 45*(9), 1527-1535. doi:10.1038/s41386-020-0709-9

Canetta, S., Bolkan, S., Padilla-Coreano, N., Song, L. J., Sahn, R., Harrison, N. L., . . . Kellendonk, C. (2016a). Maternal immune activation does not alter the number of perisomatic parvalbumin-positive boutons in the offspring prefrontal cortex. *Mol Psychiatry, 21*(7), 857. doi:10.1038/mp.2016.92

Canetta, S., Bolkan, S., Padilla-Coreano, N., Song, L. J., Sahn, R., Harrison, N. L., . . . Kellendonk, C. (2016b). Maternal immune activation leads to selective functional deficits in offspring parvalbumin interneurons. *Mol Psychiatry, 21*(7), 956-968. doi:10.1038/mp.2015.222

Canetta, S., Teboul, E., Holt, E., Bolkan, S. S., Padilla-Coreano, N., Gordon, J. A., . . . Kellendonk, C. (2020). Differential Synaptic Dynamics and Circuit Connectivity of Hippocampal and Thalamic Inputs to the Prefrontal Cortex. *Cerebral Cortex Communications, 1*(1). doi:10.1093/texcom/tgaa084

Canetta, S. E., Holt, E. S., Benoit, L. J., Teboul, E., Ogden, R. T., Harris, A. Z., & Kellendonk, C. (2021). Mature parvalbumin interneuron function in prefrontal cortex requires activity during a postnatal sensitive period. *bioRxiv*, 2021.2003.2004.433943. doi:10.1101/2021.03.04.433943

Cannon, T. D., Chung, Y., He, G., Sun, D., Jacobson, A., van Erp, T. G. M., . . . Heinssen, R. (2015). Progressive Reduction in Cortical Thickness as Psychosis Develops: A Multisite Longitudinal Neuroimaging Study of Youth at Elevated Clinical Risk. *Biological psychiatry, 77*(2), 147-157. doi:https://doi.org/10.1016/j.biopsych.2014.05.023

Caras, M. L., & Sanes, D. H. (2015). Sustained Perceptual Deficits from Transient Sensory Deprivation. *J Neurosci, 35*(30), 10831-10842. doi:10.1523/JNEUROSCI.0837-15.2015

Cardin, J. A., Carlén, M., Meletis, K., Knoblich, U., Zhang, F., Deisseroth, K., . . . Moore, C. I. (2009). Driving fast-spiking cells induces gamma rhythm and controls sensory responses. *Nature, 459*(7247), 663-667.

Chakraborty, S., Kolling, N., Walton, M. E., & Mitchell, A. S. (2016). Critical role for the mediodorsal thalamus in permitting rapid reward-guided updating in stochastic reward environments. *Elife, 5*, e13588. doi:10.7554/eLife.13588

Chandler, D. J. (2016). Evidence for a specialized role of the locus coeruleus noradrenergic system in cortical circuitries and behavioral operations. *Brain Res, 1641*(Pt B), 197-206. doi:10.1016/j.brainres.2015.11.022

Chattopadhyaya, B., Di Cristo, G., Wu, C. Z., Knott, G., Kuhlman, S., Fu, Y., . . . Huang, Z. J. (2007). GAD67-mediated GABA synthesis and signaling regulate inhibitory synaptic innervation in the visual cortex. *Neuron, 54*(6), 889-903.

Chen, C.-M. A., Stanford, A. D., Mao, X., Abi-Dargham, A., Shungu, D. C., Lisanby, S. H., . . . Kegeles, L. S. (2014). GABA level, gamma oscillation, and working memory performance in schizophrenia. *NeuroImage: Clinical, 4*, 531-539.

Chen, L., Cooper, N. G., & Mower, G. D. (2000). Developmental changes in the expression of NMDA receptor subunits (NR1, NR2A, NR2B) in the cat visual cortex and the effects of dark rearing. *Molecular Brain Research, 78*(1-2), 196-200.

Cheng, W., Palaniyappan, L., Li, M., Kendrick, K. M., Zhang, J., Luo, Q., . . . Feng, J. (2015). Voxel-based, brain-wide association study of aberrant functional connectivity in

schizophrenia implicates thalamocortical circuitry. *NPJ schizophrenia, 1*(1), 15016. doi:10.1038/npjschz.2015.16

Chien, P. L., & Bell, C. C. (2008). Racial differences and schizophrenia. *Directions in Psychiatry, 28*(4), 297-304.

Chini, M., & Hanganu-Opatz, I. L. (2021). Prefrontal Cortex Development in Health and Disease: Lessons from Rodents and Humans. *Trends Neurosci, 44*(3), 227-240. doi:10.1016/j.tins.2020.10.017

Cho, K. I., Shenton, M. E., Kubicki, M., Jung, W. H., Lee, T. Y., Yun, J. Y., . . . Kwon, J. S. (2016). Altered Thalamo-Cortical White Matter Connectivity: Probabilistic Tractography Study in Clinical-High Risk for Psychosis and First-Episode Psychosis. *Schizophr Bull, 42*(3), 723-731. doi:10.1093/schbul/sbv169

Cho, K. K., Hoch, R., Lee, A. T., Patel, T., Rubenstein, J. L., & Sohal, V. S. (2015). Gamma rhythms link prefrontal interneuron dysfunction with cognitive inflexibility in Dlx5/6(+/-) mice. *Neuron, 85*(6), 1332-1343. doi:10.1016/j.neuron.2015.02.019

Cho, K. K. A., Davidson, T. J., Bouvier, G., Marshall, J. D., Schnitzer, M. J., & Sohal, V. S. (2020). Cross-hemispheric gamma synchrony between prefrontal parvalbumin interneurons supports behavioral adaptation during rule shift learning. *Nat Neurosci, 23*(7), 892-902. doi:10.1038/s41593-020-0647-1

Cho, R., Konecky, R., & Carter, C. S. (2006). Impairments in frontal cortical γ synchrony and cognitive control in schizophrenia. *Proceedings of the National Academy of Sciences, 103*(52), 19878-19883.

Clarkson, R. L., Liptak, A. T., Gee, S. M., Sohal, V. S., & Bender, K. J. (2017). D3 Receptors Regulate Excitability in a Unique Class of Prefrontal Pyramidal Cells. *J Neurosci, 37*(24), 5846-5860. doi:10.1523/JNEUROSCI.0310-17.2017

Condé, F., Lund, J. S., Jacobowitz, D. M., Baimbridge, K. G., & Lewis, D. A. (1994). Local circuit neurons immunoreactive for calretinin, calbindin D-28k or parvalbumin in monkey prefronatal cortex: Distribution and morphology. *Journal of Comparative Neurology, 341*(1), 95-116.

Crair, M. C., & Malenka, R. C. (1995). A critical period for long-term potentiation at thalamocortical synapses. *Nature, 375*(6529), 325-328.

Cronenwett, W. J., & Csernansky, J. (2010). Thalamic pathology in schizophrenia. *Curr Top Behav Neurosci, 4*, 509-528. doi:10.1007/7854_2010_55

Cruz, D. A., Weaver, C. L., Lovallo, E. M., Melchitzky, D. S., & Lewis, D. A. (2009). Selective alterations in postsynaptic markers of chandelier cell inputs to cortical pyramidal neurons in subjects with schizophrenia. *Neuropsychopharmacology, 34*(9), 2112-2124.

Dadarlat, M. C., & Stryker, M. P. (2017). Locomotion Enhances Neural Encoding of Visual Stimuli in Mouse V1. *J Neurosci, 37*(14), 3764-3775. doi:10.1523/JNEUROSCI.2728-16.2017

Damaraju, E., Allen, E. A., Belger, A., Ford, J. M., McEwen, S., Mathalon, D. H., . . . Calhoun, V. D. (2014). Dynamic functional connectivity analysis reveals transient states of dysconnectivity in schizophrenia. *NeuroImage: Clinical, 5*, 298-308. doi:https://doi.org/10.1016/j.nicl.2014.07.003

Davidson, M., Reichenberg, A., Rabinowitz, J., Weiser, M., Kaplan, Z., & Mark, M. (1999). Behavioral and intellectual markers for schizophrenia in apparently healthy male adolescents. *American Journal of Psychiatry, 156*(9), 1328-1335.

Dazzan, P., Soulsby, B., Mechelli, A., Wood, S. J., Velakoulis, D., Phillips, L. J., . . . Pantelis, C. (2011). Volumetric Abnormalities Predating the Onset of Schizophrenia and Affective Psychoses: An MRI Study in Subjects at Ultrahigh Risk of Psychosis. *Schizophr Bull, 38*(5), 1083-1091. doi:10.1093/schbul/sbr035

de Villers-Sidani, E., Chang, E. F., Bao, S., & Merzenich, M. M. (2007). Critical period window for spectral tuning defined in the primary auditory cortex (A1) in the rat. *J Neurosci, 27*(1), 180-189. doi:10.1523/JNEUROSCI.3227-06.2007

Deakin, J., Slater, P., Simpson, M., Gilchrist, A., Skan, W., Royston, M., . . . Cross, A. (1989). Frontal cortical and left temporal glutamatergic dysfunction in schizophrenia. *J Neurochem, 52*(6), 1781-1786.

Deidda, G., Allegra, M., Cerri, C., Naskar, S., Bony, G., Zunino, G., . . . Cancedda, L. (2015). Early depolarizing GABA controls critical-period plasticity in the rat visual cortex. *Nat Neurosci, 18*(1), 87-96.

Deidda, G., Bozarth, I. F., & Cancedda, L. (2014). Modulation of GABAergic transmission in development and neurodevelopmental disorders: investigating physiology and pathology to gain therapeutic perspectives. *Frontiers in Cellular Neuroscience, 8*(119). doi:10.3389/fncel.2014.00119

Delevich, K., Klinger, M., Okada, N. J., & Wilbrecht, L. (2021). Coming of age in the frontal cortex: The role of puberty in cortical maturation. *Seminars in Cell & Developmental Biology*. doi:https://doi.org/10.1016/j.semcdb.2021.04.021

Delevich, K., Tucciarone, J., Huang, Z. J., & Li, B. (2015). The mediodorsal thalamus drives feedforward inhibition in the anterior cingulate cortex via parvalbumin interneurons. *J Neurosci, 35*(14), 5743-5753. doi:10.1523/jneurosci.4565-14.2015

DeLisi, L. E., Buchsbaum, M. S., Holcomb, H. H., Langston, K. C., King, A. C., Kessler, R., . . . Margolin, R. (1989). Increased temporal lobe glucose use in chronic schizophrenic patients. *Biological psychiatry, 25*(7), 835-851.

Di Biase, M. A., Cetin-Karayumak, S., Lyall, A. E., Zalesky, A., Cho, K. I. K., Zhang, F., . . . Pasternak, O. (2021). White matter changes in psychosis risk relate to development and are not impacted by the transition to psychosis. *Mol Psychiatry*. doi:10.1038/s41380-021-01128-8

Diagnostic and statistical manual of mental disorders: DSM-5™, 5th ed. (2013). Arlington, VA, US: American Psychiatric Publishing, Inc.

Dias, R., Robbins, T. W., & Roberts, A. C. (1996). Primate analogue of the Wisconsin Card Sorting Test: effects of excitotoxic lesions of the prefrontal cortex in the marmoset. *Behav Neurosci, 110*(5), 872-886. doi:10.1037//0735-7044.110.5.872

Divac, I., Kosmal, A., Bjorklund, A., & Lindvall, O. (1978). Subcortical projections to the prefrontal cortex in the rat as revealed by the horseradish peroxidase technique. *Neuroscience, 3*(9), 785-796. doi:10.1016/0306-4522(78)90031-3

Dunnett, S. B., Nathwani, F., & Brasted, P. J. (1999). Medial prefrontal and neostriatal lesions disrupt performance in an operant delayed alternation task in rats. *Behavioural Brain Research, 106*(1), 13-28. doi:10.1016/S0166-4328(99)00076-5

EG, J., & McCormick, D. (2007). The thalamus. In: Cambridge, UK: Cambridge University Press.[Google Scholar].

Eggan, S. M., Hashimoto, T., & Lewis, D. A. (2008). Reduced Cortical Cannabinoid 1 Receptor Messenger RNA and Protein Expression in Schizophrenia. *Archives of general psychiatry, 65*(7), 772-784. doi:10.1001/archpsyc.65.7.772

Erisir, A., & Harris, J. L. (2003). Decline of the critical period of visual plasticity is concurrent with the reduction of NR2B subunit of the synaptic NMDA receptor in layer 4. *Journal of Neuroscience, 23*(12), 5208-5218.

Fagiolini, M., Fritschy, J.-M., Löw, K., Möhler, H., Rudolph, U., & Hensch, T. K. (2004). Specific GABAA circuits for visual cortical plasticity. *Science, 303*(5664), 1681-1683.

Fagiolini, M., & Hensch, T. K. (2000a). Inhibitory threshold for critical-period activation in primary visual cortex. *Nature, 404*(6774), 183-186. doi:10.1038/35004582

Fagiolini, M., & Hensch, T. K. (2000b). Inhibitory threshold for critical-period activation in primary visual cortex. *Nature, 404*(6774), 183-186.

Feinberg, I. (1982). Schizophrenia: caused by a fault in programmed synaptic elimination during adolescence? *J Psychiatr Res, 17*(4), 319-334. doi:10.1016/0022-3956(82)90038-3

Feinberg, I., & Campbell, I. G. (2010). Sleep EEG changes during adolescence: an index of a fundamental brain reorganization. *Brain Cogn, 72*(1), 56-65. doi:10.1016/j.bandc.2009.09.008

Feldman, D. E., Nicoll, R. A., Malenka, R. C., & Isaac, J. T. (1998). Long-term depression at thalamocortical synapses in developing rat somatosensory cortex. *Neuron, 21*(2), 347-357.

Ferguson, B. R., & Gao, W. J. (2014). Development of thalamocortical connections between the mediodorsal thalamus and the prefrontal cortex and its implication in cognition. *Front Hum Neurosci, 8*, 1027. doi:10.3389/fnhum.2014.01027

Ferguson, B. R., & Gao, W. J. (2018). Thalamic Control of Cognition and Social Behavior Via Regulation of Gamma-Aminobutyric Acidergic Signaling and Excitation/Inhibition

Balance in the Medial Prefrontal Cortex. *Biol Psychiatry, 83*(8), 657-669. doi:10.1016/j.biopsych.2017.11.033

Fletcher, P. (1998). The missing link: a failure of fronto-hippocampal integration in schizophrenia. *Nat Neurosci, 1*(4), 266-267.

Flores-Barrera, E., Thomases, D. R., Heng, L. J., Cass, D. K., Caballero, A., & Tseng, K. Y. (2014). Late adolescent expression of GluN2B transmission in the prefrontal cortex is input-specific and requires postsynaptic protein kinase A and D1 dopamine receptor signaling. *Biol Psychiatry, 75*(6), 508-516. doi:10.1016/j.biopsych.2013.07.033

Frontal lobe function and dysfunction. (1991). New York, NY, US: Oxford University Press.

Fryer, S., Woods, S., Kiehl, K., Calhoun, V., Pearlson, G., Roach, B., . . . Mathalon, D. (2013). Deficient Suppression of Default Mode Regions during Working Memory in Individuals with Early Psychosis and at Clinical High-Risk for Psychosis. *Frontiers in Psychiatry, 4*(92). doi:10.3389/fpsyt.2013.00092

Fryer, S. L., Ferri, J. M., Roach, B. J., Loewy, R. L., Stuart, B. K., Anticevic, A., . . . Mathalon, D. H. (2021). Thalamic dysconnectivity in the psychosis risk syndrome and early illness schizophrenia. *Psychol Med*, 1-9. doi:10.1017/s0033291720004882

Fu, Y., Wu, X., Lu, J., & Huang, J. (2012). Presynaptic GABAB receptor regulates activity-dependent maturation and patterning of inhibitory synapses through dynamic allocation of synaptic vesicles. *Frontiers in Cellular Neuroscience, 6*, 57.

Fusar-Poli, P., Smieskova, R., Kempton, M. J., Ho, B. C., Andreasen, N. C., & Borgwardt, S. (2013). Progressive brain changes in schizophrenia related to antipsychotic treatment? A meta-analysis of longitudinal MRI studies. *Neurosci Biobehav Rev, 37*(8), 1680-1691. doi:10.1016/j.neubiorev.2013.06.001

Garcia-Garcia, A. L., Meng, Q., Canetta, S., Gardier, A. M., Guiard, B. P., Kellendonk, C., . . . Leonardo, E. D. (2017). Serotonin Signaling through Prefrontal Cortex 5-HT1A Receptors during Adolescence Can Determine Baseline Mood-Related Behaviors. *Cell Rep, 18*(5), 1144-1156. doi:10.1016/j.celrep.2017.01.021

Garey, L., Ong, W., Patel, T., Kanani, M., Davis, A., Mortimer, A., . . . Hirsch, S. (1998). Reduced dendritic spine density on cerebral cortical pyramidal neurons in schizophrenia. *Journal of Neurology, Neurosurgery & Psychiatry, 65*(4), 446-453.

Gee, S., Ellwood, I., Patel, T., Luongo, F., Deisseroth, K., & Sohal, V. S. (2012). Synaptic activity unmasks dopamine D2 receptor modulation of a specific class of layer V pyramidal neurons in prefrontal cortex. *J Neurosci, 32*(14), 4959-4971. doi:10.1523/JNEUROSCI.5835-11.2012

Giraldo-Chica, M., Rogers, B. P., Damon, S. M., Landman, B. A., & Woodward, N. D. (2017). Prefrontal-Thalamic Anatomical Connectivity and Executive Cognitive Function in Schizophrenia. *Biol Psychiatry*. doi:10.1016/j.biopsych.2017.09.022

Giraldo-Chica, M., & Woodward, N. D. (2017). Review of thalamocortical resting-state fMRI studies in schizophrenia. *Schizophrenia Research, 180*, 58-63. doi:10.1016/j.schres.2016.08.005

Glahn, D. C., Laird, A. R., Ellison-Wright, I., Thelen, S. M., Robinson, J. L., Lancaster, J. L., . . . Fox, P. T. (2008). Meta-analysis of gray matter anomalies in schizophrenia: application of anatomic likelihood estimation and network analysis. *Biol Psychiatry, 64*(9), 774-781. doi:10.1016/j.biopsych.2008.03.031

Glantz, L. A., & Lewis, D. A. (1997). Reduction of synaptophysin immunoreactivity in the prefrontal cortex of subjects with schizophrenia: regional and diagnostic specificity. *Archives of general psychiatry, 54*(10), 943-952.

Glantz, L. A., & Lewis, D. A. (2000). Decreased dendritic spine density on prefrontal cortical pyramidal neurons in schizophrenia. *Archives of general psychiatry, 57*(1), 65-73.

Gogtay, N., Vyas, N. S., Testa, R., Wood, S. J., & Pantelis, C. (2011). Age of onset of schizophrenia: perspectives from structural neuroimaging studies. *Schizophr Bull, 37*(3), 504-513. doi:10.1093/schbul/sbr030

Gomes, F. V., & Grace, A. A. (2017). Adolescent Stress as a Driving Factor for Schizophrenia Development-A Basic Science Perspective. *Schizophr Bull, 43*(3), 486-489. doi:10.1093/schbul/sbx033

Goodwill, H. L., Manzano-Nieves, G., LaChance, P., Teramoto, S., Lin, S., Lopez, C., . . . Bath, K. G. (2018). Early Life Stress Drives Sex-Selective Impairment in Reversal Learning by Affecting Parvalbumin Interneurons in Orbitofrontal Cortex of Mice. *Cell Rep, 25*(9), 2299-2307 e2294. doi:10.1016/j.celrep.2018.11.010

Goto, K., & Ito, I. (2017). The asymmetry defect of hippocampal circuitry impairs working memory in beta2-microglobulin deficient mice. *Neurobiol Learn Mem, 139*, 50-55. doi:10.1016/j.nlm.2016.12.020

Goto, K., Kurashima, R., Gokan, H., Inoue, N., Ito, I., & Watanabe, S. (2010). Left-right asymmetry defect in the hippocampal circuitry impairs spatial learning and working memory in iv mice. *PLoS One, 5*(11), e15468. doi:10.1371/journal.pone.0015468

Granon, S., Vidal, C., Thinus-Blanc, C., Changeux, J. P., & Poucet, B. (1994). Working memory, response selection, and effortful processing in rats with medial prefrontal lesions. *Behav Neurosci, 108*(5), 883-891. doi:10.1037//0735-7044.108.5.883

Green, M. F., Kern, R. S., Braff, D. L., & Mintz, J. (2000). Neurocognitive deficits and functional outcome in schizophrenia: are we measuring the "right stuff"? *Schizophr Bull, 26*(1), 119-136. doi:10.1093/oxfordjournals.schbul.a033430

Guillery, R. W. (1995). Anatomical evidence concerning the role of the thalamus in corticocortical communication: a brief review. *J Anat, 187 (Pt 3)*(Pt 3), 583-592.

Guirado, R., Umemori, J., Sipila, P., & Castren, E. (2016). Evidence for Competition for Target Innervation in the Medial Prefrontal Cortex. *Cereb Cortex, 26*(3), 1287-1294. doi:10.1093/cercor/bhv280

Guo, Z. V., Inagaki, H. K., Daie, K., Druckmann, S., Gerfen, C. R., & Svoboda, K. (2017). Maintenance of persistent activity in a frontal thalamocortical loop. *Nature, 545*(7653), 181-186. doi:10.1038/nature22324

Häfner, H., & Maurer, K. (2006). Early detection of schizophrenia: current evidence and future perspectives. *World Psychiatry, 5*(3), 130-138.

Häfner, H., Maurer, K., Löffler, W., Fätkenheuer, B., Heiden, W. A. D., Riecher-Rössler, A., . . . Gattaz, W. F. (1994). The Epidemiology of Early Schizophrenia: Influence of Age and Gender on Onset and Early Course. *British Journal of Psychiatry, 164*(S23), 29-38. doi:10.1192/S0007125000292714

Hanover, J. L., Huang, Z. J., Tonegawa, S., & Stryker, M. P. (1999). Rapid Communications (http://www. jneurosci. org)-Brain-Derived Neurotrophic Factor Overexpression Induces Precocious Critical Period in Mouse Visual Cortex. *Journal of Neuroscience, 19*(22), RC40.

Harris, J. A., Mihalas, S., Hirokawa, K. E., Whitesell, J. D., Choi, H., Bernard, A., . . . Zeng, H. (2019). Hierarchical organization of cortical and thalamic connectivity. *Nature, 575*(7781), 195-202. doi:10.1038/s41586-019-1716-z

Harrisberger, F., Buechler, R., Smieskova, R., Lenz, C., Walter, A., Egloff, L., . . . Theodoridou, A. (2016). Alterations in the hippocampus and thalamus in individuals at high risk for psychosis. *NPJ schizophrenia, 2*(1), 1-6.

Hashimoto, T., Arion, D., Unger, T., Maldonado-Aviles, J., Morris, H., Volk, D., . . . Lewis, D. (2008a). Alterations in GABA-related transcriptome in the dorsolateral prefrontal cortex of subjects with schizophrenia. *Molecular Psychiatry, 13*(2), 147-161.

Hashimoto, T., Bazmi, H. H., Mirnics, K., Wu, Q., Sampson, A. R., & Lewis, D. A. (2008b). Conserved regional patterns of GABA-related transcript expression in the neocortex of subjects with schizophrenia. *American Journal of Psychiatry, 165*(4), 479-489.

Hashimoto, T., Volk, D. W., Eggan, S. M., Mirnics, K., Pierri, J. N., Sun, Z., . . . Lewis, D. A. (2003). Gene expression deficits in a subclass of GABA neurons in the prefrontal cortex of subjects with schizophrenia. *Journal of Neuroscience, 23*(15), 6315-6326.

Heaton, R., Paulsen, J. S., McAdams, L. A., Kuck, J., Zisook, S., Braff, D., . . . Jeste, D. V. (1994). Neuropsychological deficits in schizophrenics: relationship to age, chronicity, and dementia. *Archives of general psychiatry, 51*(6), 469-476.

Heckers, S., & Konradi, C. (2010). Hippocampal pathology in schizophrenia. *Behavioral neurobiology of schizophrenia and its treatment*, 529-553.

Heckers, S., Rauch, S., Goff, D., Savage, C., Schacter, D., Fischman, A., & Alpert, N. (1998). Impaired recruitment of the hippocampus during conscious recollection in schizophrenia. *Nat Neurosci, 1*(4), 318-323.

Hensch, T. K. (2004). Critical period regulation. *Annu Rev Neurosci, 27*, 549-579. doi:10.1146/annurev.neuro.27.070203.144327

Hensch, T. K., & Bilimoria, P. M. (2012). Re-opening Windows: Manipulating Critical Periods for Brain Development. *Cerebrum, 2012*, 11.

Hensch, T. K., Fagiolini, M., Mataga, N., Stryker, M. P., Baekkeskov, S., & Kash, S. F. (1998). Local GABA circuit control of experience-dependent plasticity in developing visual cortex. *Science, 282*(5393), 1504-1508. doi:10.1126/science.282.5393.1504

Henseler, I., Falkai, P., & Gruber, O. (2010). Disturbed functional connectivity within brain networks subserving domain-specific subcomponents of working memory in schizophrenia: relation to performance and clinical symptoms. *Journal of Psychiatric Research, 44*(6), 364-372.

Hill, R. A., Wu, Y. W., Kwek, P., & van den Buuse, M. (2012). Modulatory effects of sex steroid hormones on brain-derived neurotrophic factor-tyrosine kinase B expression during adolescent development in C57Bl/6 mice. *J Neuroendocrinol, 24*(5), 774-788. doi:10.1111/j.1365-2826.2012.02277.x

Hill, S. K., Bishop, J. R., Palumbo, D., & Sweeney, J. A. (2010). Effect of second-generation antipsychotics on cognition: current issues and future challenges. *Expert Rev Neurother, 10*(1), 43-57. doi:10.1586/ern.09.143

Hirano, Y., Oribe, N., Kanba, S., Onitsuka, T., Nestor, P. G., & Spencer, K. M. (2015). Spontaneous gamma activity in schizophrenia. *JAMA Psychiatry, 72*(8), 813-821.

Ho, N. F., Chong, P. L. H., Lee, D. R., Chew, Q. H., Chen, G., & Sim, K. (2019). The Amygdala in Schizophrenia and Bipolar Disorder: A Synthesis of Structural MRI, Diffusion Tensor Imaging, and Resting-State Functional Connectivity Findings. *Harvard Review of Psychiatry, 27*(3), 150-164. doi:10.1097/hrp.0000000000000207

Hoffman, R. P. (2017). The Complex Inter-Relationship Between Diabetes and Schizophrenia. *Curr Diabetes Rev, 13*(3), 528-532. doi:10.2174/1573399812666161201205322

Hoover, W. B., & Vertes, R. P. (2007). Anatomical analysis of afferent projections to the medial prefrontal cortex in the rat. *Brain Struct Funct, 212*(2), 149-179. doi:10.1007/s00429-007-0150-4

Hoptman, M. J., D'Angelo, D., Catalano, D., Mauro, C. J., Shehzad, Z. E., Kelly, A. M., . . . Milham, M. P. (2010). Amygdalofrontal functional disconnectivity and aggression in schizophrenia. *Schizophr Bull, 36*(5), 1020-1028. doi:10.1093/schbul/sbp012

Hsiao, K., Noble, C., Pitman, W., Yadav, N., Kumar, S., Keele, G. R., . . . Rajasethupathy, P. (2020). A Thalamic Orphan Receptor Drives Variability in Short-Term Memory. *Cell, 183*(2), 522-536.e519. doi:https://doi.org/10.1016/j.cell.2020.09.011

Hu, H., Gan, J., & Jonas, P. (2014). Fast-spiking, parvalbumin+ GABAergic interneurons: From cellular design to microcircuit function. *Science, 345*(6196).

Huang, A. S., Rogers, B. P., Anticevic, A., Blackford, J. U., Heckers, S., & Woodward, N. D. (2019). Brain function during stages of working memory in schizophrenia and psychotic bipolar disorder. *Neuropsychopharmacology, 44*(12), 2136-2142. doi:10.1038/s41386-019-0434-4

Huang, A. S., Rogers, B. P., Sheffield, J. M., Jalbrzikowski, M. E., Anticevic, A., Blackford, J. U., . . . Woodward, N. D. (2020). Thalamic Nuclei Volumes in Psychotic Disorders and in Youths With Psychosis Spectrum Symptoms. *Am J Psychiatry, 177*(12), 1159-1167. doi:10.1176/appi.ajp.2020.19101099

Huang, P., Xi, Y., Lu, Z.-L., Chen, Y., Li, X., Li, W., . . . Yin, H. (2015). Decreased bilateral thalamic gray matter volume in first-episode schizophrenia with prominent hallucinatory symptoms: A volumetric MRI study. *Scientific Reports, 5*(1), 14505. doi:10.1038/srep14505

Huang, X., Pu, W., Li, X., Greenshaw, A. J., Dursun, S. M., Xue, Z., . . . Liu, Z. (2017). Decreased Left Putamen and Thalamus Volume Correlates with Delusions in First-Episode Schizophrenia Patients. *Frontiers in Psychiatry, 8*(245). doi:10.3389/fpsyt.2017.00245

Huang, Z. J., Kirkwood, A., Pizzorusso, T., Porciatti, V., Morales, B., Bear, M. F., . . . Tonegawa, S. (1999). BDNF regulates the maturation of inhibition and the critical period of plasticity in mouse visual cortex. *Cell, 98*(6), 739-755.

Hubel, D. H., & Wiesel, T. N. (1970). The period of susceptibility to the physiological effects of unilateral eye closure in kittens. *J Physiol, 206*(2), 419-436. Retrieved from http://www.ncbi.nlm.nih.gov/pubmed/5498493

Hunt, P. R., & Aggleton, J. P. (1998). Neurotoxic lesions of the dorsomedial thalamus impair the acquisition but not the performance of delayed matching to place by rats: a deficit in shifting response rules. *J Neurosci, 18*(23), 10045-10052. Retrieved from https://www.ncbi.nlm.nih.gov/pubmed/9822759. (Accession No. 9822759)

Hyman, J. M., Zilli, E. A., Paley, A. M., & Hasselmo, M. E. (2010). Working Memory Performance Correlates with Prefrontal-Hippocampal Theta Interactions but not with Prefrontal Neuron Firing Rates. *Front Integr Neurosci, 4*, 2. doi:10.3389/neuro.07.002.2010

Ingvar, D. H., & Franzen, G. (1974). Abnormalities of cerebral blood flow distribution in patients with chronic schizophrenia. *Acta Psychiatr Scand, 50*(4), 425-462. Retrieved from https://www.ncbi.nlm.nih.gov/pubmed/4423855

Insel, T. R. (2010). Rethinking schizophrenia. *Nature, 468*(7321), 187-193. doi:10.1038/nature09552

Jones, E. G. (2012). *The thalamus*: Springer Science & Business Media.

Kahn, J. B., Ward, R. D., Kahn, L. W., Rudy, N. M., Kandel, E. R., Balsam, P. D., & Simpson, E. H. (2012). Medial prefrontal lesions in mice impair sustained attention but spare maintenance of information in working memory. *Learn Mem, 19*(11), 513-517. doi:10.1101/lm.026302.112

Kamigaki, T., & Dan, Y. (2017). Delay activity of specific prefrontal interneuron subtypes modulates memory-guided behavior. *Nat Neurosci, 20*(6), 854-863. doi:10.1038/nn.4554

Kaneko, M., Fu, Y., & Stryker, M. P. (2017). Locomotion Induces Stimulus-Specific Response Enhancement in Adult Visual Cortex. *J Neurosci, 37*(13), 3532-3543. doi:10.1523/JNEUROSCI.3760-16.2017

Kann, O. (2016). The interneuron energy hypothesis: Implications for brain disease. *Neurobiology of Disease, 90*, 75-85. doi:https://doi.org/10.1016/j.nbd.2015.08.005

Karam, C. S., Ballon, J. S., Bivens, N. M., Freyberg, Z., Girgis, R. R., Lizardi-Ortiz, J. E., . . . Javitch, J. A. (2010). Signaling pathways in schizophrenia: emerging targets and therapeutic strategies. *Trends in Pharmacological Sciences, 31*(8), 381-390. doi:https://doi.org/10.1016/j.tips.2010.05.004

Karlsgodt, K. H., Sanz, J., van Erp, T. G. M., Bearden, C. E., Nuechterlein, K. H., & Cannon, T. D. (2009). Re-evaluating dorsolateral prefrontal cortex activation during working memory in schizophrenia. *Schizophrenia Research, 108*(1-3), 143-150. doi:10.1016/j.schres.2008.12.025

Katz, M., Buchsbaum, M. S., Siegel, B. V., Jr., Wu, J., Haier, R. J., & Bunney, W. E., Jr. (1996). Correlational patterns of cerebral glucose metabolism in never-medicated schizophrenics. *Neuropsychobiology, 33*(1), 1-11. Retrieved from http://www.ncbi.nlm.nih.gov/pubmed/8821368

Kawasaki, Y., Suzuki, M., Maeda, Y., Urata, K., Yamaguchi, N., Matsuda, H., . . . Takashima, T. (1992). Regional cerebral blood flow in patients with schizophrenia. *European Archives of Psychiatry and Clinical Neuroscience, 241*(4), 195-200. doi:10.1007/BF02190252

Kellendonk, C., Simpson, E. H., Polan, H. J., Malleret, G., Vronskaya, S., Winiger, V., . . . Kandel, E. R. (2006). Transient and selective overexpression of dopamine D2 receptors in the striatum causes persistent abnormalities in prefrontal cortex functioning. *Neuron, 49*(4), 603-615. doi:10.1016/j.neuron.2006.01.023

Keller, C. J., Chen, C., Lado, F. A., & Khodakhah, K. (2016). The Limited Utility of Multiunit Data in Differentiating Neuronal Population Activity. *PLoS One, 11*(4), e0153154. doi:10.1371/journal.pone.0153154

Kirihara, K., Rissling, A. J., Swerdlow, N. R., Braff, D. L., & Light, G. A. (2012). Hierarchical organization of gamma and theta oscillatory dynamics in schizophrenia. *Biological psychiatry, 71*(10), 873-880.

Klingner, C. M., Langbein, K., Dietzek, M., Smesny, S., Witte, O. W., Sauer, H., & Nenadic, I. (2014). Thalamocortical connectivity during resting state in schizophrenia. *European*

Archives of Psychiatry and Clinical Neuroscience, 264(2), 111-119. doi:10.1007/s00406-013-0417-0

Kolb, B., & Whishaw, I. Q. (1983). Performance of schizophrenic patients on tests sensitive to left or right frontal, temporal, or parietal function in neurological patients. *J Nerv Ment Dis, 171*(7), 435-443. doi:10.1097/00005053-198307000-00008

Konopaske, G. T., Balu, D. T., Presti, K. T., Chan, G., Benes, F. M., & Coyle, J. T. (2018). Dysbindin-1 contributes to prefrontal cortical dendritic arbor pathology in schizophrenia. *Schizophr Res, 201*, 270-277. doi:10.1016/j.schres.2018.04.042

Konstantoudaki, X., Chalkiadaki, K., Vasileiou, E., Kalemaki, K., Karagogeos, D., & Sidiropoulou, K. (2018). Prefrontal cortical-specific differences in behavior and synaptic plasticity between adolescent and adult mice. *J Neurophysiol, 119*(3), 822-833. doi:10.1152/jn.00189.2017

Kraepelin, E., Robertson, G. M., & Barclay, R. M. (1919). *Dementia praecox and paraphrenia*. [Chicago]: Chicago Medical Book Co.

Kubota, M., Miyata, J., Sasamoto, A., Sugihara, G., Yoshida, H., Kawada, R., . . . Murai, T. (2013). Thalamocortical disconnection in the orbitofrontal region associated with cortical thinning in schizophrenia. *JAMA Psychiatry, 70*(1), 12-21. doi:10.1001/archgenpsychiatry.2012.1023

Kupferschmidt, D. A., & Gordon, J. A. (2018). The dynamics of disordered dialogue: Prefrontal, hippocampal and thalamic miscommunication underlying working memory deficits in schizophrenia. *Brain and Neuroscience Advances, 2*, 2398212818771821. doi:10.1177/2398212818771821

Lang, P. J., & Davis, M. (2006). Emotion, motivation, and the brain: Reflex foundations in animal and human research. In S. Anders, G. Ende, M. Junghofer, J. Kissler, & D. Wildgruber (Eds.), *Progress in brain research* (Vol. 156, pp. 3-29): Elsevier.

Larsen, B., & Luna, B. (2018a). Adolescence as a neurobiological critical period for the development of higher-order cognition. *Neuroscience & Biobehavioral Reviews, 94*, 179-195. doi:https://doi.org/10.1016/j.neubiorev.2018.09.005

Larsen, B., & Luna, B. (2018b). Adolescence as a neurobiological critical period for the development of higher-order cognition. *Neurosci Biobehav Rev, 94*, 179-195. doi:10.1016/j.neubiorev.2018.09.005

Larsen, J. K., & Divac, I. (1978). Selective ablations within the prefrontal cortex of the rat and performance of delayed alternation. *Physiological Psychology, 6*(1), 15-17. doi:10.3758/bf03326684

Lee, H., Dvorak, D., Kao, H.-Y., Duffy, Áine M., Scharfman, Helen E., & Fenton, André A. (2012). Early Cognitive Experience Prevents Adult Deficits in a Neurodevelopmental Schizophrenia Model. *Neuron, 75*(4), 714-724. doi:https://doi.org/10.1016/j.neuron.2012.06.016

Levin, H. S., Eisenberg, H. M., & Benton, A. L. (1991). *Frontal lobe function and dysfunction*: Oxford University Press, USA.

Lewis, D. A. (2012). Cortical circuit dysfunction and cognitive deficits in schizophrenia – implications for preemptive interventions. *European Journal of Neuroscience, 35*(12), 1871-1878. doi:https://doi.org/10.1111/j.1460-9568.2012.08156.x

Lewis, D. A., Curley, A. A., Glausier, J. R., & Volk, D. W. (2012). Cortical parvalbumin interneurons and cognitive dysfunction in schizophrenia. *Trends in Neurosciences, 35*(1), 57-67. doi:https://doi.org/10.1016/j.tins.2011.10.004

Li, T., Wang, Q., Zhang, J., Rolls, E. T., Yang, W., Palaniyappan, L., . . . Feng, J. (2016). Brain-Wide Analysis of Functional Connectivity in First-Episode and Chronic Stages of Schizophrenia. *Schizophr Bull, 43*(2), 436-448. doi:10.1093/schbul/sbw099

Liang, M., Zhou, Y., Jiang, T., Liu, Z., Tian, L., Liu, H., & Hao, Y. (2006). Widespread functional disconnectivity in schizophrenia with resting-state functional magnetic resonance imaging. *Neuroreport, 17*(2), 209-213.

Liddle, P., Friston, K., Frith, C., Hirsch, S., Jones, T., & Frackowiak, R. (1992). Patterns of cerebral blood flow in schizophrenia. *The British Journal of Psychiatry, 160*(2), 179-186.

Light, G. A., Hsu, J. L., Hsieh, M. H., Meyer-Gomes, K., Sprock, J., Swerdlow, N. R., & Braff, D. L. (2006). Gamma band oscillations reveal neural network cortical coherence dysfunction in schizophrenia patients. *Biological psychiatry, 60*(11), 1231-1240.

Little, J. P., & Carter, A. G. (2012). Subcellular synaptic connectivity of layer 2 pyramidal neurons in the medial prefrontal cortex. *J Neurosci, 32*(37), 12808-12819. doi:10.1523/JNEUROSCI.1616-12.2012

Lodge, D. J., & Grace, A. A. (2009). Gestational methylazoxymethanol acetate administration: a developmental disruption model of schizophrenia. *Behavioural Brain Research, 204*(2), 306-312.

Lunsford-Avery, J. R., Orr, J. M., Gupta, T., Pelletier-Baldelli, A., Dean, D. J., Watts, A. K. S., . . . Mittal, V. A. (2013). Sleep dysfunction and thalamic abnormalities in adolescents at ultra high-risk for psychosis. *Schizophrenia Research, 151*(1-3), 148-153.

Malaspina, D., Harkavy-Friedman, J., Corcoran, C., Mujica-Parodi, L., Printz, D., Gorman, J. M., & Van Heertum, R. (2004). Resting neural activity distinguishes subgroups of schizophrenia patients. *Biological psychiatry, 56*(12), 931-937. doi:https://doi.org/10.1016/j.biopsych.2004.09.013

Malhi, G. S., Bell, E., Hamilton, A., & Morris, G. (2021). Early intervention for risk syndromes: What are the real risks? *Schizophrenia Research, 227*, 4-9. doi:https://doi.org/10.1016/j.schres.2020.04.006

Marenco, S., Stein, J. L., Savostyanova, A. A., Sambataro, F., Tan, H. Y., Goldman, A. L., . . . Weinberger, D. R. (2012). Investigation of anatomical thalamo-cortical connectivity and

FMRI activation in schizophrenia. *Neuropsychopharmacology, 37*(2), 499-507. doi:10.1038/npp.2011.215

Marín, O. (2012). Interneuron dysfunction in psychiatric disorders. *Nature Reviews Neuroscience, 13*(2), 107-120. doi:10.1038/nrn3155

Markham, J. A., & Greenough, W. T. (2004). Experience-driven brain plasticity: beyond the synapse. *Neuron glia biology, 1*(4), 351-363.

Markowitsch, H. J., Pritzel, M., & Divac, I. (1978). The prefrontal cortex of the cat: anatomical subdivisions based on retrograde labeling of cells in the mediodorsal thalamic nucleus. *Exp Brain Res, 32*(3), 335-344. doi:10.1007/bf00238706

Markram, H., Toledo-Rodriguez, M., Wang, Y., Gupta, A., Silberberg, G., & Wu, C. (2004). Interneurons of the neocortical inhibitory system. *Nature Reviews Neuroscience, 5*(10), 793-807. doi:10.1038/nrn1519

Marmolejo, N., Paez, J., Levitt, J. B., & Jones, L. B. (2012). Early postnatal lesion of the medial dorsal nucleus leads to loss of dendrites and spines in adult prefrontal cortex. *Dev Neurosci, 34*(6), 463-476. doi:10.1159/000343911

Marton, T. F., Seifikar, H., Luongo, F. J., Lee, A. T., & Sohal, V. S. (2018). Roles of Prefrontal Cortex and Mediodorsal Thalamus in Task Engagement and Behavioral Flexibility. *J Neurosci, 38*(10), 2569-2578. doi:10.1523/JNEUROSCI.1728-17.2018

McEvoy, J. P. (2007). The importance of early treatment of schizophrenia. *Behav Healthc, 27*(4), 40-43.

McGee, A. W., Yang, Y., Fischer, Q. S., Daw, N. W., & Strittmatter, S. M. (2005). Experience-driven plasticity of visual cortex limited by myelin and Nogo receptor. *Science, 309*(5744), 2222-2226.

McGlashan, T. H., & Hoffman, R. E. (2000). Schizophrenia as a disorder of developmentally reduced synaptic connectivity. *Archives of general psychiatry, 57*(7), 637-648.

McGrath, J., Saha, S., Chant, D., & Welham, J. (2008). Schizophrenia: a concise overview of incidence, prevalence, and mortality. *Epidemiol Rev, 30*, 67-76. doi:10.1093/epirev/mxn001

McRae, P. A., Rocco, M. M., Kelly, G., Brumberg, J. C., & Matthews, R. T. (2007). Sensory deprivation alters aggrecan and perineuronal net expression in the mouse barrel cortex. *Journal of Neuroscience, 27*(20), 5405-5413.

Medoff, D. R., Holcomb, H. H., Lahti, A. C., & Tamminga, C. A. (2001). Probing the human hippocampus using rCBF: contrasts in schizophrenia. *Hippocampus, 11*(5), 543-550.

Mei, L., & Nave, K.-A. (2014). Neuregulin-ERBB Signaling in the Nervous System and Neuropsychiatric Diseases. *Neuron, 83*(1), 27-49. doi:https://doi.org/10.1016/j.neuron.2014.06.007

Melchitzky, D. S., González-Burgos, G., Barrionuevo, G., & Lewis, D. A. (2001). Synaptic targets of the intrinsic axon collaterals of supragranular pyramidal neurons in monkey prefrontal cortex. *Journal of Comparative Neurology, 430*(2), 209-221.

Meyer-Lindenberg, A. S., Olsen, R. K., Kohn, P. D., Brown, T., Egan, M. F., Weinberger, D. R., & Berman, K. F. (2005). Regionally specific disturbance of dorsolateral prefrontal–hippocampal functional connectivity in schizophrenia. *Archives of general psychiatry, 62*(4), 379-386.

Millan, M. J. (2006). Multi-target strategies for the improved treatment of depressive states: Conceptual foundations and neuronal substrates, drug discovery and therapeutic application. *Pharmacol Ther, 110*(2), 135-370. doi:10.1016/j.pharmthera.2005.11.006

Millan, M. J., Agid, Y., Brune, M., Bullmore, E. T., Carter, C. S., Clayton, N. S., . . . Young, L. J. (2012a). Cognitive dysfunction in psychiatric disorders: characteristics, causes and the quest for improved therapy. *Nat Rev Drug Discov, 11*(2), 141-168. doi:10.1038/nrd3628

Millan, M. J., Agid, Y., Brüne, M., Bullmore, E. T., Carter, C. S., Clayton, N. S., . . . Young, L. J. (2012b). Cognitive dysfunction in psychiatric disorders: characteristics, causes and the quest for improved therapy. *Nat Rev Drug Discov, 11*(2), 141-168. doi:10.1038/nrd3628

Millan, M. J., Andrieux, A., Bartzokis, G., Cadenhead, K., Dazzan, P., Fusar-Poli, P., . . . Weinberger, D. (2016). Altering the course of schizophrenia: progress and perspectives. *Nature Reviews Drug Discovery, 15*(7), 485-515. doi:10.1038/nrd.2016.28

Mirnics, K., Middleton, F. A., Marquez, A., Lewis, D. A., & Levitt, P. (2000). Molecular characterization of schizophrenia viewed by microarray analysis of gene expression in prefrontal cortex. *Neuron, 28*(1), 53-67.

Mitelman, S. A., Byne, W., Kemether, E. M., Hazlett, E. A., & Buchsbaum, M. S. (2005). Metabolic disconnection between the mediodorsal nucleus of the thalamus and cortical Brodmann's areas of the left hemisphere in schizophrenia. *Am J Psychiatry, 162*(9), 1733-1735. doi:162/9/1733 [pii]

10.1176/appi.ajp.162.9.1733

Miyamae, T., Chen, K., Lewis, D. A., & Gonzalez-Burgos, G. (2017a). Distinct Physiological Maturation of Parvalbumin-Positive Neuron Subtypes in Mouse Prefrontal Cortex. *J Neurosci, 37*(19), 4883-4902. doi:10.1523/JNEUROSCI.3325-16.2017

Miyamae, T., Chen, K., Lewis, D. A., & Gonzalez-Burgos, G. (2017b). Distinct physiological maturation of parvalbumin-positive neuron subtypes in mouse prefrontal cortex. *Journal of Neuroscience, 37*(19), 4883-4902.

Molina, V., Reig, S., Pascau, J., Sanz, J., Sarramea, F., Gispert, J. D., . . . Desco, M. (2003). Anatomical and functional cerebral variables associated with basal symptoms but not risperidone response in minimally treated schizophrenia. *Psychiatry Research: Neuroimaging, 124*(3), 163-175. doi:https://doi.org/10.1016/S0925-4927(03)00107-0

Mondelli, V., Cattaneo, A., Belvederi Murri, M., Di Forti, M., Handley, R., Hepgul, N., . . . Pariante, C. M. (2011). Stress and inflammation reduce brain-derived neurotrophic factor expression in first-episode psychosis. *a pathway to smaller hippocampal volume, 72*(12), 1677-1684. doi:10.4088/JCP.10m06745

Moreno-Küstner, B., Martín, C., & Pastor, L. (2018). Prevalence of psychotic disorders and its association with methodological issues. A systematic review and meta-analyses. *PLoS One, 13*(4), e0195687. doi:10.1371/journal.pone.0195687

Morgunova, A., & Flores, C. (2021). MicroRNA regulation of prefrontal cortex development and psychiatric risk in adolescence. *Semin Cell Dev Biol*. doi:10.1016/j.semcdb.2021.04.011

Morita, Y., Callicott, J. H., Testa, L. R., Mighdoll, M. I., Dickinson, D., Chen, Q., . . . Hyde, T. M. (2014). Characteristics of the Cation Cotransporter NKCC1 in Human Brain: Alternate Transcripts, Expression in Development, and Potential Relationships to Brain Function and Schizophrenia. *The Journal of Neuroscience, 34*(14), 4929-4940. doi:10.1523/jneurosci.1423-13.2014

Morris, H. M., Hashimoto, T., & Lewis, D. A. (2008). Alterations in somatostatin mRNA expression in the dorsolateral prefrontal cortex of subjects with schizophrenia or schizoaffective disorder. *Cerebral Cortex, 18*(7), 1575-1587.

Mount, C. W., & Monje, M. (2017). Wrapped to Adapt: Experience-Dependent Myelination. *Neuron, 95*(4), 743-756. doi:https://doi.org/10.1016/j.neuron.2017.07.009

Mukherjee, A., Bajwa, N., Lam, N. H., Porrero, C., Clasca, F., & Halassa, M. M. (2020). Variation of connectivity across exemplar sensory and associative thalamocortical loops in the mouse. *Elife, 9*. doi:10.7554/eLife.62554

Mukherjee, A., Carvalho, F., Eliez, S., & Caroni, P. (2019a). Long-lasting rescue of network and cognitive dysfunction in a genetic schizophrenia model. *Cell, 178*(6), 1387-1402. e1314.

Mukherjee, A., Carvalho, F., Eliez, S., & Caroni, P. (2019b). Long-Lasting Rescue of Network and Cognitive Dysfunction in a Genetic Schizophrenia Model. *Cell, 178*(6), 1387-1402 e1314. doi:10.1016/j.cell.2019.07.023

Muller, N. G., Machado, L., & Knight, R. T. (2002). Contributions of subregions of the prefrontal cortex to working memory: evidence from brain lesions in humans. *J Cogn Neurosci, 14*(5), 673-686. doi:10.1162/08989290260138582

Murray, C. J. L. (1990). The Global Burden of Disease : A Comprehensive Assessment of Mortality and Disability from Diseases, Injuries, and Risk Factors in 1990 and Projected to 2020. *Global Burden of Disease and Injury Series*. Retrieved from https://ci.nii.ac.jp/naid/10022001078/en/

Murray, E. A., & Izquierdo, A. (2007). Orbitofrontal cortex and amygdala contributions to affect and action in primates. *Ann N Y Acad Sci, 1121*, 273-296. doi:10.1196/annals.1401.021

Nabel, E. M., Garkun, Y., Koike, H., Sadahiro, M., Liang, A., Norman, K. J., . . . Morishita, H. (2020). Adolescent frontal top-down neurons receive heightened local drive to establish

adult attentional behavior in mice. *Nat Commun, 11*(1), 3983. doi:10.1038/s41467-020-17787-0

Nabel, E. M., & Morishita, H. (2013). Regulating critical period plasticity: insight from the visual system to fear circuitry for therapeutic interventions. *Front Psychiatry, 4*, 146. doi:10.3389/fpsyt.2013.00146

Narayanan, N. S., & Laubach, M. (2009). Methods for studying functional interactions among neuronal populations. *Methods Mol Biol, 489*, 135-165. doi:10.1007/978-1-59745-543-5_7

Neil D. Woodward, Ph.D. ,, Haleh Karbasforoushan, M.S. , and, & Stephan Heckers, M.D., M.Sc. (2012). Thalamocortical Dysconnectivity in Schizophrenia. *American Journal of Psychiatry, 169*(10), 1092-1099. doi:10.1176/appi.ajp.2012.12010056

Nelson, M. D., Saykin, A. J., Flashman, L. A., & Riordan, H. J. (1998). Hippocampal Volume Reduction in Schizophrenia as Assessed by Magnetic Resonance Imaging: A Meta-analytic Study. *Archives of general psychiatry, 55*(5), 433-440. doi:10.1001/archpsyc.55.5.433

O'Donnell, P. (2012). Cortical disinhibition in the neonatal ventral hippocampal lesion model of schizophrenia: New vistas on possible therapeutic approaches. *Pharmacology & Therapeutics, 133*(1), 19-25. doi:https://doi.org/10.1016/j.pharmthera.2011.07.005

Ohnuma, T., Augood, S., Arai, H., McKenna, P., & Emson, P. (1999). Measurement of GABAergic parameters in the prefrontal cortex in schizophrenia: focus on GABA content, GABAA receptor α-1 subunit messenger RNA and human GABA transporter-1 (HGAT-1) messenger RNA expression. *Neuroscience, 93*(2), 441-448.

Okada, N., Fukunaga, M., Yamashita, F., Koshiyama, D., Yamamori, H., Ohi, K., . . . Hashimoto, R. (2016). Abnormal asymmetries in subcortical brain volume in schizophrenia. *Mol Psychiatry, 21*(10), 1460-1466. doi:10.1038/mp.2015.209

Olbert, C. M., Nagendra, A., & Buck, B. (2018). Meta-analysis of Black vs. White racial disparity in schizophrenia diagnosis in the United States: Do structured assessments attenuate racial disparities? *J Abnorm Psychol, 127*(1), 104-115. doi:10.1037/abn0000309

Olfson, M., Gerhard, T., Huang, C., Crystal, S., & Stroup, T. S. (2015). Premature Mortality Among Adults With Schizophrenia in the United States. *JAMA Psychiatry, 72*(12), 1172-1181. doi:10.1001/jamapsychiatry.2015.1737

Ouhaz, Z., Fleming, H., & Mitchell, A. S. (2018). Cognitive Functions and Neurodevelopmental Disorders Involving the Prefrontal Cortex and Mediodorsal Thalamus. *Frontiers in Neuroscience, 12*(33). doi:10.3389/fnins.2018.00033

Ouhaz, Z., Perry, B. A., Nakamura, K., & Mitchell, A. S. (2021). Mediodorsal thalamus is critical for updating during extra-dimensional shifts but not reversals in the attentional set-shifting task. *bioRxiv*, 2021.2004.2013.439610. doi:10.1101/2021.04.13.439610

Pakan, J. M., Francioni, V., & Rochefort, N. L. (2018). Action and learning shape the activity of neuronal circuits in the visual cortex. *Curr Opin Neurobiol, 52*, 88-97. doi:10.1016/j.conb.2018.04.020

Park, A. J., Harris, A. Z., Martyniuk, K. M., Chang, C. Y., Abbas, A. I., Lowes, D. C., . . . Gordon, J. A. (2021). Reset of hippocampal-prefrontal circuitry facilitates learning. *Nature, 591*(7851), 615-619. doi:10.1038/s41586-021-03272-1

Parnaudeau, S., Bolkan, S. S., & Kellendonk, C. (2018). The Mediodorsal Thalamus: An Essential Partner of the Prefrontal Cortex for Cognition. *Biol Psychiatry, 83*(8), 648-656. doi:10.1016/j.biopsych.2017.11.008

Parnaudeau, S., O'Neill, P. K., Bolkan, S. S., Ward, R. D., Abbas, A. I., Roth, B. L., . . . Kellendonk, C. (2013). Inhibition of mediodorsal thalamus disrupts thalamofrontal connectivity and cognition. *Neuron, 77*(6), 1151-1162. doi:10.1016/j.neuron.2013.01.038

Pattwell, S. S., Liston, C., Jing, D., Ninan, I., Yang, R. R., Witztum, J., . . . Lee, F. S. (2016). Dynamic changes in neural circuitry during adolescence are associated with persistent attenuation of fear memories. *Nat Commun, 7*, 11475. doi:10.1038/ncomms11475

Paus, T., Keshavan, M., & Giedd, J. N. (2008). Why do many psychiatric disorders emerge during adolescence? *Nat Rev Neurosci, 9*(12), 947-957. doi:10.1038/nrn2513

Pergola, G., Selvaggi, P., Trizio, S., Bertolino, A., & Blasi, G. (2015). The role of the thalamus in schizophrenia from a neuroimaging perspective. *Neurosci Biobehav Rev, 54*, 57-75. doi:10.1016/j.neubiorev.2015.01.013

Perrone-Bizzozero, N. I., Sower, A. C., Bird, E. D., Benowitz, L. I., Ivins, K. J., & Neve, R. L. (1996). Levels of the growth-associated protein GAP-43 are selectively increased in association cortices in schizophrenia. *Proceedings of the National Academy of Sciences, 93*(24), 14182-14187.

Pessoa, L. (2008). On the relationship between emotion and cognition. *Nat Rev Neurosci, 9*(2), 148-158. doi:10.1038/nrn2317

Pettersson-Yeo, W., Allen, P., Benetti, S., McGuire, P., & Mechelli, A. (2011). Dysconnectivity in schizophrenia: where are we now? *Neuroscience & Biobehavioral Reviews, 35*(5), 1110-1124.

Pierri, J. N., Volk, C. L., Auh, S., Sampson, A., & Lewis, D. A. (2001). Decreased somal size of deep layer 3 pyramidal neurons in the prefrontal cortex of subjects with schizophrenia. *Archives of general psychiatry, 58*(5), 466-473.

Pillinger, T., Beck, K., Gobjila, C., Donocik, J. G., Jauhar, S., & Howes, O. D. (2017). Impaired Glucose Homeostasis in First-Episode Schizophrenia: A Systematic Review and Meta-analysis. *JAMA Psychiatry, 74*(3), 261-269. doi:10.1001/jamapsychiatry.2016.3803

Pinault, D., & Deschenes, M. (1998). Projection and innervation patterns of individual thalamic reticular axons in the thalamus of the adult rat: a three-dimensional, graphic, and

morphometric analysis. *J Comp Neurol, 391*(2), 180-203. Retrieved from https://www.ncbi.nlm.nih.gov/pubmed/9518268

Price, J. L. (2007). Definition of the orbital cortex in relation to specific connections with limbic and visceral structures and other cortical regions. *Ann N Y Acad Sci, 1121*, 54-71. doi:10.1196/annals.1401.008

Rajkowska, G., Selemon, L. D., & Goldman-Rakic, P. S. (1998). Neuronal and glial somal size in the prefrontal cortex: a postmortem morphometric study of schizophrenia and Huntington disease. *Archives of general psychiatry, 55*(3), 215-224.

Rao, N. P., Kalmady, S., Arasappa, R., & Venkatasubramanian, G. (2010). Clinical correlates of thalamus volume deficits in anti-psychotic-naïve schizophrenia patients: A 3-Tesla MRI study. *Indian J Psychiatry, 52*(3), 229-235. doi:10.4103/0019-5545.70975

Rapoport, J. L., Giedd, J. N., & Gogtay, N. (2012). Neurodevelopmental model of schizophrenia: update 2012. *Mol Psychiatry, 17*(12), 1228-1238. doi:10.1038/mp.2012.23

Rapoport, J. L., & Gogtay, N. (2008). Brain neuroplasticity in healthy, hyperactive and psychotic children: insights from neuroimaging. *Neuropsychopharmacology, 33*(1), 181-197.

Rasetti, R., Sambataro, F., Chen, Q., Callicott, J. H., Mattay, V. S., & Weinberger, D. R. (2011). Altered cortical network dynamics: a potential intermediate phenotype for schizophrenia and association with ZNF804A. *Archives of general psychiatry, 68*(12), 1207-1217.

Ray, J. P., & Price, J. L. (1992). The organization of the thalamocortical connections of the mediodorsal thalamic nucleus in the rat, related to the ventral forebrain–prefrontal cortex topography. *Journal of Comparative Neurology, 323*(2), 167-197. doi:https://doi.org/10.1002/cne.903230204

Rikhye, R. V., Gilra, A., & Halassa, M. M. (2018a). Thalamic regulation of switching between cortical representations enables cognitive flexibility. *Nat Neurosci, 21*(12), 1753-1763. doi:10.1038/s41593-018-0269-z

Rikhye, R. V., Wimmer, R. D., & Halassa, M. M. (2018b). Toward an Integrative Theory of Thalamic Function. *Annu Rev Neurosci, 41*, 163-183. doi:10.1146/annurev-neuro-080317-062144

Rios, O., & Villalobos, J. (2004). Postnatal development of the afferent projections from the dorsomedial thalamic nucleus to the frontal cortex in mice. *Brain Res Dev Brain Res, 150*(1), 47-50. doi:10.1016/j.devbrainres.2004.02.005

Robinson, S. E., & Sohal, V. S. (2017). Dopamine D2 Receptors Modulate Pyramidal Neurons in Mouse Medial Prefrontal Cortex through a Stimulatory G-Protein Pathway. *J Neurosci, 37*(42), 10063-10073. doi:10.1523/JNEUROSCI.1893-17.2017

Rossi, M. A., Hayrapetyan, V. Y., Maimon, B., Mak, K., Je, H. S., & Yin, H. H. (2012). Prefrontal cortical mechanisms underlying delayed alternation in mice. *J Neurophysiol, 108*(4), 1211-1222. doi:10.1152/jn.01060.2011

Saalmann, Y. B. (2014). Intralaminar and medial thalamic influence on cortical synchrony, information transmission and cognition. *Front Syst Neurosci, 8*, 83. doi:10.3389/fnsys.2014.00083

Sakurai, T., & Gamo, N. J. (2019). Cognitive functions associated with developing prefrontal cortex during adolescence and developmental neuropsychiatric disorders. *Neurobiology of Disease, 131*, 104322. doi:https://doi.org/10.1016/j.nbd.2018.11.007

Sale, A., Vetencourt, J. F. M., Medini, P., Cenni, M. C., Baroncelli, L., De Pasquale, R., & Maffei, L. (2007). Environmental enrichment in adulthood promotes amblyopia recovery through a reduction of intracortical inhibition. *Nat Neurosci, 10*(6), 679-681.

Salzman, C. D., & Fusi, S. (2010). Emotion, cognition, and mental state representation in amygdala and prefrontal cortex. *Annu Rev Neurosci, 33*, 173-202. doi:10.1146/annurev.neuro.051508.135256

Samantha J. Fung, Ph.D. ,, Maree J. Webster, Ph.D. ,, Sinthuja Sivagnanasundaram, Ph.D. ,, Carlotta Duncan, Ph.D. ,, Michael Elashoff, Ph.D. , and, & Cynthia Shannon Weickert, Ph.D. (2010). Expression of Interneuron Markers in the Dorsolateral Prefrontal Cortex of the Developing Human and in Schizophrenia. *American Journal of Psychiatry, 167*(12), 1479-1488. doi:10.1176/appi.ajp.2010.09060784

Santana, N., & Artigas, F. (2017). Laminar and Cellular Distribution of Monoamine Receptors in Rat Medial Prefrontal Cortex. *Frontiers in Neuroanatomy, 11*(87). doi:10.3389/fnana.2017.00087

Saykin, A. J., Shtasel, D. L., Gur, R. E., Kester, D. B., Mozley, L. H., Stafiniak, P., & Gur, R. C. (1994). Neuropsychological deficits in neuroleptic naive patients with first-episode schizophrenia. *Archives of general psychiatry, 51*(2), 124-131.

Schafer, D. P., & Stevens, B. (2013). Phagocytic glial cells: sculpting synaptic circuits in the developing nervous system. *Current Opinion in Neurobiology, 23*(6), 1034-1040. doi:https://doi.org/10.1016/j.conb.2013.09.012

Scheffer-Teixeira, R., Belchior, H., Leao, R. N., Ribeiro, S., & Tort, A. B. (2013). On high-frequency field oscillations (>100 Hz) and the spectral leakage of spiking activity. *J Neurosci, 33*(4), 1535-1539. doi:10.1523/JNEUROSCI.4217-12.2013

Schmitt, L. I., Wimmer, R. D., Nakajima, M., Happ, M., Mofakham, S., & Halassa, M. M. (2017). Thalamic amplification of cortical connectivity sustains attentional control. *Nature, 545*(7653), 219-223. doi:10.1038/nature22073

Schobel, S. A., Chaudhury, N. H., Khan, U. A., Paniagua, B., Styner, M. A., Asllani, I., . . . Small, S. A. (2013). Imaging patients with psychosis and a mouse model establishes a spreading pattern of hippocampal dysfunction and implicates glutamate as a driver. *Neuron, 78*(1), 81-93. doi:10.1016/j.neuron.2013.02.011

Schoenbaum, G., Nugent, S. L., Saddoris, M. P., & Setlow, B. (2002). Orbitofrontal lesions in rats impair reversal but not acquisition of go, no-go odor discriminations. *Neuroreport, 13*(6), 885-890.

Schwartz, R. C., & Blankenship, D. M. (2014). Racial disparities in psychotic disorder diagnosis: A review of empirical literature. *World journal of psychiatry, 4*(4), 133-140. doi:10.5498/wjp.v4.i4.133

Seamans, J. K., Floresco, S. B., & Phillips, A. G. (1995). Functional differences between the prelimbic and anterior cingulate regions of the rat prefrontal cortex. *Behav Neurosci, 109*(6), 1063-1073. doi:10.1037//0735-7044.109.6.1063

Seamans, J. K., & Yang, C. R. (2004). The principal features and mechanisms of dopamine modulation in the prefrontal cortex. *Prog Neurobiol, 74*(1), 1-58. doi:10.1016/j.pneurobio.2004.05.006

Sekar, A., Bialas, A. R., de Rivera, H., Davis, A., Hammond, T. R., Kamitaki, N., . . . McCarroll, S. A. (2016). Schizophrenia risk from complex variation of complement component 4. *Nature, 530*(7589), 177-183. doi:10.1038/nature16549

Sellgren, C. M., Gracias, J., Watmuff, B., Biag, J. D., Thanos, J. M., Whittredge, P. B., . . . Perlis, R. H. (2019). Increased synapse elimination by microglia in schizophrenia patient-derived models of synaptic pruning. *Nat Neurosci, 22*(3), 374-385. doi:10.1038/s41593-018-0334-7

Seong, H. J., & Carter, A. G. (2012). D1 receptor modulation of action potential firing in a subpopulation of layer 5 pyramidal neurons in the prefrontal cortex. *J Neurosci, 32*(31), 10516-10521. doi:10.1523/JNEUROSCI.1367-12.2012

Sherman, A. D., Davidson, A. T., Baruah, S., Hegwood, T. S., & Waziri, R. (1991). Evidence of glutamatergic deficiency in schizophrenia. *Neuroscience letters, 121*(1-2), 77-80.

Sherman, S. M. (2016). Thalamus plays a central role in ongoing cortical functioning. *Nat Neurosci, 19*(4), 533-541. doi:10.1038/nn.4269

Sherman, S. M., & Guillery, R. (1998). On the actions that one nerve cell can have on another: distinguishing “drivers” from “modulators”. *Proceedings of the National Academy of Sciences, 95*(12), 7121-7126.

Sigurdsson, T., & Duvarci, S. (2016). Hippocampal-Prefrontal Interactions in Cognition, Behavior and Psychiatric Disease. *Frontiers in Systems Neuroscience, 9*(190). doi:10.3389/fnsys.2015.00190

Silbersweig, D. A., Stern, E., Frith, C., Cahill, C., Holmes, A., Grootoonk, S., . . . Schnorr, L. (1995). A functional neuroanatomy of hallucinations in schizophrenia. *Nature, 378*(6553), 176-179.

Sim, K., Cullen, T., Ongur, D., & Heckers, S. (2006). Testing models of thalamic dysfunction in schizophrenia using neuroimaging. *J Neural Transm (Vienna), 113*(7), 907-928. doi:10.1007/s00702-005-0363-8

Singh, S., Singh, K., Trivedi, R., Goyal, S., Kaur, P., Singh, N., . . . Khushu, S. (2016). Microstructural abnormalities of uncinate fasciculus as a function of impaired cognition in schizophrenia: A DTI study. *J Biosci, 41*(3), 419-426. doi:10.1007/s12038-016-9631-z

Sohal, V. S., Zhang, F., Yizhar, O., & Deisseroth, K. (2009). Parvalbumin neurons and gamma rhythms enhance cortical circuit performance. *Nature, 459*(7247), 698-702.

Spellman, T., Rigotti, M., Ahmari, S. E., Fusi, S., Gogos, J. A., & Gordon, J. A. (2015). Hippocampal-prefrontal input supports spatial encoding in working memory. *Nature, 522*(7556), 309-314. doi:10.1038/nature14445

Spellman, T., Svei, M., Kaminsky, J., Manzano-Nieves, G., & Liston, C. (2021). Prefrontal deep projection neurons enable cognitive flexibility via persistent feedback monitoring. *Cell, 184*(10), 2750-2766 e2717. doi:10.1016/j.cell.2021.03.047

Spolidoro, M., Baroncelli, L., Putignano, E., Maya-Vetencourt, J., Viegi, A., & Maffei, L. (2011). Food restriction enhances visual cortex plasticity in adulthood. Nat Commun 2: 320. In.

Spronk, M., Keane, B. P., Ito, T., Kulkarni, K., Ji, J. L., Anticevic, A., & Cole, M. W. (2021). A Whole-Brain and Cross-Diagnostic Perspective on Functional Brain Network Dysfunction. *Cereb Cortex, 31*(1), 547-561. doi:10.1093/cercor/bhaa242

Stamm, J. S., & Weber-Levine, M. L. (1971). Delayed alternation impairments following selective prefrontal cortical ablations in monkeys. *Exp Neurol, 33*(2), 263-278. doi:10.1016/0014-4886(71)90020-3

Stefanini, F., Kushnir, L., Jimenez, J. C., Jennings, J. H., Woods, N. I., Stuber, G. D., . . . Fusi, S. (2020). A Distributed Neural Code in the Dentate Gyrus and in CA1. *Neuron, 107*(4), 703-716 e704. doi:10.1016/j.neuron.2020.05.022

Stilo, S. A., & Murray, R. M. (2019). Non-Genetic Factors in Schizophrenia. *Curr Psychiatry Rep, 21*(10), 100. doi:10.1007/s11920-019-1091-3

Stryker, M. P. (2014). A Neural Circuit That Controls Cortical State, Plasticity, and the Gain of Sensory Responses in Mouse. *Cold Spring Harb Symp Quant Biol, 79*, 1-9. doi:10.1101/sqb.2014.79.024927

Sumich, A., Chitnis, X. A., Fannon, D. G., O'Ceallaigh, S., Doku, V. C., Falrowicz, A., . . . Sharma, T. (2002). Temporal lobe abnormalities in first-episode psychosis. *American Journal of Psychiatry, 159*(7), 1232-1235.

Sun, Y. J., Espinosa, J. S., Hoseini, M. S., & Stryker, M. P. (2019). Experience-dependent structural plasticity at pre- and postsynaptic sites of layer 2/3 cells in developing visual cortex. *Proc Natl Acad Sci U S A, 116*(43), 21812-21820. doi:10.1073/pnas.1914661116

Szeszko, P. R., Goldberg, E., Gunduz-Bruce, H., Ashtari, M., Robinson, D., Malhotra, A. K., . . . Kane, J. M. (2003). Smaller anterior hippocampal formation volume in antipsychotic-naive patients with first-episode schizophrenia. *American Journal of Psychiatry, 160*(12), 2190-2197.

Takesian, A. E., & Hensch, T. K. (2013a). Balancing plasticity/stability across brain development. *Progress in brain research, 207*, 3-34.

Takesian, A. E., & Hensch, T. K. (2013b). Balancing plasticity/stability across brain development. *Prog Brain Res, 207*, 3-34. doi:10.1016/B978-0-444-63327-9.00001-1

Tanaka-Koshiyama, K., Koshiyama, D., Miyakoshi, M., Joshi, Y. B., Molina, J. L., Sprock, J., . . . Light, G. A. (2020). Abnormal Spontaneous Gamma Power Is Associated With Verbal Learning and Memory Dysfunction in Schizophrenia. *Frontiers in Psychiatry, 11*(832). doi:10.3389/fpsyt.2020.00832

Tanaka, S. (2008). Dysfunctional GABAergic inhibition in the prefrontal cortex leading to "psychotic" hyperactivation. *BMC Neurosci, 9*, 41. doi:10.1186/1471-2202-9-41

Tanibuchi, I., & Goldman-Rakic, P. S. (2003). Dissociation of spatial-, object-, and sound-coding neurons in the mediodorsal nucleus of the primate thalamus. *Journal of neurophysiology, 89*(2), 1067-1077.

Taylor, S. F., Welsh, R. C., Chen, A. C., Velander, A. J., & Liberzon, I. (2007). Medial frontal hyperactivity in reality distortion. *Biol Psychiatry, 61*(10), 1171-1178. doi:10.1016/j.biopsych.2006.11.029

Thune, J. J., Uylings, H. B., & Pakkenberg, B. (2001). No deficit in total number of neurons in the prefrontal cortex in schizophrenics. *Journal of Psychiatric Research, 35*(1), 15-21.

Tian, L., Meng, C., Yan, H., Zhao, Q., Liu, Q., Yan, J., . . . Zhang, D. (2011). Convergent evidence from multimodal imaging reveals amygdala abnormalities in schizophrenic patients and their first-degree relatives. *PLoS One, 6*(12), e28794. doi:10.1371/journal.pone.0028794

Tooley, U. A., Bassett, D. S., & Mackey, A. P. (2021). Environmental influences on the pace of brain development. *Nature Reviews Neuroscience, 22*(6), 372-384. doi:10.1038/s41583-021-00457-5

Uhlhaas, P. J. (2013). Dysconnectivity, large-scale networks and neuronal dynamics in schizophrenia. *Current Opinion in Neurobiology, 23*(2), 283-290. doi:https://doi.org/10.1016/j.conb.2012.11.004

Uhlhaas, P. J., & Singer, W. (2011). The development of neural synchrony and large-scale cortical networks during adolescence: relevance for the pathophysiology of schizophrenia and neurodevelopmental hypothesis. *Schizophr Bull, 37*(3), 514-523. doi:10.1093/schbul/sbr034

Uhlhaas, P. J., & Singer, W. (2012). Neuronal dynamics and neuropsychiatric disorders: toward a translational paradigm for dysfunctional large-scale networks. *Neuron, 75*(6), 963-980.

Van Eden, C. (1986). Development of connections between the mediodorsal nucleus of the thalamus and the prefrontal cortex in the rat. *Journal of Comparative Neurology, 244*(3), 349-359.

Van Eden, C., Kros, J., & Uylings, H. (1991). The development of the rat prefrontal cortex: Its size and development of connections with thalamus, spinal cord and other cortical areas. *Progress in brain research, 85*, 169-183.

Van Eden, C. G., & Uylings, H. B. (1985). Postnatal volumetric development of the prefrontal cortex in the rat. *J Comp Neurol, 241*(3), 268-274. doi:10.1002/cne.902410303

van Erp, T. G., Hibar, D. P., Rasmussen, J. M., Glahn, D. C., Pearlson, G. D., Andreassen, O. A., . . . Turner, J. A. (2016). Subcortical brain volume abnormalities in 2028 individuals with schizophrenia and 2540 healthy controls via the ENIGMA consortium. *Mol Psychiatry, 21*(4), 547-553. doi:10.1038/mp.2015.63

Vertes, R. P., Fortin, W. J., & Crane, A. M. (1999). Projections of the median raphe nucleus in the rat. *J Comp Neurol, 407*(4), 555-582. Retrieved from https://www.ncbi.nlm.nih.gov/pubmed/10235645

Vetencourt, J. F. M., Sale, A., Viegi, A., Baroncelli, L., De Pasquale, R., O'Leary, O. F., . . . Maffei, L. (2008). The antidepressant fluoxetine restores plasticity in the adult visual cortex. *Science, 320*(5874), 385-388.

Vinck, M., van Wingerden, M., Womelsdorf, T., Fries, P., & Pennartz, C. M. (2010). The pairwise phase consistency: a bias-free measure of rhythmic neuronal synchronization. *Neuroimage, 51*(1), 112-122. doi:10.1016/j.neuroimage.2010.01.073

Volk, D. W., & Lewis, D. A. (2010). Prefrontal Cortical Circuits in Schizophrenia. In N. R. Swerdlow (Ed.), *Behavioral neurobiology of schizophrenia and its treatment* (pp. 485-508). Berlin, Heidelberg: Springer Berlin Heidelberg.

Volk, D. W., Pierri, J. N., Fritschy, J.-M., Auh, S., Sampson, A. R., & Lewis, D. A. (2002). Reciprocal alterations in pre-and postsynaptic inhibitory markers at chandelier cell inputs to pyramidal neurons in schizophrenia. *Cerebral Cortex, 12*(10), 1063-1070.

Watanabe, Y., & Funahashi, S. (2004a). Neuronal activity throughout the primate mediodorsal nucleus of the thalamus during oculomotor delayed-responses. I. Cue-, delay-, and response-period activity. *Journal of neurophysiology, 92*(3), 1738-1755.

Watanabe, Y., & Funahashi, S. (2004b). Neuronal activity throughout the primate mediodorsal nucleus of the thalamus during oculomotor delayed-responses. II. Activity encoding visual versus motor signal. *Journal of neurophysiology, 92*(3), 1756-1769.

Watanabe, Y., & Funahashi, S. (2012). Thalamic mediodorsal nucleus and working memory. *Neuroscience & Biobehavioral Reviews, 36*(1), 134-142.

Weinberger, D. R. (1987). Implications of Normal Brain Development for the Pathogenesis of Schizophrenia. *Archives of general psychiatry, 44*(7), 660-669. doi:10.1001/archpsyc.1987.01800190080012

Weinberger, D. R., & Berman, K. F. (1996). Prefrontal function in schizophrenia: confounds and controversies. *Philos Trans R Soc Lond B Biol Sci, 351*(1346), 1495-1503. doi:10.1098/rstb.1996.0135

Weinberger, D. R., Berman, K. F., Suddath, R., & Torrey, E. F. (1992). Evidence of dysfunction of a prefrontal-limbic network in schizophrenia: a magnetic resonance imaging and

regional cerebral blood flow study of discordant monozygotic twins. *Am J Psychiatry, 149*(7), 890-897.

Welham, J., Isohanni, M., Jones, P., & McGrath, J. (2009). The antecedents of schizophrenia: a review of birth cohort studies. *Schizophr Bull, 35*(3), 603-623. doi:10.1093/schbul/sbn084

Wen, W., & Turrigiano, G. G. (2021). Developmental Regulation of Homeostatic Plasticity in Mouse Primary Visual Cortex. *bioRxiv*, 2021.2006.2011.448148. doi:10.1101/2021.06.11.448148

Wiesel, T. N. (1982). Postnatal development of the visual cortex and the influence of environment. *Nature, 299*(5884), 583-591.

Wiesel, T. N., & Hubel, D. H. (1963). Single-Cell Responses in Striate Cortex of Kittens Deprived of Vision in One Eye. *J Neurophysiol, 26*, 1003-1017. doi:10.1152/jn.1963.26.6.1003

Woo, T.-U., Miller, J. L., & Lewis, D. A. (1997). Schizophrenia and the parvalbumin-containing class of cortical local circuit neurons. *American Journal of Psychiatry, 154*(7), 1013-1015.

Woo, T.-U., Whitehead, R. E., Melchitzky, D. S., & Lewis, D. A. (1998). A subclass of prefrontal γ-aminobutyric acid axon terminals are selectively altered in schizophrenia. *Proceedings of the National Academy of Sciences, 95*(9), 5341-5346.

Woo, T.-U. W., Spencer, K., & McCarley, R. W. (2010). Gamma Oscillation Deficits and the Onset and Early Progression of Schizophrenia. *Harvard Review of Psychiatry, 18*(3), 173-189. doi:10.3109/10673221003747609

Woods, S. W., Bearden, C. E., Sabb, F. W., Stone, W. S., Torous, J., Cornblatt, B. A., . . . Anticevic, A. (2021). Counterpoint. Early intervention for psychosis risk syndromes: Minimizing risk and maximizing benefit. *Schizophr Res, 227*, 10-17. doi:10.1016/j.schres.2020.04.020

Woodward, N. D., & Heckers, S. (2016a). Mapping Thalamocortical Functional Connectivity in Chronic and Early Stages of Psychotic Disorders. *Biol Psychiatry, 79*(12), 1016-1025. doi:10.1016/j.biopsych.2015.06.026

Woodward, N. D., & Heckers, S. (2016b). Mapping Thalamocortical Functional Connectivity in Chronic and Early Stages of Psychotic Disorders. *Biological psychiatry, 79*(12), 1016-1025. doi:https://doi.org/10.1016/j.biopsych.2015.06.026

Woodward, N. D., Karbasforoushan, H., & Heckers, S. (2012). Thalamocortical dysconnectivity in schizophrenia. *Am J Psychiatry, 169*(10), 1092-1099. doi:10.1176/appi.ajp.2012.12010056

Wu, C. H., Ramos, R., Katz, D. B., & Turrigiano, G. G. (2021). Homeostatic synaptic scaling establishes the specificity of an associative memory. *Curr Biol, 31*(11), 2274-2285 e2275. doi:10.1016/j.cub.2021.03.024

Wu, X., Fu, Y., Knott, G., Lu, J., Di Cristo, G., & Huang, Z. J. (2012). GABA signaling promotes synapse elimination and axon pruning in developing cortical inhibitory interneurons. *Journal of Neuroscience, 32*(1), 331-343.

Yamamuro, K., Bicks, L. K., Leventhal, M. B., Kato, D., Im, S., Flanigan, M. E., . . . Morishita, H. (2020). A prefrontal-paraventricular thalamus circuit requires juvenile social experience to regulate adult sociability in mice. *Nat Neurosci, 23*(10), 1240-1252. doi:10.1038/s41593-020-0695-6

Yanagi, M., Joho, R. H., Southcott, S. A., Shukla, A. A., Ghose, S., & Tamminga, C. A. (2014). Kv3.1-containing K+ channels are reduced in untreated schizophrenia and normalized with antipsychotic drugs. *Molecular Psychiatry, 19*(5), 573-579. doi:10.1038/mp.2013.49

Yang, E.-J., Lin, E. W., & Hensch, T. K. (2012). Critical period for acoustic preference in mice. *Proceedings of the National Academy of Sciences, 109*(Supplement 2), 17213-17220.

Yang, J.-M., Zhang, J., Yu, Y.-Q., Duan, S., & Li, X.-M. (2014a). Postnatal development of 2 microcircuits involving fast-spiking interneurons in the mouse prefrontal cortex. *Cerebral Cortex, 24*(1), 98-109.

Yang, J. M., Zhang, J., Yu, Y. Q., Duan, S., & Li, X. M. (2014b). Postnatal development of 2 microcircuits involving fast-spiking interneurons in the mouse prefrontal cortex. *Cereb Cortex, 24*(1), 98-109. doi:10.1093/cercor/bhs291

Yilmaz, M., Yalcin, E., Presumey, J., Aw, E., Ma, M., Whelan, C. W., . . . Carroll, M. C. (2021). Overexpression of schizophrenia susceptibility factor human complement C4A promotes excessive synaptic loss and behavioral changes in mice. *Nat Neurosci, 24*(2), 214-224. doi:10.1038/s41593-020-00763-8

Yoon, T., Okada, J., Jung, M. W., & Kim, J. J. (2008). Prefrontal cortex and hippocampus subserve different components of working memory in rats. *Learn Mem, 15*(3), 97-105. doi:10.1101/lm.850808

Yuste, R. (2015). From the neuron doctrine to neural networks. *Nat Rev Neurosci, 16*(8), 487-497. doi:10.1038/nrn3962

Zhou, Y., Shu, N., Liu, Y., Song, M., Hao, Y., Liu, H., . . . Jiang, T. (2008). Altered resting-state functional connectivity and anatomical connectivity of hippocampus in schizophrenia. *Schizophrenia Research, 100*(1-3), 120-132.

Zuo, Y., Lin, A., Chang, P., & Gan, W.-B. (2005). Development of Long-Term Dendritic Spine Stability in Diverse Regions of Cerebral Cortex. *Neuron, 46*(2), 181-189. doi:https://doi.org/10.1016/j.neuron.2005.04.001